

**DEVELOPMENT OF MOBILITY CONTROL METHODS
TO IMPROVE OIL RECOVERY BY CO₂**

Second Annual Report, Oct. 1, 1980-Sept. 30, 1981

Work Performed for the Department of Energy
Under Contract No. DE-AC21-79MC10689

Date Published—August 1982

New Mexico Petroleum Recovery Research Center
New Mexico Institute of Mining and Technology
Socorro, New Mexico



U. S. DEPARTMENT OF ENERGY

DISCLAIMER

"This book was prepared as an account of work sponsored by an agency of the United States Government. Neither the United States Government nor any agency thereof, nor any of their employees, makes any warranty, express or implied, or assumes any legal liability or responsibility for the accuracy, completeness, or usefulness of any information, apparatus, product, or process disclosed, or represents that its use would not infringe privately owned rights. Reference herein to any specific commercial product, process, or service by trade name, trademark, manufacturer, or otherwise, does not necessarily constitute or imply its endorsement, recommendation, or favoring by the United States Government or any agency thereof. The views and opinions of authors expressed herein do not necessarily state or reflect those of the United States Government or any agency thereof."

Available from the National Technical Information Service, U.S. Department of Commerce, Springfield, Virginia 22161.

NTIS price codes

Paper copy: \$10.50
Microfiche copy: \$4.00

**DEVELOPMENT OF MOBILITY CONTROL METHODS
TO IMPROVE OIL RECOVERY BY CO₂**

Second Annual Report, Oct. 1, 1980–Sept. 30, 1981

John P. Heller and Joseph J. Taber, *Principal Investigators*
New Mexico Petroleum Recovery Research Center
New Mexico Institute of Mining and Technology
Socorro, New Mexico 87801

Albert B. Yost II, *Technical Project Officer*
Morgantown Energy Technology Center
P.O. Box 880
Morgantown, West Virginia 26505

Work Performed for the Department of Energy
Under Contract No. DE-AC21-79MC10689

Date Published—August 1982

CONTENTS

Abstract	1
History and Status of the Project	2
Introduction	2
A. Displacement Efficiency	3
B. Flow Non-uniformities	3
C. Gravitational Effects	4
D. The Mobility Ratio Problem	4
E. Water Alternated with Gas	5
F. High-Pressure Dispersions of CO ₂ in Water (or "Foams")	6
G. Direct Thickening of CO ₂ by Polymers	6
H. Flow Tests	7
I. Practical Considerations with Field Use of Mobility Control Agents	7
Summary of Progress	8
A. Foams	8
B. Direct Thickening	12
C. General Description of Core Flooding Tests	15
D. Specific Progress and Problems	17
1. Core Mounting	17
2. The "Overburden" System	18
3. The Primary Fluid System	19
4. Pressure Measurement	20
5. Computer Monitoring	21
6. Conductivity Measurement	21
7. A Miscible Displacement	22

E. Project Plans	23
Acknowledgement	25
APPENDIX A-1.....	26
VISCOSITY MEASUREMENT BY FALL TIME OF A CYLINDER IN A TUBE.....	26
Introduction	26
Mathematical Analysis	26
Definition of Idealized System.....	26
The Fluid Velocity Distribution in the Annulus.....	28
Dynamics of the Motion.....	32
The Inertial Effective Mass.....	33
The Total Viscous Force.....	35
The Gravitational Force and Coefficients of the Equation.....	36
Viscosity Computations	38
The Dimensionless Coefficients.....	38
Computing Fall Time between Stations, and Viscosity.....	40
Presentation of Results.....	40
Experimental Realization	41
FIGURE A1	42
FIGURE A2	43
FIGURE A3	44
APPENDIX A-2	45
APPENDIX A-3	46
APPENDIX A-4	50
APPENDIX B-1	51
APPENDIX B-2	53
APPENDIX B-3	58
APPENDIX C-1	61

APPENDIX C-262
TABLES67
FIGURES71
REFERENCES86

Abstract

Carbon Dioxide (CO₂) shows certain advantages over water as a displacement fluid in Enhanced Oil Recovery (EOR). Chief among these is the significantly higher microscopic displacement efficiency by CO₂ which is in the liquified or dense-gas state. Such high efficiencies are observed in laboratory experiments in which oil is recovered from long, thin, sand-packed tubes. The high efficiencies, approaching unity, are possible because of the "developed miscibility" in front-stabilized displacements. The objective of this project is to develop means by which the indicated possibility, of recovering more oil from reservoirs, may be achieved in practice. The work is guided by the following widely accepted principle, based on evidence observed by many investigators over the last three decades: Development of non-uniformities in a two- or three-dimensional displacement in a permeable medium, is severely aggravated by the frontal instability resulting from an unfavorable mobility ratio. Such a ratio occurs when the displacing fluid is less viscous than the displaced, as is the case in a CO₂ flood, unless compensated by a uniform and opposite ratio of the relative permeabilities. The goal of this project has been to develop methods to counteract the harmful influence of the naturally unfavorable mobility ratio in CO₂ floods. This goal is to be achieved by thickening the CO₂ while retaining those properties and circumstances that lead to the high microscopic displacement efficiency.

Our efforts have been directed towards the development of two distinct methods for increasing the effective viscosity of dense CO₂. One of these involves the use of water-CO₂ emulsions or "foams" as the displacement fluid. The second type of mobility control additives being investigated are direct thickeners--solutions of certain polymers in the CO₂. Significant progress has been made in both these areas of development.

In conjunction with the development of means of thickening the CO₂ displacement fluid, the need also exists to assess the behavior and effectiveness of the additives. The assessment is to be performed in a standardized, repeatable core-flooding test which has been developed as a third part of the project's laboratory work. As with the development of the thickeners themselves, good progress has also been made here, and the experimental and measuring system has been brought to operating condition.

This report describes significant results which have been obtained in research directed towards each of the three goals enunciated above. Some of these accomplishments are:

- 1) The construction and operation of a foam generator for the laboratory production of liquid-liquid, foam-like dispersions for injection into rock as mobility controlled displacement fluids. The apparatus and procedures have been designed for use with high-pressure CO₂ as the non-aqueous phase, and successful operation has already been achieved using iso-octane in that role.
- 2) The development and use of equipment for measuring both the solubility of polymers in dense CO₂ and the viscosity

of such solutions. About a dozen soluble polymers have been found, and some correlation guidelines observed for polymers which might be effective as direct thickeners.

- 3) An instrumented core-flooding system has been designed and brought to operational condition, to assess the field usefulness of mobility control agents in high-pressure CO₂ floods of tertiary oil. This system has already been used for several preliminary flooding and fluid distribution experiments.

History and Status of the Project

This project resulted from PRRC response to a request for proposal from the Morgantown Energy Technology Center of the DOE. Award of contract (designated DE-AC21-79MC10689) was made on October 1, 1979. A cost-sharing research contract was also granted from the New Mexico Energy and Minerals Department, by which the State paid approximately half the cost of the project.

The first major task of the project was the production of a comprehensive literature survey to explore published work applicable to CO₂ floods which concerned the problem of adverse mobility ratio, and proposed remedies. This was completed in mid-1980 and published¹ by the DOE Fossil Energy Program. In conjunction with this, detailed plans were made for our experimental program for development of mobility control agents for CO₂ floods. These plans were approved by the DOE in August 1980; early progress on them was described in the First Annual Report.²

Because it was not possible to pursue these laboratory plans as rapidly as anticipated, and because some of the investigators' efforts were required by a parallel field project* being discussed with the DOE, no-cost extensions were negotiated for both this project, DE-AC21-79MC10689, and its New Mexico EMD equivalent. Under these extensions the concluding dates of the project were extended until September 1982, at no additional cost to the contracting agencies. Thus, it is anticipated that a Final Report on the activities of this project will be forthcoming next year. The current document, a Second Annual Report, discusses the project as a whole and describes progress made in concepts and in apparatus development, and experimental results available at this time.

Introduction

This section is intended to provide background to one of the central problems of oil production, and to the efforts made in this research project

*This parallel project, DE-AC21-81MC16426, is for laboratory support to a field project being operated by Pennzoil for the DOE, for use of Mobility Control Agents in the Rock Creek field of Roane County, West Virginia.

to solve it. The lettered sections below give brief descriptions of each of these topics. Thus the initial section discusses the efficiency with which oil can be displaced from reservoir rock, and leads into the next three topics, about factors which affect that efficiency - especially in CO₂ floods. Next are discussed three different possibilities for control of non-uniform displacement. The latter two of these sections emphasize the concepts underlying those means of mobility control which are investigated in the project. A further section discusses the laboratory flow tests designed to assess the usefulness of the mobility control agents that are developed, and the last topic of the Introduction is concerned with practical matter involved in the use of such agents or procedures in the oilfield.

A. Displacement Efficiency

In any displacement program, many conditions and variables affect the efficiency of oil recovery. In considering these, it has been traditional in Petroleum Engineering to recognize two major factors in the overall efficiency of displacement, dealing with microscopic and macroscopic phenomena. Microscopic flooding efficiency expresses the fraction of oil recovered from a small region of the reservoir which is fully contacted or swept by the flooding fluid. It may be measured in the laboratory by the use of core samples so mounted that the flow is predominately linear. In the case of displacement processes involving partial miscibility between displaced and displacing fluid, and in which the mass transport of components can lead to a "developed miscibility zone"³, the above view of the microscopic efficiency needs to be extended. For such situations, laboratory studies of the microscopic displacement efficiency demand rather long samples in which the extraction and transport processes can fully develop. Such is the case for CO₂ floods, in which laboratory tests are run in long thin tubes⁴ to find the microscopic flooding efficiency. The results are greatly influenced by the phase behavior of mixtures of CO₂ with the reservoir crude, at appropriate conditions of temperature and pressure.^{5,6} In any flooding situation, though, the microscopic displacement efficiency can be regarded as the upper limit of oil recovery from a formation.

B. Flow Non-uniformities

Macroscopic effects cause the actual oil recovery to be always less than that indicated by the above limit. This is because such effects can prevent the entire reservoir from being fully contacted or swept by the displacing fluid. Such large-scale effects include those due to the heterogeneity of the reservoir rock. In particular, such flow non-uniformity is due to the stratification of the pay zone, but it is also caused by horizontal variations of rock properties over the extent of the field. Another

"geometrical" macroscopic effect follows from the pattern of flow between production and injection wells, which is necessarily non-uniform.

A major effect, however, which can cause flow heterogeneities throughout a wide range of characteristic sizes, is due to unfavorable differences in the properties between displaced and displacing fluid. Such differences in either the mobility or the density can cause the growth of flow non-uniformities.^{7,8,9,10} These can originate either at existing, major permeability or porosity heterogeneities, or can form and grow spontaneously from practically infinitesimal ones.^{11,12}

C. Gravitational Effects

In a predominately horizontal flood, the effect of a density difference is to cause a "parasitic" modification of the flow, by which the displacing fluid will either "over-ride" or "tongue under" the displaced fluid, depending on whether it is of the lower or higher density. In either case, of course, the orientation in which the heavier fluid lies below the less dense one is gravitationally stable. The rate at which such an orientation is approached (and thus the seriousness of the situation) in a horizontal flood, is approximately proportional to the fluid density difference, to an average mobility of the fluids, and to the sine of the angle between the concentration gradient vector and the vertical.

D. The Mobility Ratio Problem

A somewhat different "parasitic flow" results from a mobility difference between the two fluids. When the displacing fluid has higher mobility (the unstable case) the growth of flow non-uniformities is driven by the energy of the displacement itself. After an initial period of more gradual elongation, the flow rate of displacing fluid within a "finger" becomes greater than that of the less mobile fluid surrounding it by a factor about equal to the mobility ratio.¹³

The details of growth of these flow non-uniformities are still the subjects of research. They are dependent on the miscibility of the fluids, on the diffusion rates of chemical components within the individual phases, and on the interfacial tension and rates of transport of the components across the interfaces between those phases. Despite the still-existing uncertainties about many of these questions, the remedy for oil production is fairly clear. If the mobility ratio is much greater than one in a flooding project, displacement efficiency will be improved by "mobility control techniques" - by decreasing the mobility of the displacing fluid. This rule of thumb applies strongly to CO₂ floods.

CO₂ is by now rather widely used for EOR, but because of the unfavorable

mobility ratio even against light crudes, early breakthrough of the injected CO_2 is common and the sweep efficiency is poor. These difficulties are quite evident in their effect on the foremost economic indicator - the number of thousand standard cubic feet of CO_2 which are injected per barrel of oil recovered. In a one-for-one displacement* this number would be between 2 and 3 MSCF/Bbl (depending on reservoir temperature and pressure), and the cost of the injected CO_2 would be an affordable fraction of the selling price of the oil. But if the figure were to exceed 10 or 15 MSCF/Bbl, the flood project could be too costly to operate. It is evident that a powerful incentive exists to improve the sweep efficiency of CO_2 floods.

E. Water Alternated with Gas

The only method which has up to now been used for mobility control in CO_2 field projects is one which was first proposed and utilized for gas and solvent floods, called WAG (as an abbreviation for Water Alternated with Gas).^{14,15} This method, by which water is injected either simultaneously or alternately with the CO_2 , has been used to decrease the average mobility of the injected solvent or gas. The effect is to reduce the rate of formation and growth of the flow non-uniformities. It results, of course, from the reduced relative permeability of the solvent consequent to the increase in average water saturation.^{16,17} But this same increase in water saturation, it has been suggested, will decrease the microscopic displacement efficiency. Thus while WAG can improve the macroscopic sweep pattern and delay breakthrough of the injected CO_2 , it may prevent effective extraction of oil from trapped globules that are surrounded by water. In order to retain the high microscopic displacement efficiency of a solvent or CO_2 flood, it is essential that all or most of the oil be accessible to the displacing fluid. Otherwise zones which appear, in a macroscopic view to be contacted by the solvent, will contain a significant fraction of trapped or un-mobilized oil after passage of the front.

The mobility control methods which have been emphasized in this project have, in contrast to WAG, attempted to maintain the CO_2 content of the displacing fluid as high as possible while simultaneously reducing its mobility. With high CO_2 content, the advancing front of displacing fluid can increase local CO_2 concentrations to a high level. It is expected that CO_2 can then reach and mobilize more of the isolated oil which would remain trapped in a higher water content displacement. The goal is to retain the high microscopic displacement efficiency observed in thin tube tests. If a high enough CO_2 saturation is reached behind the front, this goal might be attained even in tertiary floods in which water must be the initial fluid displaced. Two approaches have been investigated in the development of additives to decrease the mobility of predominately- CO_2 displacing fluids.

*Such a one-for-one displacement would be observed at the start of a hypothetical primary recovery flood in which the same reservoir volume of oil is produced as CO_2 is injected.

F. High-Pressure Dispersions of CO₂ in Water (or "Foams")

The first of these methods involves the use, as a displacing fluid, of an emulsion or "foam" in which the CO₂ is confined in bubbles or cells surrounded by water films chemically stabilized by a suitable surfactant.¹⁸ The aqueous phase is continuous, although the major constituent of the dispersion is dense CO₂ in accordance with the requirements stated above. While it is much less compressible, this high-pressure dispersion is similar to an ordinary foam formed at atmospheric pressure by gas and foamant-containing liquid. In particular, the "high-pressure foam" also shows a high apparent viscosity. Also like an ordinary foam, this dispersion does not persist for long without a stabilizing agent to prevent rapid coalescence of the non-aqueous cells. The required foamants should have similar characteristics in the two cases as well. Firstly they should be surface active so as to concentrate themselves at the surfaces of the aqueous films, and secondly, for long foam life, they should retard flow in those films.

As a foam decays, the films of the continuous phase become thinner as fluid drains out of them. Certain foamants are much more effective than others in impeding such flow by mechanisms which are not fully understood. Some sort of surface viscosity effects, which could be quite non-linear, must be involved.¹⁹ The latter stages of the thinning process can also be retarded by electrical forces between those surfactant molecules which are congregated at the opposite surfaces of the films. In a container that is large compared to the cell size of the foam, fluid drained from each of the films is collected in its boundary edges. These so-called Plateau boundaries form a network of channels by which the drained fluid is conducted toward the walls, or to a free fluid surface. In a porous medium one could expect, on the other hand, that this latter process could not proceed far, because the film boundaries would be continually changing as a result of the flow. In fact, forward flow of continuous phase through the pore system would be needed in order to maintain the fluid supply for the films. Anything which slowed down this process would then interfere with the propagation of a foam-like dispersion through rock. The property of high bulk viscosity, which tends to retard drainage through the Plateau network in a large container of air-water foam, might actually be detrimental in a mobility control "foam". There is, unfortunately, a lack of comprehensive or quantitative theory concerning both the fundamental processes which occur during the transport of foam-like dispersions through porous rock, and the detailed properties needed in such a dispersion for optimum mobility control. Consequently the development work being pursued in this project on mobility control "foams" is empirical, though based on the qualitative views of the situation presented above.

G. Direct Thickening of CO₂ by Polymers

The second CO₂-thickening method being investigated in the project is the direct solution of suitable polymers in the CO₂.²⁰ At the pressures required for efficient displacement of oil, the specific gravity of CO₂ is in

the range from .75 to .9 - about the same as that of the oil itself. This high density must be achieved to attain a high microscopic displacement efficiency, whether the temperature is below CO₂'s critical point of 88°F (when the gas can be liquified) or above it (when even high-density fluid cannot be called a liquid, but is referred to as a "dense gas"). In both of these states, the fluid is capable of dissolving certain chemicals. Our efforts have consisted in searching for and testing polymers which are soluble in CO₂ and could increase its viscosity. Our goal is to synthesize or to discover on the existing market one or more polymers which can produce a viscosity increase by a factor of ten to twenty, in low enough concentrations to be economically feasible.

H. Flow Tests

In conjunction with efforts towards the thickening of the CO₂ displacement fluid by the above two methods, a further need in this project is to test the behavior and effectiveness of the additives. These further tests utilize flood experiments in which oil is displaced from rock. The range of variation of rock and fluid types with which such tests could be conducted is so large as to preclude trials under all or most of these conditions. But a repeatable, standardized flooding test has been designed by which much of the needed information can be obtained. In this test, a synthetic oil is displaced from a dolomite rock by a CO₂ displacement fluid against a back pressure high enough to maintain CO₂ density in a range typical of field EOR projects. In addition to the usual measurements of produced fluid, which enable the overall efficiency of displacement in the rock sample to be calculated, the sample itself is highly instrumented. The additional instrumentation provides the facility for two further indications of displacement behavior. These are internal indicators, which reveal some detail of the mobility and saturation conditions in the body of the rock. One is of the pressure gradient along the core - which is measured by four pairs of pressure taps connected to differential pressure transducers. Divided into the Darcy velocity, these give a continuous and direct measure of the mobility, at four locations along the rock sample. The second indication is provided by a set of electrodes which allow the measurement of a profile of conductivity along the rock, at any time when the saturation of an electrically conducting fluid is not too low. The measurement of voltage drops from each voltage electrode to its adjacent neighbors, and across a standard resistor in series with the supply and the current electrodes at each end of the core, are made by a fast analog-to-digital converter (ADC) operated by a small computer. The same computer performs the necessary calculations to draw a "conductivity profile" of the rock.

I. Practical Considerations with Field Use of Mobility Control Agents

Motivating the development of mobility control methods is the need to

increase the macroscopic efficiency of displacement. Decreasing the mobility of the displacing fluid is the only known way to slow the growth of the frontal instabilities that magnify displacement non-uniformities and lead to early breakthrough and bypassed oil. The needed mobility decrease is to be attained here by thickening the CO₂. This goal seems achievable by either or both of the two classes of additives being developed in this project. But it is not too early to refer also to a potential difficulty with both of them - and with any foreseeable mobility control method.

The difficulty results from a simple fact - that the rate of oil production, in any constant-pressure flooding program, is proportional to the rate of injection of the displacing fluid. The use of a mobility control agent will require a greater injection pressure if a given rate is to be maintained. In many cases - particularly in CO₂ floods - the injection rate is limited primarily by the supply of fluid to be injected, and is not affected by thickening it or otherwise decreasing the mobility. Sometimes, however, the limit is set by the maximum pressure which can safely be applied at the input wells. In this latter situation the use of mobility control necessitates a decrease in injection and production rates. An economic compromise must then be struck between the rate of current production and the promise of greater displacement efficiency, with oil production extending further into the future.

The matter is raised here to emphasize an important secondary requirement in the application of mobility control. The degree of thickening attained by the mobility control agents should not be excessive. It is in fact highly desirable - and essential, in some cases - that the decrease in mobility should be independently and predictably variable by some positive control such as additive concentration. Then the reservoir engineer will have the opportunity to specify the extent of mobility control, in order to optimize a particular field project.

The objective of the above introductory remarks has been to present brief descriptions of the basis and some oilfield ramifications of the mobility control problem, and of the research tasks being performed in the project. The succeeding parts of this report will expand on the latter, paying special attention to the progress and problems experienced during the last year.

Summary of Progress

A. Foams

The objective of this section of the project has been to develop and test dispersions of CO₂ in surfactant/brine solutions. We presume in this work that the usefulness of the "high pressure foams" for mobility control will be determined by several properties:

1. They should display a relatively high apparent viscosity.

In direct measurements of flow in rock samples, a low mobility should be observed. This should be adjustable to some extent, so that it should be possible to formulate a "foam" with mobility in the range from 1/2 to 1/5 the mobility of water.

2. The aqueous phase should be continuous so that the CO₂ is present in disconnected bubbles or cells.
3. The aqueous phase should be present in low volume fraction.

These requirements are of course related - the literature shows that, in general, high apparent viscosities are characteristic of emulsions with low fractional content of the continuous phase.

Such is the case, for instance, in common low-pressure foams which have served as the model for the desired emulsion of dense CO₂ in brine. But these dispersions are not identical, and some differences are of significance to our goal. One such point is that air and water differ greatly in density. This affects the relative stability of the foam-like and the inverse emulsions. The latter consist of isolated droplets of the minor-volume-fraction phase suspended in the major constituent which is the continuous phase. In an air-water system, the relatively large density difference reduces the lifetimes of water droplets, and therefore of any inverse emulsion which may be present. This limitation does not prevent the stability of inverse emulsions in all situations, of course - water droplets can stay effectively suspended in air if they are sufficiently small or if the container* is large. But the density difference is not great between water and the dense CO₂ needed for displacement of oil, and consequently both types of emulsion might be expected to be simultaneously present in the mobility control "foam". It is of course possible that such a situation might be of some assistance in the displacement process. While the isolated droplets of surfactant-water, suspended in dense CO₂, would not be of much use in increasing apparent viscosity, they could be useful in providing the material to replace films broken or dangerously thinned during propagation of the dispersion.

Another difference between the required high pressure dispersion and common air or gas foams is a result of their relative compressibility in the range of absolute pressure of use. Low pressure, air-water foams can be expanded by a factor of more than ten by a pressure decrease of less than 200 psi. This can be of major significance both in the generation of the foam, and in increasing the "quality" or volume fraction of the discontinuous component. A much smaller fractional expansion would take place as a result of this pressure change in a CO₂-water dispersion at reservoir pressures. However, the difference might be of considerable importance in laboratory simulation of the flow of mobility control foam in porous media.

With this background, the generation of "mobility control foams" in laboratory or field can be discussed. The generation process involves more

*Such a large "container" might be a layer of the earth's atmosphere, in which the persistence of clouds is also extended by upward convection currents.

than simply the application of a suitable quantity of energy to a mixture of dense CO₂ with the surfactant-water mixture. The energy required to produce the interfacial surface per unit volume of foam is in fact relatively modest. It is of the order of magnitude of five or ten times the interfacial tension divided by the radius of the average bubbles or cells contained in it. Thus the generation process does not seem to be limited by the energy available except in quiescent situations, and the lowering of the interfacial tension cannot be the only function of the surfactant.

It is the manner in which this energy is applied that determines its effectiveness in producing the desired type of emulsion. High pressure dispersions or "mobility control foams" may be produced by many of the same methods which have been successfully applied at atmospheric pressure for common gas-liquid foams.* One way which has not been tried in this project, but might be quite effective, is an analog of the Waring blender method, such as has been used as a screening technique by Patton, et al.²¹ Liquified or dense-gas CO₂ would replace atmospheric-pressure air in the upper portion of a high-pressure mixing chamber. The lower part of the chamber would contain the aqueous phase which would cover a submerged high speed, rotating mixing blade. A foam-like dispersion would then be produced as CO₂ was drawn down into the water and broken up into bubbles. Relatively simple plumbing could convert the dispersion production from a batch into a continuous process. Of course some cut-and-try redesign of the propeller blade and other features might be necessary to compensate for the decreased density difference between the fluid components.

A method which has been used and reported in the literature is the in situ process. In this method, the aqueous phase and the CO₂ are simultaneously or alternately injected into a section of porous and permeable material.¹⁸ This can be either the rock to be tested or a specially constructed bead or sand pack.

In the New Mexico Tech Mobility Control project, foams have been generated using a method somewhat similar to the separate-porous-pack version of the above. In this case a fritted stainless steel disk, a simple stainless-steel screen, or a stack of two or three screens is used instead of a bead pack. This method also is modelled after one which has been successfully used for the production of atmospheric pressure foams. In this high pressure system, surfactant solution is introduced above the screen, and the CO₂ below. The dense CO₂ is formed into bubbles of fairly regular size as it passes upward out of the screens or frit into the water. The method is operated as a continuous process, with foam emerging from the top of the high pressure generation chamber as the constituent fluids are pumped into their separate entry ports below. This method was shown and discussed in the First Annual Report, and it was evaluated in auxiliary experiments early in 1981, in which its product was pumped through a short core, and thence through a

*One important and familiar exception springs to mind. A classic way of generating gas-water foams is by conducting to the atmosphere, from a pressurized container, a stream of surfactant-laden liquid saturated with gas at high pressure. The resulting expansion to atmospheric pressure of (possibly pre-nucleated) gas bubbles produces a low liquid fraction foam. This method can't be used in our case; no such large expansion ratio is available.

back-pressure regulator to the atmosphere. The system also contained a high-pressure capillary tube sight glass for visual examination of the dispersion, upstream of the rock. These experiments utilized liquified CO_2 at room temperature, and water solutions of the surfactant CD 128.

Although foams were produced at the higher rates, they were difficult to control and the apparatus did not operate consistently at the low total rates (of CO_2 plus surfactant - water) which were deemed necessary for the main core test experiments. The operation of these auxiliary experiments also exposed several other problems with the high-pressure flow system. These difficulties centered around the contamination of the system and the plugging of part of it by fine particles resulting both from corrosion and from detachment of particles from the rock sample itself. Modification of the apparatus to correct these problems made it temporarily unavailable for further testing of the static foam generator.

The experiences also showed the need for some changes in the foam generator. Because of its disappointing behavior at low flow rates, an active energy source or mixer seemed necessary inside the chamber. At the same time, it had been observed that the fritted disks gave rise to intermittent operation that was difficult to control. Consequently, a new foam generator was designed. The flow routes were similar to those in the earlier model, but the new model was constructed of a non-magnetic stainless steel, and contained a magnetic stir-bar which rested directly on the screen. This could be turned by an external rotating field by mounting the chamber on a commercial magnetic stirring table. A cross-sectional schematic is shown in Figure 1.

During the preliminary foam generation experiments conducted previously, we also learned that operation at high pressure was quite expensive in terms of time. It was therefore decided that a set of low pressure experiments would be valuable to check out the new, "active foam generator". The purpose of these would be to determine procedures of use, and the operating regions of total rate and of rate ratio. The magnetic spin-bar would hopefully fulfill its design function and make possible the production of foam at low total rates. In these low-pressure experiments, isooctane was used to simulate dense CO_2 , in order to minimize artifacts from density and compressibility differences. To examine the produced high-density foam, a high-pressure, flat-windowed observation cell had been constructed. This was used in the low-pressure experiments also, with a low-power microscope to observe and photograph the dispersion for uniformity, shape and size of bubble-cells, and to verify the relative absence of inverse emulsion.

A schematic diagram of these foam generation tests is shown in Figure 2, and a photomicrograph of a produced foam-like dispersion is shown in Figure 3. (Surfactant used here was ADFA, at 10% in distilled water. Relative aqueous solution flow rate was 6.7%). The effects of changing screen size (from tightly woven 80 x 700 to open square, 100 x 100 mesh), total fluid rate, and rate fraction of the aqueous component were tested. The latter number is also the volumetric fraction during times when the entire output of the generator is foam. In all of the tests, the magnetic spin table was run at its maximum rate, and rotation of the spin bar was verified by its sound.

A further advantage of low-pressure simulation, with isooctane used in

place of high density CO₂, has been that the product emulsion is available for examination and collection under ambient conditions. This has proved especially useful in observing the effect of screen size variation. Not surprisingly, finer mesh screens produce smaller-cell emulsions. It is also qualitatively evident from their behavior while emerging from a tube, that the foam-like emulsions composed of these smaller cells have a greater apparent viscosity. In consequence of this observation, and in accord with the need to avoid excessive thickening, the foam generator will be operated with the coarser screens.

Five surfactants, which are described as "good foamers" by McCutcheon,²² are referred to in Table 1. They have been tested in the low-pressure foam generation experiments and are listed in order of the stability of the produced dispersions. Also noted was some variation in the range of fractional aqueous phase concentration over which the "foams" can be produced. Experiments to explore this range more fully have not yet been completed. Because it is strongly felt that microscopic recovery efficiency would be strongly degraded by excessive water content, however, the lower end of this range will be pursued even if surfactant concentration in the water phase must be increased. The foams listed in the table were all produced with 10% surfactant concentration in the water. A foam with 10% aqueous phase in which surfactant concentration is 10% would cost about the same as a 5% foam in which surfactant concentration in the water is 20%. Yet the latter would presumably be a more effective mobility control agent because, with less aqueous phase content, it would allow the CO₂ to contact more of the residual oil.

B. Direct Thickening

Two early publications by Francis^{23,24} discuss liquid miscibilities, and show many phase diagrams of liquid CO₂ with various organic liquids. Not a great deal has been published, though, about the kind of high molecular weight chemicals which might be soluble either in liquified or in dense, supercritical CO₂. No information is available about the viscosity of such solutions. In fact, some doubt had been expressed as to whether it was possible for any solid or liquid material at all to be dissolved in a gas, no matter what its density. But molecular-scale mixtures of evaporated liquids or sublimated solids with even low density gas are facts of common experience. Recently the dissolving power of supercritical CO₂ and other gases has been examined microanalytically by Stahl et al.²⁵ Knowing no fundamental reason such mixtures could not exist at higher concentration and at high pressure, a search was commenced - at first merely for polymers likely to be soluble in CO₂.

Preliminary experiments were performed at low pressure, in which carbon disulfide (CS₂) was used to simulate dense CO₂. It was reasoned that because of the similarity of the molecules (both being isoelectronic), CS₂ would be a reasonable screening or test solvent. It was rapidly found that the common water-soluble polymers, already known or in use in EOR operations, would not dissolve in CS₂. Different polymers were found, though, which were soluble, although with no striking increase in the CS₂'s viscosity.

An apparatus designed to enable the experimenter to measure the solubilities of these and other polymers in high-pressure CO₂ (pictured and briefly described in the First Annual Report) has been perfected and brought into routine operation. The operating version of this device is shown in Figures 4, 5, and 6. The latter two are detailed drawings of the sapphire tube mixing chamber and of the assay chamber.

In operation, a polymer sample is placed in the mixing chamber. After evacuation of air from the apparatus, it is pressurized with CO₂ from the constant displacement pump, up to that required for the test. A mixing assembly consisting of a commercial teflon-covered magnetic stir-bar, together with a machined steel lower extension, is manipulated vertically by use of an external permanent magnet. The lower part of the steel mixing extension has protrusions which can fit into the annulus surrounding the inlet tube at the lower end of the mixing chamber. The up-and-down motion of the mixing assembly is then able to stir the undissolved polymer which settles into the annulus. After enough stirring to produce a saturated solution at the given pressure and temperature, the external magnet is clamped into a holding position, so the mixing assembly is held midway up the tube. Any undissolved polymer is then allowed to settle into the annulus, leaving only clear solution in the tube above it.

At this point the positive displacement pump is used again to force a known amount (about 2.9 ml) of this solution out of the mixing chamber and over into the lower end of the assay tube. (The entire assay chamber had previously been pressurized with Nitrogen gas, at the same pressure as the CO₂ in the mixing chamber. Thus the transfer of the small quantity of dense CO₂/polymer solution is not accompanied by any decrease in pressure.) When the transfer is complete, the valve from the mixing chamber is closed, and the nitrogen gas slowly bled off to the atmosphere from around the test tube. As the pressure decreases and CO₂ evaporates, the polymer condenses out of solution onto the glass beads in the lower part of the test tube. When pressure in the assay chamber has decreased to atmospheric, it is disassembled and the test tube weighed to determine how much polymer has been dissolved in the transferred volume of CO₂. Further verification is available by extracting the glass beads in a conventional solvent for IR or other analysis.

It has become apparent that CS₂ was a good choice for a preliminary test fluid. Many polymers which are soluble in CS₂ or in light hydrocarbons are soluble in dense CO₂. About two dozen polymers have been tested - of which more than half showed solubility in the parts-per-thousand range or greater. Although no final criteria have been established, it is apparent that in addition to the density of the CO₂, several properties of the polymer are important in determining its solubility. Among these are the structure, the molecular weight and the tacticity. A list of various polymers together with some of their properties, their solubilities in CO₂, and the temperatures and pressures of the tests, are given in Table 2a, b and c.

With the successful measurement of polymer solubilities in dense CO₂, the determination of the viscosities of these solutions became of vital importance before consideration could be given to their use as direct mobility control additives. Although there are no commercial instruments known which could be used for the measurements of these viscosities at high

pressure, two possibilities for the tests exist here at PRRC. Both are under development.

One of these methods has been used by Dr. Dwain Diller and his colleagues at the National Bureau of Standards in Boulder, Colorado, to measure the viscosities of condensed pure gases. It uses a torsionally oscillating, rod-shaped quartz crystal. Damping of the oscillation is proportional to the square root of the product of viscosity and density. Work is going on in the companion DOE project here at New Mexico's PRRC, directed by Dr. F.M. Orr, Jr., to adapt the technique to a high-pressure, low fluid volume, flow-through cell.

A second method is being pursued in this project, and consists of a modification in the solubility-measuring apparatus described above. The modification makes it possible to measure the time of fall of a smooth cylinder substituted for the teflon-covered stir bar in its sapphire mixing chamber tube. A U section plastic insert, containing two light source-photo diode pairs, can be fixed in place against the sapphire tube. Electronic amplification of the photo-diode's signals provides start and stop pulses for a commercial high speed counter, the Intersil 7226. Schematic diagrams of the electronics are shown in Figures 7 and 8.

The fall of a cylinder in a concentric tube has previously been used in viscometry.²⁶ There is a feature here, however, which renders the present use unique. Because of the shortness of the available sample tube, and because it is not feasible to increase the viscous drag by using a very close-fitting cylinder (this in turn is because the single-crystal sapphire tube is not precisely cylindrical) the fall velocity is not independent of time. The falling cylinder does not (for all fluids) reach its terminal velocity by the time it passes the first (or sometimes even the second) observing station. In these cases the cylinder is accelerated during its fall, and the measured time is not simply proportional to the fluid viscosity.

Consequently, there is no simple "viscometer constant" which can be multiplied by any fall time to give the viscosity of the fluid in the tube. A mathematical analysis of the motion is presented in Appendix A. There, it is shown that the fall of the cylinder is describable by two quantities. The first of these is the terminal velocity U , and the second is the characteristic time T_c for the exponential decay of the acceleration. If the tube is long enough, or the fluid viscous enough for the fall time to be large compared to T_c , then the acceleration may be ignored. It is only then that the use of a single "viscometer constant" becomes a good approximation. Both U and T_c are inversely proportional to the fluid viscosity. They also depend on the fluid density, on the average density of the cylinder, and on the radii of the cylinder and tube. These relationships make it possible to compute a table of "acceleration correction times" to be subtracted from the measured time of fall. The viscosity may then be calculated as the product of the "corrected fall time" by a constant C . For greater fall times, the acceleration correction time becomes quite small, and the computation reduces to the simple case. Unfortunately the values of the "correction times" are characteristic for the dimensions of a particular instrument. (They are especially dependent on the ratio of tube-to-cylinder radii, and on the location of the observing stations below the release point of the cylinder.)

Thus the correction table calculated for any given viscometer will not be valid for a different instrument. Details on the computation of these tables are also given in the appendix.

Plans for the immediate future in this phase of the project are to measure the viscosities of a number of different solutions of various polymers in CO₂, and also to continue the determination of solubilities of new polymers. Most of the polymers we have found to be soluble in CO₂, dissolve also in light hydrocarbon solvents. We anticipate experimenting with the joint solution (formed by mixing into the CO₂ a near-saturated solution of polymer in such a solvent). This will require a slight further modification in our apparatus, to enable introduction of liquid, high vapor pressure samples. This modification, however, will enable us to look at more materials of possible use in the oilfield.

A direct-thickening polymer could be applied simply in CO₂ floods by injection from a separate metering pump directly into the well head or into a mixing chamber connected to it, during CO₂ injection. If the pure polymer were available only in solid form, it would be most economic to have made up for injection a solution of the polymer in a light hydrocarbon solvent. As in the laboratory situation, the use of such an auxiliary solvent would hasten dispersion and the attainment of a homogeneous mixture of the polymer into the CO₂. The hydrocarbon solvent itself would probably not have much effect on the displacement efficiency, but (if anything) might improve total recovery by decreasing the pressure required, and thus extending somewhat further into the reservoir the region in which high microscopic efficiency is attained.

C. General Description of Core Flooding Tests

The purpose of the laboratory work discussed here is to assess the EOR utility of the mobility control additives and procedures developed elsewhere in the project. This assessment is intended to test in the laboratory the same characteristics which will determine the effectiveness of the agents in the field. The core flooding tests are thus designed to give information not only about the overall efficiency with which oil is displaced from a relatively small test core, but also about the uniformity of the displacement.

The "core sample" was cut from a slab of quarried dolomite.²⁷ It is rectangular in cross section 1.93 x 2.01 inches (4.9 x 5.1 cm) and 29.88 inches long (75.8 cm). Despite the sample's rather uniform and featureless appearance, like most limestones it contains permeability and porosity heterogeneities. The high mobility ratio of unprotected CO₂ displacements can be expected to accentuate the flow rate non-uniformities which occur even in M = 1 floods in this rock. The resulting production curve, when CO₂ is injected in a tertiary-type flood, will probably show early breakthrough and very little oil recovery. This rock sample, then, should demonstrate the ability of mobility control additives to improve the displacement pattern. Both the amount of delay of CO₂ breakthrough and the increase in oil recovery

can be taken as measures of the usefulness of an additive, and of the likelihood it can work a similar improvement in the reservoir's performance.

Nevertheless the rock sample is not in fact a complete oil reservoir-or even part of one. The numerical results from the laboratory measurement of displacement efficiency are not really direct predictions of reservoir behavior. After all, the reservoir is complicated by its own special 3-dimensional geometry, heterogeneities and well layout - to mention only a few of its points of distinction. Thus it would be useful to the reservoir engineer to obtain some more general information, from a core flood, about the influence of the additive on the laboratory displacement.

To provide such additional information, the project's core-flooding tests were made somewhat more complex. To enable the direct and continuous evaluation of mobility (the ratio of flow rate to pressure drop) during the displacement, one of the zero-flow boundaries along the side of the core was pierced for four pairs of pressure taps. With a differential pressure transducer connected to each of the pairs, pressure gradients can be measured at these locations along the core. These results can be interpreted directly to give the mobility changes to be expected in a reservoir with the use of the particular mobility control agent.

A second complicating addition to the more standard core flooding test is a set of electrodes by which the changing electrical conductivity of the core can be measured. These measurements are made rapidly and at many locations along the flow direction. The local core conductivity is related to the rock texture, and also to both the ionic concentration and the saturation of the aqueous fluid present in the rock's pores. In the absence of firm information on the ion concentration, the data cannot be directly interpreted to give the saturation. The major purpose during the CO₂ floods, though, is to show a qualitative picture of the variation due to displacement, as an independent indication of the effect of the mobility control agent.

Before starting the descriptions of progress in the various sub-tasks of the core flooding tests, it may be valuable to mention a few operational points, representing decisions which have been made about the conduct of the tests. First, these tests will ordinarily be of tertiary-type floods. The general preparation of the core prior to each of them will be:

- 1) Cleaning, by light hydrocarbon and alcohol floods - using enough fluid to dissolve all brine, oil and surfactant from former tests.
- 2) Brine saturation, by miscible displacement of the alcohol. This will also remove any excess salt left by the previous brine and not dissolved by the alcohol.
- 3) Oil saturation, by displacement of the brine.
- 4) Resaturation with brine, by displacement of the oil.

This procedure will leave a residual oil saturation, probably in the range of 25 to 40%, which will be the target for both unprotected and mobility-controlled CO₂ floods.

The next questions concern the fluids to use - particularly the oil - and the flow rates at which to operate the displacements. In order to be able to have repetitive, comparable tests, it is necessary to return the core to the same condition at the end of each test by flooding with a mild solvent that has no effect on the epoxy side boundaries. This rules out the use of crude oil, because its heavy components could not be cleaned from the rock without more powerful solvents. Presumably though, the restriction will not detract from the value of the mobility control tests. For these tests, crude will be simulated by a synthetic oil mixture of 90% Soltrol 130* and 10% Paraffin oil.** Tests of chemical compatibility of mobility control agents with crude will in any case have to be run with the particular oils, at a later stage of testing.

The choice of brines is not so critical, since it can be made anew for each run. Test displacements so far have been made with 0.1% NaCl by weight in distilled water. The influence of different ions, and of brine concentration on particular foamants may also be best determined in separate tests.

The auxiliary displacements during the different stages of core cleaning described above can in general be performed as rapidly as possible consistent with the needs:

- 1) To avoid too high a pressure drop.
- 2) In immiscible floods, to keep the capillary number below the range at which isolated blobs of residual phase start being displaced.
- 3) In miscible floods, to provide enough time for diffusion to transfer material out of the more isolated or "dead end" pores into channels where flow is at a higher rate.

The CO₂ floods themselves should be performed at near nominal reservoir rate of one foot per day. Lower displacement efficiency may be expected at higher rates, if the criterion #3 above is violated.

D. Specific Progress and Problems

1. Core Mounting

The work of cutting, coating and otherwise preparing the rock sample was completed early in the year. The chief requirements were the need for high pressure operation of the flow tests with CO₂. The core mounting

*Soltrol is a proprietary core test fluid sold by Phillips Petroleum Company.

**Anderson Laboratories "BANCO" standard paraffin oil, Saybolt viscosity 180-190 at 100°F. IC# 46980.

procedure was also designed to be consistent with the decision to make both electrical and pressure measurements at intermediate locations along the core. The flow was confined and made to be macroscopically one dimensional by a coat of epoxy resin* on the sides. Fluid access to the ends of the core is through Lucite** end plates in which distribution channels were machined. Also pressed against the ends are full cross-sectional-area current electrodes made of squares of gold-plated, 100 mesh stainless steel screen. The end plates and current electrodes were secured with fiberglass strips and another coat of epoxy. Down one side of the core, at a spacing of 0.26 inches (.6604 cm) are embedded 115 gold-plated pins to serve as voltage electrodes. These were each sealed into a hole drilled through the epoxy into the core. Eleven more electrodes, called the asymmetry electrodes, are located on two other sides of the rock sample. Along the fourth side of the core are eight pressure taps - holes drilled through the epoxy into the rock, in which were sealed 1/16 inch (.159 cm) stainless steel tubes. The locations of all electrodes and pressure taps on the sides of the core are shown in Figure 9. Also sealed onto the sides of the epoxy-coated core were a number of brass "feet" to support the rock sample in its high-pressure container during horizontal flow, and to make it easy to slide the rock into the tube without damage.

2. The "Overburden" System

"Sleeve" or "overburden" pressurization is required to protect the epoxy coating on the sides of the rock sample from the high pressure within it, especially during CO₂ floods. The system is complete and operational. The high-pressure container is a 5 inch outside diameter steel pipe with 4 inch inside diameter. The annular region between the pipe and the epoxy-coated core sample is filled with oil.*** This oil is pressurized by an auxiliary high-pressure pump**** which is switched automatically by an electronic circuit, to keep the "sleeve" or annular pressure above the input flowing pressure by an adjustable "pressure margin". The analog circuit to accomplish this, shown in Figure 10, takes its input from two pressure transducers and operates a solid state switch to control the pump.

The high-pressure container is closed at one end with a threaded-on cap through which passes the fluid input connection to the core. Two sleeve-oil connections are also made through the end cap. The other end of the high-pressure container is closed with an end plate bolted to a 7-1/4 inch OD flange welded onto the pipe. A flange closure is used at this end to permit eight connection tubes from the pressure taps, as well as the centrally located fluid output connections, to pass through the pressure wall. In addition, a large piece of printed circuit board with 128 radial connectors

*Emerson and Cuming Eccobond 285, with catalyst 9 at 3.4 wt. percent.

**Dupont trademark for polymerized methyl methacrylate resin.

***For this purpose, a (mechanical) vacuum pump oil is used, for its fairly high viscosity and very low content of low boiling components.

****This auxiliary pump is an Eldex series B-100-S rated at a maximum flow rate of 480 ml/hour at 5,000 psig. This is a single piston, positive displacement pump commonly used in High-Pressure Liquid Chromatography.

is held between O-rings in both the flange and the end-plate. The function of these printed connections is to carry out the electrical signals from the voltage electrodes on the sides of the rock sample. These connectors lead to the multiplex switching circuits mounted on the part of the circuit board outside of the pressure vessel.

Several sudden sleeve-pressure-release accidents, resulting from failure of one or another of the seals, have caused local breaks in the epoxy coating of the rock sample during initial assembly and testing. These have all been repaired, and procedures worked out to avoid the same kind of mishaps in the future. The fluid pumping and sleeve pressure systems are both in operating condition, although they have not yet been tested to the maximum pressure desired (2,600 psi). Some accidental saturation of heavy vacuum pump oil from the sleeve system has not yet been cleaned out of the rock.

3. The Primary Fluid System

Three types of CO₂ floods are planned under various input conditions. The three are:

- 1) "Unprotected CO₂ Floods", in which liquid or supercritical CO₂ is injected directly into the core from a single Ruska Pump with 1,000 ml cylinder capacity.
- 2) "Mobility Control by Foam" floods, in which CO₂ will be pumped from one Ruska pump, and surfactant/brine will be discharged from a monel transfer cylinder into which oil is pumped from a second Ruska pump. The two cylinders on the Ruska pump cart are powered independently. A high-pressure dispersion of CO₂ in surfactant/brine will be formed in a foam generator through which the fluids pass on their way to the core.
- 3) "Mobility Control by Direct Thickening" floods, in which a batch of solution of an appropriate polymer in liquid CO₂ is made up in the cylinder of one Ruska pump, and discharged directly into the core for the flood.

For the auxiliary displacements in which the core is cleaned and prepared for later tests, an Eldex positive displacement pump is used for fluid input to the core. Fluid intake to such pumps is through a fritted stainless steel filter cylinder immersed in the input fluid. This auxiliary pump has given some trouble with erratic operation, apparently because of leaking piston seal and check valves. Consequently the pump rate has been uncertain during many of the auxiliary displacements which have been performed. New seals and valves have now been installed and more consistent service is anticipated. Other elements of the flow system are an electronic back pressure regulator* (BPR), a particle filter to protect it, and a hot

*The BPR is modelled after one developed at PRRC in an earlier DOE/New Mexico EMD project, "Displacement of Oil by Carbon Dioxide."

water bath to keep it from freezing. Appropriate collectors for measuring gas and liquid output are also required parts of the system.

4. Pressure Measurement

This system is complete and operational. Several different transducers are used to monitor operating pressures, and Bourdon-type mechanical gauges are used as back-ups in several critical locations. For standardization purposes, most of the transducers are of a single type* except for two used in special situations. Greater precision is needed for measurements of the output pressure, since this signal is used also by the BPR. A capacitance-type gauge** of greater stability is therefore used to measure the output pressure from the core. Because the sleeve pressure does not need to be known to as high a precision, a less expensive, silicon strain gauge transducer*** was used in this application.

The four differential pressure transducers connected to the pressure tape in the side of the core are of the standard Validyne variable reluctance type. Some difficulties have been experienced with them in this application due to the larger-than-expected "hydraulic capacitance." This quantity, a direct analog of electrical capacitance, measures the volume of fluid which must be forced into the transducer to cause its reading to increase by one unit of pressure. It can be denoted by C_H and expressed in units of cc/psi. Unfortunately, this characteristic of a pressure gauge is not generally specified in the data furnished by the manufacturer. More unfortunately still, the investigator did not anticipate that C_H would be large enough to cause trouble with the sensitive diaphragms**** which had been selected. The trouble experienced is in slow response. If the fluid path to the transducer has a total "hydraulic resistance" (another electrical analogy) of R_H , in units of psi sec/cc, then a time constant of $R_H C_H$ will be involved in the response of the transducers to a changing pressure. Specifically, if an instantaneous change of pressure were to occur in the core, the transducer reading would approach its eventual value along an exponential curve. The reading error would be decreased by the factor e ($= 2.71\dots$) in each successive time interval of $R_H C_H$ sec. Measurements of the rates of change of the four transducer readings indicated the time constants were in the range of 30 to 90 sec. These are long enough to increase significantly the uncertainty in dynamic measurements of mobility change with passage of displacement fronts.

Stiffer diaphragms in the transducers would reduce C_H but would also decrease the sensitivity and resolution in the same proportion. As a compromise, a factor of four was judged to be reasonable, and ± 5 psi diaphragms have now been installed.

*Validyne type DP-15 differential pressure transducer, which has a replaceable diaphragm.

**Setra type 304.

***Foxboro type L-100.

**** ± 1.25 psi for full-scale reading.

5. Computer Monitoring

Automatic data acquisition is achieved by use of a dedicated TERA microcomputer which operates under the PASCAL software system. A 16-channel analog to digital converter (ADC) and a 16-bit digital input-output circuit (DIO) have been installed in the computer to enable recognition of electrical signals from the experimental apparatus. This system is also complete and in operation. With appropriate programs, the computer monitors pressure signals from the input and output, from the sleeve system and also from the four differential pressure transducers. It is also able to control measuring current flow and calculate conductivity from the voltages measured at the electrodes. Appendix B lists several of these programs, and in Appendix C are given some examples of data taken during some preliminary measurements and displacements. As an example, Appendix B-1 is a listing of the calibration program for the differential pressure transducers. For this, the four gauges are connected to two common manifolds to which are connected flexible transparent tubes. With the system filled with a test fluid, the interface in one of the transparent tubes is raised in steps to different heights above the interface level in the tube from the other manifold. For each pressure step the computer makes a number of readings, and at the conclusion of the readings it calculates least-squares straight line approximations for the pressure-voltage calibration of each gauge. Appendix C-1 shows the output from this program - in this case, recent data after the stiffer diaphragms referred to above were installed in the transducers.

A computer program used during operation of the auxiliary displacements is listed in Appendix B-2. This program, of filename DEL2, displays input and output pressures on the computer's monitor screen and also prints a record of these (at less frequent intervals) along with the date and time. When initiated, the program calls on the operator to enter the starting date and time. Subsequently, it monitors the "pressure margin" between the "sleeve" pressure and the input pressure to the core, and sounds an alarm if the value of the margin sinks below a preset limit.

6. Conductivity Measurement

This sub-system, which has been complete and operational since August 1981, makes possible the measurement of average conductivity in each of 114 "slices" of the rock. These volume regions are of the cross-sectional size of the core, and a thickness of .26 inches. To gauge the conductivity, current is passed from end to end of the rock, using the screen-wire current electrodes described above. During the passage of the current, the ohmic potential drop between a selected, adjacent pair of voltage electrodes along the side of the core is measured, using a high input impedance instrumentation amplifier whose output is sent to the computer. Voltage drop is also measured across a standard resistor in series with the rock, and then the current is reversed and the measurements made again. A conductivity ratio is calculated from

$$CR = (SRA - SRB) / (CA - CB)$$

where SRA and SRB are the voltages measured across the standard resistor during the two current directions, and CA and CB are the voltages across the particular electrode pair. The average conductivity of the rock within the boundaries of the "slice" defined by the electrodes is then

$$C = L \cdot CR / A \cdot R_{stan}$$

Here, L is the distance between the voltage electrodes measured, A is the cross-sectional area, and R_{stan} is the value of the standard resistance in ohms. If L and A respectively are expressed in meters and in square meters, C will be in siemens/meter.

The particular pair of voltage electrodes which is selected is determined by an array of electronic switches, a multiplexor to which an address is sent by the DIO circuit card of the computer. The analog multiplexor, the instrumentation amplifier and the circuits controlling the measuring current (the schematics of which are shown in Figures 11-15), are wire-wrapped onto four small cards. These are mounted on the corner areas of the large printed circuit board that is held between the flange and endplate of the core-holding pressure vessel, and on which are printed 128 radial electrical connections. In the controlling program each successive, adjacent pair is selected in sequence for a conductivity measurement. The collection of all of these is referred to as a "conductivity profile" of the core, and can be displayed on the printed record as a small graph. A program by which the computer performs all these steps is listed in Appendix B-3. In operation, the measurements and calculations for a complete conductivity profile are made in somewhat less than a second.

7. A Miscible Displacement

As a test of the operation and resolution of both the pressure monitoring and conductivity measurement systems, a miscible displacement of one brine by another was performed. During the displacement, periodic conductivity profiles were taken in the manner discussed above. An initial core saturation of 0.1% NaCl brine was displaced with 0.02% brine. A special program combined the monitoring of pressures with the measurement of conductivity profiles. Input from an auxiliary keyboard was also used to make possible changes in program operation. By this means, during the early phase of the experiment, before the fluid input was switched to the displacing fluid, several conductivity profiles were taken and averaged. When the lower conductivity brine was introduced, the mode of program operation was changed. From this time, each new conductivity profile was compared, point by point, with the average that had been made with the original brine. The graph printed out presented these ratios of conductivity, and effectively showed the distribution of concentrations inside the core. Selected sections of the data print-out is reproduced in Appendix C-2.

Analysis of the successive concentration profiles gives data to calculate an average dispersion coefficient for this displacement. Using the well-known formula for the thickness of a front between the 10% to the 90% iso-concentration surfaces,

$$\Delta x = 3.62\sqrt{Dt}$$

where Δx = front thickness in direction of flow, cm.

D = dispersion coefficient, cm^2/sec .

t = time, sec.

a dispersion coefficient , may be calculated as $0.0058 \text{ cm}^2/\text{sec}$. The average displacement velocity during this experiment was $0.044 \text{ cm}/\text{sec}$.

E. Project Plans

There is little doubt that a significant fraction of future project effort will probably be spent on maintenance and unforeseen-but-necessary modifications. It is anticipated, though, that this fraction will be small, since all major apparatus and instrumentation is in place and operational. The object of this section is to recapitulate in more detail plans for the remaining laboratory and other work of the project. The latter includes those steps which must be taken to enable oilfield operators to make use of the product of our research with the least delay.

Under the heading of "foams" for mobility control, we have made some preliminary tests on several surfactants and are encouraged by the response of four or five of them. After completion of several more low pressure, rate-and-concentration-defining experiments in which isooctane is used to simulate dense CO_2 , we plan to return immediately to high-pressure tests. It is anticipated that a minimum number of these CO_2 tests will be required to verify information gained in the simulation experiments. They will make it possible to plan the details of a number of core-flooding tests in which these "foamant" additives are used in low water-content, aqueous phase continuous, mobility controlled displacements.

The other group of possible mobility control additives are the "direct thickeners" which are intended to be used in CO_2 floods without added water. They are generally hydrocarbon-based polymers which are soluble in dense CO_2 and which increase its viscosity directly. More than two dozen chemicals have been tested for solubility in CO_2 at high pressure, with about half of them showing a significant amount, in the parts-per-thousand range or more. These tests will continue as new candidate polymers are encountered. However, it is also necessary to measure the viscosity of the high-pressure solutions. This can be done in the same apparatus, using techniques which have already been developed. Viscosity increases by a factor of ten to

twenty are probably required. Unfortunately, some uncertainty about the usefulness of particular polymer solutions will remain even after the viscosity tests. This is because the increased viscosity generated by polymer solution is frequently not Newtonian. This pessimistic view is of course based only on industry experience with water-soluble polymers. The increase observed in our viscometer may not be the same as that which will be effective during flow of the solution through porous rock. Core flow tests are thus also a necessity to determine the effectiveness of direct thickening additives.

Both of the types of mobility control additives will be tested by tertiary core floods in a dolomite rock sample. It is expected that the core can be cleaned and returned to the same condition prior to each such test. The sample is enclosed in a high-pressure container to make it possible to run these floods at moderate reservoir conditions of temperature and pressure. It is also instrumented in ways described above so that significant data can be gathered on the effect of the additives. In particular, direct measurements of the mobility - the ratio of flow rate to pressure drop - can be made at four locations along the rock. These measurements, and the change in them as the flood progresses, should provide direct and convincing evidence of the usefulness of the mobility control additives being developed.

Acknowledgement

Work on this project has been performed by many staff members of the Petroleum Recovery Research Center, and students at the New Mexico Institute of Mining and Technology. Most of the work on CO₂ solubility has been done by Dr. Dileep Dandge. Consultation with him and with the principal investigators in this area has been performed by Dr. L. Guy Donaruma throughout most of the year. Dr. Melvin Hatch has also served in this capacity.

The great burden of construction, maintenance and operation of the diverse kinds of apparatus assembled for this research, has fallen on James McLemore, Andrew Rosenthal, and Susan Weber. Consultants on design of electronic instrumentation have been Prof. Edwin Szymanski and student Brent Gordon, who was also involved in construction and maintenance of that equipment. Other students who have rendered assistance are Nick Valdivia, David Goranson, and Alex Miller. This and other reports of the project could not have been prepared without the aid of Ann Irby.

VISCOSITY MEASUREMENT BY FALL TIME OF A CYLINDER IN A TUBE

Introduction

This note describes the use of a method of viscosity measurement which, though not well adapted to all situations, does have application in some special cases. It is useful for the measurement of viscosities of compressed or liquified gases -- where the pressure is above ambient and where no interface is available by which the flow of a standard volume can be detected. Briefly, the measurement procedure is as follows. The fluid sample is contained in a vertical, transparent tube. A cylindrical magnet which fits more or less closely in the tube, is raised, by an external magnetic field, to an upper stop in the tube and then released. The time of fall between two observation stations is then measured. This fall time depends not only on the viscosity of the fluid filling the sample space, but also on its density and on the density of the falling cylinder, on the ratio of cylinder diameter to the tube's inner diameter and on the position of the observing stations. For very viscous fluids, the latter dependence will be simply on the vertical distance between the two stations. But for low viscosity fluids, the cylinder does not attain its terminal velocity by the time it passes the first--or perhaps even the second--station. In that event the acceleration of the cylinder, during its fall, leads to a non-linear relation between the fall time and the viscosity.

The first two parts of the discussion below are mathematical and computational. They are concerned with an idealization of the above described viscometer with the goal of deriving the numerical relationship between the fall time and the viscosity while making proper allowance for all of the factors mentioned. The third part deals with a realization of the device which can be used for viscosity measurements of solutions of various polymers which may be of possible use in Enhanced Oil Recovery, in liquid and in supercritical CO₂.

Mathematical Analysis

Definition of Idealized System

In this section, we consider the fall of a cylinder in a tube, asking ourselves what is the influence on the cylinder's motion of a fluid which fills all the space above and below the cylinder, as well as the annular space between the cylinder and the tube. As the cylinder falls, the fluid

below it must move through that annular space, into the space above the cylinder. Motion need only occur in the fluid, in fact, within the annular space itself in a direction parallel to the axis, and within very small sections of the spaces above and below the cylinder. In these spaces, only enough non-zero radial velocity components need exist to distribute fluid into and out of the annulus from the larger diameter spaces.

For convenience, some major simplifications are made in describing the flow, as follows:

- 1) That the cylinder and tubes are coaxial and concentric throughout the motions.
- 2) a. That both the radial and axial velocities in the spaces above and below the cylinder are small and can be ignored.
b. That the vertical extent of the regions in which these extra-annular motions take place are also negligible.
- 3) a. That the compressibility of the fluid is low enough that its density above the cylinder is the same as below it.
b. Thus, that the fluid velocity in the annulus is not only parallel to the axis, but dependent only on the radial distance -- not at all on the vertical or on the azimuthal coordinates.

The assumption of incompressibility could be relaxed -- with minor additional complications we could undertake to consider the increase of the fluid velocities in the annulus with vertical distance. Thus, the slightly lower density of the fluid above the cylinder than that of the fluid below it could be accounted for. But it appears that little would be gained by this extra complication, and it will be omitted in this treatment.

A diagram of the idealized situation is given as Figure A1. The radial coordinate is denoted by r . By assumption 3b, we have no need to consider the azimuthal or vertical distance coordinates. All of the interesting activity in the fluid is assumed to take place in that portion of the annulus (i.e., the radius range described by $r_c < r < r_t$) which is at a given time adjacent to the moving cylinder.

The mathematical analysis will be considered under two separate headings - the radial velocity distribution in the fluid, and the dynamical problems dealing with the changes in time of the velocities. These topics are of course related and cannot really be discussed independently. It is reasonable, though, to consider first the relations between the velocities of the fluid in different parts of the annulus with the velocity of the cylinder.

The Fluid Velocity Distribution in the Annulus

In the constant cross-section channel contained between concentric circular boundaries, the laminar or creeping flow of a viscous liquid is one dimensional. In steady flow, the streamlines are parallel to each other and to the axis of the annular channel. The velocity in the axial direction - call it v_z - is a function only of the radial coordinate, and is given as a solution of the one dimensional Navier-Stokes equation, which itself takes the form of an inhomogeneous second degree differential equation with constant coefficients:

$$\frac{d^2 v_z(r)}{dr^2} + \frac{1}{r} \frac{d v_z(r)}{dr} = \frac{1}{\mu} \frac{dp}{dz} \quad (1)$$

where $v_z(r)$ = velocity in axial direction
 r = radial coordinate
 μ = viscosity
 dp/dz = pressure gradient in axial direction

On the right hand side is contained the pressure gradient along the axis, and the viscosity of the fluid.

The general solution to this equation is

$$v_z(r) = \frac{1}{4\mu} \frac{dp}{dz} r^2 + B + C \ln r \quad (2)$$

where B and C are arbitrary constants

The presence of the term with coefficient C is due to the existence of an inner boundary in flow, at the radial coordinate r_c , at which an independent boundary condition must be specified. In the particular situation to be considered here, the inner boundary for the fluid is the outer surface of the cylinder, which is able to move relative to the tube in which the fluid is contained.

The two independent boundary conditions can be taken up in order. First, the outer boundary. The aforementioned tube containing the fluid requires, by the usual no-slip condition, that at the radial coordinate r_t the velocity must be zero. Thus, from equation (2) we obtain:

$$0 = \frac{1}{4\mu} \frac{dp}{dz} r_t^2 + B + C \ln r_t$$

or

$$B = -\frac{1}{4\mu} \frac{dp}{dz} r_t^2 - C \ln r_t \quad (3)$$

Putting this expression for B into the general solution gives us:

$$V_z(r) = -\frac{1}{4\mu} \frac{dp}{dz} (r_t^2 - r^2) + C \ln(r/r_t) \quad (4)$$

Equation (3) expresses the fact that $v_{z(r)}$ goes to zero at $r = r_t$. The same procedure allows the still arbitrary constant C to be fixed also, in such a way that velocity at the inner boundary condition can be specified. Let V_c designate the axial velocity of the cylinder and therefore of the fluid in contact with it. Then equation (4) must give:

$$V_c = -\frac{1}{4\mu} \frac{dp}{dz} (r_t^2 - r_c^2) + C \ln(r_c/r_t)$$

or

$$C = \frac{V_c + \frac{1}{4\mu} \frac{dp}{dz} (r_t^2 - r_c^2)}{\ln(r_c/r_t)} \quad (5)$$

Now, putting this expression for C into equation (4), we get an expression which contains no arbitrary constants and satisfies both boundary conditions.

$$V_z(r) = \left(V_c + \frac{1}{4\mu} \frac{dp}{dz} (r_t^2 - r_c^2) \right) \frac{\ln(r/r_t)}{\ln(r_c/r_t)} - \frac{1}{4\mu} \frac{dp}{dz} (r_t^2 - r^2) \quad (6)$$

This expression for $v_{z(r)}$ refers to two independent variables, by which an experimenter could influence the outcome. These independent variables are the pressure drop along the annulus, dp/dz , and the velocity of the cylinder V_c .

For the viscometric purposes of the apparatus being considered here, however, a particular relationship between these two variables is imposed by the conditions of the experiment. The top and bottom ends of the tube are closed, so that there can be no net flow in any parts of the tube which at a given moment do not surround the moving cylinder. In fact, it may be supposed that fluid motion occurs only in the annulus, where there is just enough flow to clear space ahead of the cylinder, and to fill the space behind it. This condition can be written

$$-\pi r_c^2 V_c = 2\pi \int_{r_c}^{r_t} V_z(r) r dr$$

or simply

$$-\frac{r_c^2 V_c}{2} = \int_{r_c}^{r_t} v_z(r) r dr \quad (7)$$

In the equation above, the left hand side is the rate at which space is displaced by the moving cylinder, and the right hand side is the integral of flow over the radial interval r_c to r_t , which represents the annulus. To make use of equation (7), the expression (6) for the velocity must be integrated. Putting that expression for $v_z(r)$ into equation (7), there is obtained:

$$\begin{aligned} -\frac{r_c^2 V_c}{2} &= \frac{(V_c + \frac{1}{4\mu} \frac{dp}{dz} (r_c^2 - r_t^2))}{\ln(r_c/r_t)} \int_{r_c}^{r_t} \ln(r/r_c) r dr \\ &\quad - \frac{1}{4\mu} \frac{dp}{dz} r_t^2 \int_{r_c}^{r_t} r dr \\ &\quad + \frac{1}{4\mu} \frac{dp}{dz} \int_{r_c}^{r_t} r^3 dr \end{aligned} \quad (8)$$

As can be seen, there are three terms, whose integrals are given below:

$$\int_{r_c}^{r_t} r dr = \frac{r_t^2 - r_c^2}{2} \quad (9a)$$

$$\int_{r_c}^{r_t} r^3 dr = \frac{r_t^4 - r_c^4}{4} = \frac{(r_t^2 - r_c^2)(r_t^2 + r_c^2)}{4} \quad (9b)$$

$$\int_{r_c}^{r_t} \ln(r/r_t) r dr = -\frac{r_c^2}{2} \ln(r_c/r_t) - \frac{(r_t^2 - r_c^2)}{4} \quad (9c)$$

Substituting these into equation (8) and simplifying, the result is obtained

that

$$\frac{dp}{dz} = - \frac{4\mu V_c}{(r_t^2 + r_c^2) \ln(r_c/r_t) + (r_t^2 - r_c^2)} \quad (10)$$

This is the relation between cylinder velocity V_c and axial pressure gradient dp/dz which is induced in the annulus under the condition stated -- that the ends of the tube are closed. Now we are able to put this expression for dp/dz into equation (6), so as to obtain a formula for the velocity of the fluid in the annulus, in terms only of V_c and the radial dimensions:

$$V_z(r) = V_c \left\{ \frac{(r_t^2 - r^2) - (r_t^2 - r_c^2) \cdot \frac{\ln(r/r_t)}{\ln(r_c/r_t)}}{(r_t^2 + r_c^2) \ln(r_c/r_t) + (r_t^2 - r_c^2)} + \frac{\ln(r/r_t)}{\ln(r_c/r_t)} \right\} \quad (11a)$$

It may be noticed that this expression does not contain the viscosity of the fluid. This is because the flow pattern is independent of the viscosity, although of course, the force required to move the cylinder is not. The flow pattern is also independent of the tube and cylinder sizes, although fairly strongly influenced by the ratio of their diameters.

In fact, the radial distribution of fluid velocity in the annulus can perhaps best be expressed in dimensionless terms.

$$\text{If we define } \left. \begin{array}{l} P = r/r_t \\ B = r_c/r_t \end{array} \right\} \quad (11b)$$

Then we are interested in fluid velocities in the annular region defined by $(B \leq P \leq 1)$. The fluid velocity as a function of P and B is then

$$V_z(r) = V_c W(P,B) \equiv V_z(P,B)$$

$$W(P,B) = \left\{ \frac{(1-P^2) - (1-B^2) \frac{\ln P}{\ln B}}{(1+B^2) \ln B + (1-B^2)} + \frac{\ln P}{\ln B} \right\} \quad (11c)$$

Before going further, it is instructive to compute and display this pattern of variation of fluid velocity with radius. Figure A2 shows this variation of the dimensionless velocity function $W(P,B)$ for a fairly wide annulus, $B = 0.81$. Note that the horizontal and vertical scales are different, and that the horizontal scale runs only from $P = .81$ on the left. For larger B (that is for relatively narrower annuli), the inner portion of

the annulus in which W is positive (that is, in which the fluid velocity is in the same direction as the cylinder velocity) becomes an even smaller fraction of the total annular distance.

It is to be noted that equations (11) give the axial velocity of the fluid as everywhere proportional to V_c . This is only to be expected; the proportionality is a general characteristic of "creeping flows" in which inertial forces are small enough to be insignificant, and where the local velocity at any particular place can be increased or decreased by varying the driving force in the desired proportion.

It will be seen in the next section that this proportionality is involved in one further assumption about the flow, which is made in addition to those idealizations enumerated earlier. Briefly, the added assumption is a dynamic one: that the aforementioned proportionality between v_z and V_c holds true at early times as well, while the cylinder is being accelerated towards its terminal velocity but before it has reached it. In operation, the viscometer will not usually be used with the cylinder moving through the observation region at a constant velocity, except when rather viscous fluids are being tested. It is thus necessary to consider the dynamical situation, while acceleration is taking place just after release of the cylinder.

Dynamics of the Motion

After the cylinder's release, its downward velocity increases monotonically, approaching a terminal velocity in an exponential manner. This behavior is of course typical of any object falling in a gravitational field and subject to viscous forces. But if the gravity field is considered uniform over the fall distances involved (the "flat earth" assumption), if the viscous forces are Newtonian (that is, strictly proportional to velocity), and if the velocity and consequently the Reynolds Number are low enough that inertial forces are insignificant and the flow is not turbulent, then the motion can be simply described. This simple description involves a linear differential equation with constant coefficients.

$$I \frac{dV_c}{dt} + DV_c + A = 0 \quad (12)$$

Here, I is the system mass that is accelerated, D is the frictional force per unit cylinder velocity, and A is the gravitational force on the moving system. With the noted assumptions, the coefficients I , D , and A are all positive constants.

Taking into account the condition that the initial downward velocity of the cylinder is zero, one integration yields for the velocity at later times:

$$V_c(t) = -\frac{A}{D} \left(1 - e^{-Dt/I} \right) \quad (13)$$

It can be seen that the acceleration of the cylinder decays exponentially towards zero from an initial value of $(-A/I)$, as the velocity becomes more negative and approaches the terminal velocity $(-A/D)$.

One more integration, with the specification that the release point is the origin of the vertical coordinate z , gives the position of the cylinder as a function of time:

$$z(t) = -\frac{A}{D} \left(t + \frac{I}{D} \left(e^{-Dt/I} - 1 \right) \right) \quad (14)$$

It may now be apparent why a detailed assumption is required of the proportionality of the fluid velocities to the cylinder velocity. Particularly, in order to calculate the effective mass coefficient in the dynamic equation, it is to be assumed that the distribution of fluid velocities described previously in equations (11) holds true during the process of acceleration, as $(-V_c)$ increases up to the terminal velocity. Thus, it is assumed that

$$\frac{dV_z(P,B)}{dt} = W_{(P,B)} \frac{dV_c}{dt} \quad (15)$$

While $|V_c| \leq -A/D$, and where $W_{(P,B)}$ is as defined in equation (11c).

The Inertial Effective Mass

The major consequence of this, for our purposes, is that the inertial reaction of the cylinder's motion is not only that due to the mass and changing velocity of the cylinder itself, but also that of the fluid in the annulus.* The constant I consists not only of the mass of the cylinder, but must also include terms proportional to the mass of fluid in the annulus, modified by the ratio of fluid to cylinder velocity. Furthermore, account must be taken of the fact that some fluid in the annulus moves in the positive and some in the negative direction. Because of this change in the

*Of course, for many situations this might be a rather small correction. It is possible though, to imagine a situation in which it would be large. Consider using this viscometer with a low density cylinder which moves upward, under the influence of its buoyancy, in a tube of mercury. In this case the importance of the fluid's inertia would be paramount.

direction of the velocity, an integral taken with the same sign over the entire annulus would result in some of the effect being erroneously subtracted from the rest.

The annular velocity distribution is described by the function W derived above, which is positive in the region defined by $(B < P < P_c)$ and negative in the outer region $(P_c < P < 1)$. This corresponds to the fact that the fluid within a "sheath" of radial thickness Δr moves in the same direction as the cylinder. Here, $\Delta r = (r_{crit} - r_c) = r_t(P_c - B)$. Outside of that sheath, to the tube wall at r_t (or to $P = 1$ in the dimensionless form), the fluid motion is in the opposite direction to that of the cylinder. The critical value, P_c , is obtained by solving the equation

$$W(P_c, B) = 0 \quad (16a)$$

This reduces to the implicit expression

$$\sqrt{-1 - \frac{1 - P_c^2}{\ln P_c}} = B \quad (16b)$$

which can be solved numerically to give $P_c(B)$. Figure A3 displays P_c graphically in terms of the annular descriptor B . Note that for narrower annuli (i.e., as $B \rightarrow 1$), P_c exceeds B by ever smaller amounts.

The "effective mass", insofar as the inertial term of equation (12) is concerned, will then consist of three parts. The first of these is the mass of the cylinder itself, the second is the contribution due to the fluid within the "sheath" referred to above, and the third is due to the fluid outside P_c . The latter two are proportional to integrals of the fluid velocity - integrals which have already been evaluated, although not between these limits.

The inertial effective mass, following this prescription, is

$$I = \pi r_c^2 l \left(B^2 \rho_c + 2 \rho_f \left[\int_B^{P_c} W(P, B) P dP - \int_{P_c}^1 W(P, B) P dP \right] \right) \quad (17)$$

Evaluation of the integral over the full range, to obtain the net volume moved in the annulus, led earlier to equation (10). Because the sheath of fluid moving in the same direction as the cylinder is fairly thin, i.e., because P_c is not much greater than B , the first integral is much less than the second. The two of them together are of the same order of magnitude as $B^2/2$ so that the ratio of the average density of the cylinder to that of the fluid is most important in determining which contributes more to the inertial effective mass.

The Total Viscous Force

The dynamic proportionality expressed in equation (15) is also assumed in calculating the forces, proportional to the velocity, which oppose the motion. These viscous forces are calculable in two parts.

The first of these could be considered to be direct -- it is the skin friction which is directly exerted at the outer surface of the cylinder. If the fluid is Newtonian, this force is simply the negative product of the side area of the cylinder, the viscosity and the radial derivative of the velocity at the radius of the cylinder, r_c .

$$F_{v_1} = -2\pi r_c l \mu \left. \frac{dV_c}{dr} \right|_{r=r_c} \quad (18a)$$

But the derivative can be obtained from equation (11c);

$$\left. \frac{dV_z(r)}{dr} \right|_{r=r_c} = \frac{V_c}{r_c} \left. \frac{dW(P, B)}{dP} \right|_{P=B}$$

Thus

$$F_{v_1} = -2\pi l B \mu V_c \left[-\frac{2B}{Q} + \frac{1 - \frac{1-B^2}{Q}}{B \ln B} \right] \quad (18b)$$

$$\text{where } Q \equiv (1 + B^2) \ln B + (1 - B^2) \quad (18c)$$

There is also a second retarding force that is proportional to V_c . This force is due to the pressure difference between the fluid at the two ends of the cylinder, the same pressure difference that forces net fluid upward through the annulus to provide space into which the cylinder can move. It may be calculated as the product of the area of end of the cylinder, its length, and of the pressure gradient along it.

$$F_{v_2} = \pi r_c^2 l \frac{dp}{dz} \quad (19a)$$

The pressure gradient was given in equation (10) and is readily transformed to use the dimensionless radius ratio B :

$$\frac{dp}{dz} = - \frac{4\mu V_c}{r_c^2 [(1+B^2)\ln B + 1-B^2]} = - \frac{4\mu V_c}{r_c^2 Q}$$

using Q , the abbreviation introduced above. Thus

$$F_{v2} = - \frac{4\pi B^2 l \mu V_c}{Q} \quad (19b)$$

The sum of these gives the total viscous force to go into the differential equation (12).

$$DV_c = F_{v1} + F_{v2} .$$

By strange good fortune, the second term cancels out part of the first and we are left with:

$$D = -2\pi l \mu \left(1 - \frac{1-B^2}{Q}\right) \cdot \frac{1}{\ln B} \quad (20)$$

The Gravitational Force and Coefficients of the Equation

The effective force of gravity is simply the weight of the cylinder corrected for buoyancy, to allow for the equivalent volume of fluid which moves upward to replace the falling cylinder:

$$A = \pi r_c^2 l (\rho_c - \rho_f) g \quad (21)$$

Here, g is the acceleration of gravity, ρ_c is the average density of the cylinder and ρ_f the density of the fluid.

It is to be noted that the length l appears to the first power in each of the three coefficients I , D , and A and thus cancels out of the differential equation. Within the limits set by the assumptions made in the derivation, then, it is to be expected that the motion will be independent of the cylinder length. The initial value of cylinder acceleration is obtained by combining equations (17) and (21):

$$-\frac{A}{I} = - \frac{B^2 (\rho_c - \rho_f) g}{(B^2 \rho_c + 2\rho_f \left[\int_B^{\rho_c} W P dP - \int_{\rho_c}^1 W P dP \right])} \quad (22)$$

It is expressed completely in terms of the dimensionless radius ratios B and P_c -- in which the latter is a function of B. Thus, this parameter depends only on this ratio, and is independent of the actual size of the apparatus.

On the other hand, the terminal velocity of the cylinder, obtained from equations (17) and (20), is denoted by U:

$$U \equiv -\frac{A}{D} = \frac{r_c^2 g (\rho_c - \rho_f) \ln B}{2\mu \left(1 - \frac{1-B^2}{Q}\right)} \quad (23)$$

This is proportional to the square of the actual cylinder radius as well as to dimensionless functions of the radius ratios, to gravity and the density difference, and inversely to the viscosity. As is to be expected, only the single difference of the densities is important by the time terminal velocity is reached. (A more complicated dependence on the densities of fluid and cylinder holds during the early acceleration period, as seen in equation (22).)

Finally, it is of interest to examine the ratio (I/D), which represents the characteristic time interval over which the acceleration decays to $(1/e)^{th}$ of its starting value. This characteristic time is labelled T_c :

$$T_c \equiv \frac{I}{D} = - \frac{r_c^2 \left(B^2 \rho_c + 2\rho_f \left[\int_B^{P_c} W P dP - \int_{P_c}^1 W P dP \right] \right) \ln B}{2\mu \left(1 - (1-B^2)/Q\right)} \quad (24)$$

This decay time is proportional to the square of the tube radius, as well as to the densities and inversely to the viscosity.

Equation (14) for the position coordinate of the cylinder can now be rewritten in terms of these newly defined quantities:

$$z(t) = U \left(t + T_c (e^{-t/T_c} - 1) \right) \quad (25)$$

This completes the mathematical analysis of the idealized system. One task remaining is to develop a computational method by which the measurements resulting from fall-time experiments can be combined with equation (25) and the others to give viscosity values. This includes numerical evaluation of the factors and the assessment of sensitivity to errors in the necessary measurements. A further need is to discuss the design of an actual apparatus, with particular emphasis on the extent to which it can be made to conform with the idealizations which were so convenient mathematically.

Viscosity Computations

There are several computational problems in applying the above results, which are dealt with briefly in this section. They have to do with:

1. Computation of the dimensionless coefficients used in equations (23) and (24), that are functions of the radius ratio B .
2. The lack of an inverse form of equation (25). Fall times cannot be computed directly from the viscosity and positions of the observing stations. A similar difficulty then occurs in the computation of the viscosity from the fall parameters.
3. The presentation of results in a form convenient for use, to obtain viscosity from the measured time of fall. As noted previously, the results of the calculation are presented as "correction times" to be subtracted from the measured times. A conventional viscometer constant is then used with the "corrected fall time" to calculate the viscosity.

The Dimensionless Coefficients

In both the expressions for U in equation (23) and T_c in (24), there appears a combination which can be labelled as $X(B)$:

$$X(B) = \frac{\ln B}{(1 - (1-B^2)/Q)} \quad (26)$$

which may be computed directly. It may also be of use to repeat here the definition of $Q(B)$ from equation (18c):

$$Q = (1+B^2)\ln B + (1-B^2)$$

There also appears in equation (24) a dimensionless function of B that involves two integrals of the (dimensionless) fluid velocity $W(P,B)$. The indefinite integral, defined as $J_{(P,B)}$, can be evaluated analytically, with the result:

$$J(P, B) \equiv \int W(P', B) P' dP'$$

$$= \frac{P^2}{2Q} \left(1 - \frac{P^2}{2} + \frac{(\ln P - 1/2)(Q - 1 + B^2)}{\ln B} \right) \quad (27)$$

Then if

$$Y(B) \equiv \int_B^{P_c} W(P', B) P' dP' - \int_{P_c}^1 W(P', B) P' dP'$$

$$Y(B) = 2J(P_c, B) - J(B, B) - J(1, B) \quad (28)$$

The dimensionless function, $Y(B)$, can be calculated directly from equation (28), with $J(P, B)$ specified as a function subroutine. Because $Y(B)$ is a small difference between large numbers, though, the accuracy of the value computed in this way is badly eroded by roundoff error. Fortunately $Y(B)$ occurs only in the calculation of T_c , and as the coefficient of the smaller term in a sum. This inaccuracy is thereby reduced in importance. It would assume greater import in two cases: if the fluid were of higher density relative to that of the falling cylinder, and for very low viscosity fluids where the acceleration becomes relatively more important.

It may be recalled that P_c , the dimensionless radius at which the fluid velocity is zero, and which is needed in the evaluation of equation (28), is obtained by numerical solution of equation (16b):

$$\sqrt{-1 - \frac{1 - P_c^2}{\ln P_c}} = B \quad (16b)$$

Because some of these functions vary rapidly with B , it may be of interest to be able to refer to their dependence on this radius ratio. A table of values over a reasonable range of B has thus been computed and is given as Appendix A-2.

The two parameters of the fall, the terminal velocity U and the decay time T_c , are thus given by:

$$U = \frac{r_c^2 g (\rho_c - \rho_f) X(B)}{2\mu} \quad (29)$$

$$T_c = \frac{r_c^2}{2\mu} X(B) (B^2 \rho_c - 2Y(B) \rho_f) \quad (30)$$

Computing Fall Time between Stations, and Viscosity

Equation (25) gives the distance explicitly for time after release. Inverting it to make possible the calculation of fall time as a function of the fluid viscosity, the densities and the positions of the observing stations is best done numerically. The computation, contained in a function subroutine labelled TFALM, uses the Newton root-finding method to obtain the fall time to distance S from the release point. The direct evaluation of equation (25) is done in function ESM in one of three ways depending on the value of T/Tc, the negative of the argument of the exponential.

A similar use of the Newton method is required to calculate the viscosity itself, given the fall time between observing stations and the other relevant parameters. This is performed in function MUFT.

Presentation of Results

A minimum fall time would be measured between the two observing stations if the tube contained a fluid of zero viscosity (such as a high vacuum). At low viscosities greater than zero, the rate of increase in the fall time with increasing viscosity is low, and increases gradually at larger times. This non-linearity is of course the result of the acceleration of the cylinder towards its terminal velocity. For fall times which are long compared to the minimum time, the rate of increase of fall time with viscosity approaches a maximum. This occurs when the terminal velocity has been nearly reached over most of the fall distance.

Rather than listing the calculated viscosities themselves for each fall time, the table of results lists "correction times" CT. The correction time is to be subtracted from the measured time, and the difference multiplied by a conventional "viscometer constant" C to give the viscosity.

$$\mu = C(T_{\text{meas}} - CT) \quad (31)$$

At large enough values of T_{meas} the correction time is very small and is negligible in comparison with measurement errors. This is the limit described above, of course, when terminal velocity has been reached by the cylinder.

The PASCAL program VISFAL, listed as Appendix A-2, calculates tables such as those given in A-3. These tables are divided into six columns, for six chosen fluid density values. For each density the viscometer constant C is given at the top of the table. Below it are listed values of the correction time, for increasing values of the measured time of fall. The use of these tables in data reduction involves selection of the proper fluid density, interpolation to find the appropriate correction time for a given measured fall time, subtraction to obtain a "corrected fall time" and

multiplication by C. If the measured time is in seconds, the viscosity obtained in this way will be in centipoise.

Experimental Realization

The viscometer constructed according to the above principles uses a sapphire tube in which to contain the sample to be measured.* The falling cylinder is made of steel so that it may be lifted to its release point by an external magnet. The two observation stations each consist of a light-emitting diode and a photo diode detector. These are built into a plexiglas block which has a channel milled out of it, to fit around the sapphire tube. The stations are separated by a distance of 9.42 cm., and when the block is installed around the tube, the upper observing station lies 1.24 cm. below the lower end of the steel cylinder before the latter's release.

Because the sapphire tube is grown as a single crystal,** its inner diameter is not precisely cylindrical. Thus it does not conform exactly with the idealization which had been assumed for mathematical convenience in the derivation. The numerical value which should be used for the "radius ratio" B, which is a very sensitive variable in the calculations, is therefore in some doubt. In this situation it has seemed most reasonable to construct several tables using different assumed values of B. From these, one table is selected that gives viscosities nearest to the handbook values of several known fluids. This particular table will then be used for all further tests, since it will presumably contain a value of B which most closely describes the real, non-cylindrical geometry of the tube and cylinder.

*The viscometer is a modification of the device originally designed to measure solubilities in condensed CO₂, and the two versions are convertible into each other. The sapphire tube serves as a mixing chamber in the solubility apparatus. Though thin walled enough for manipulation of a magnet within it, it is able to contain an internal pressure of 4000 psi or greater.

**The sapphire tube is manufactured by the Tyco Corporation, Saphikon Division, 51 Powers Street, Milford, New Hampshire 03055.

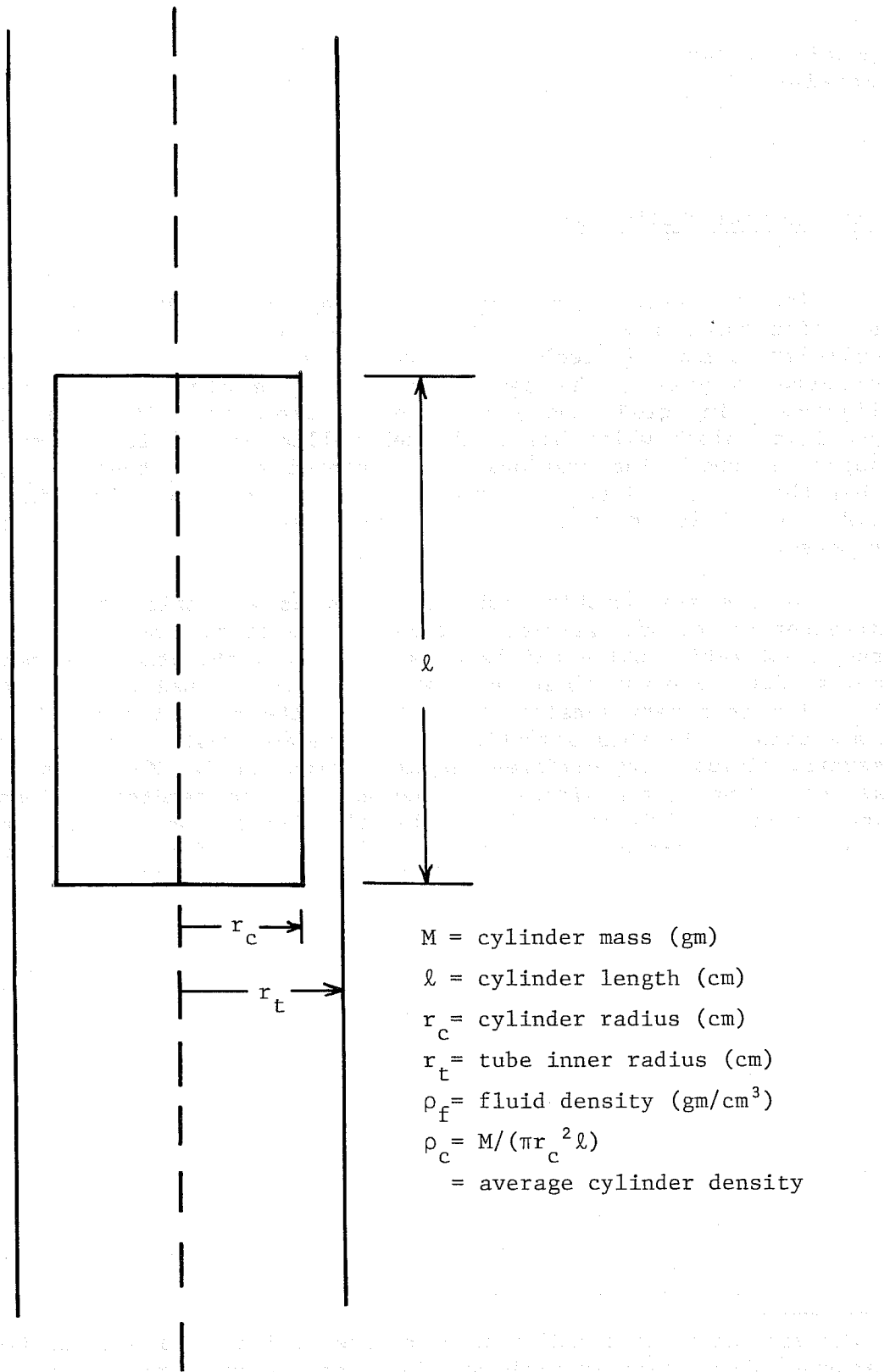


Figure A1 Cylinder-in-Tube Viscometer

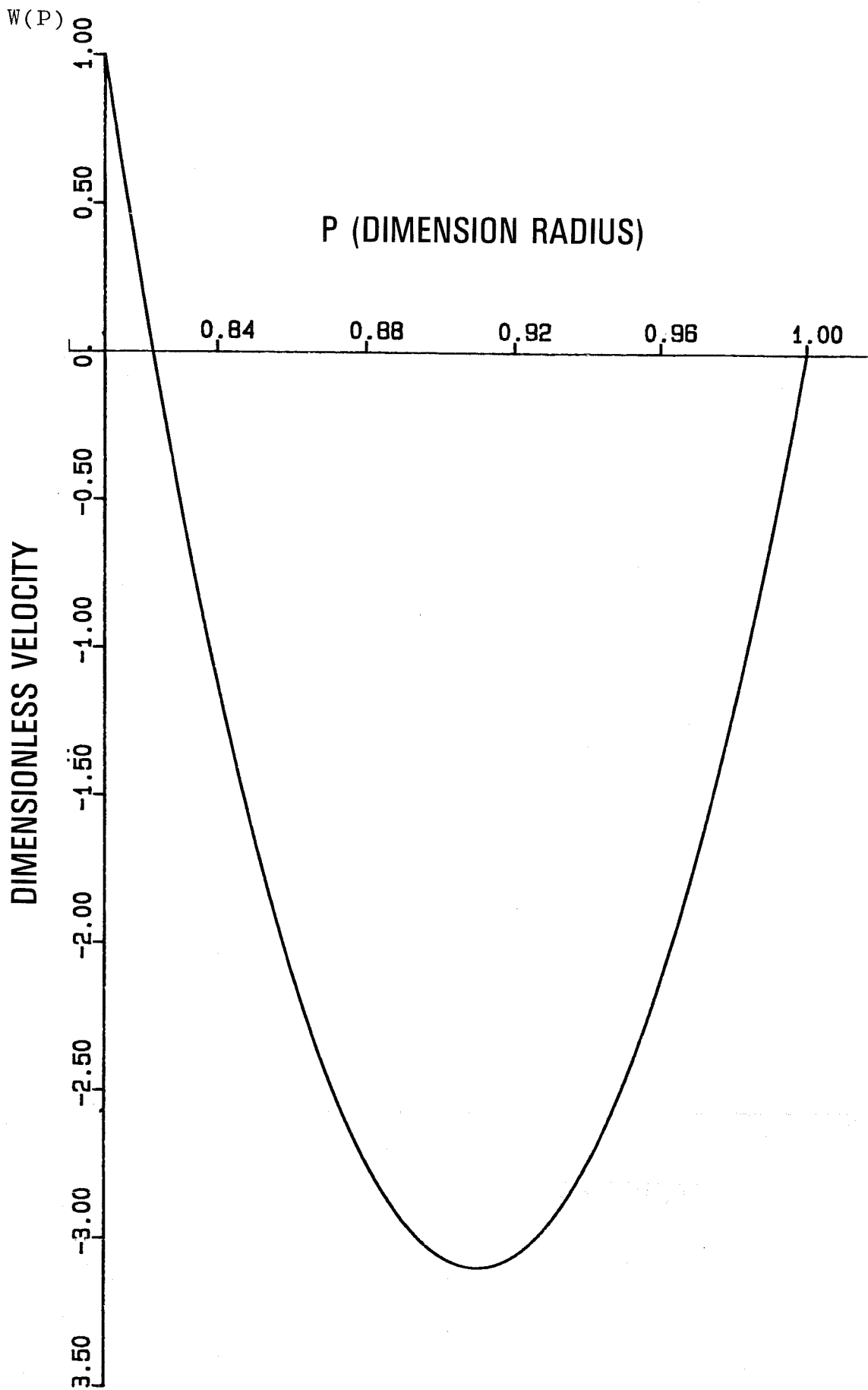


FIGURE A2 - Dimensionless Velocity Distribution in Annulus, for $B = 0.81$

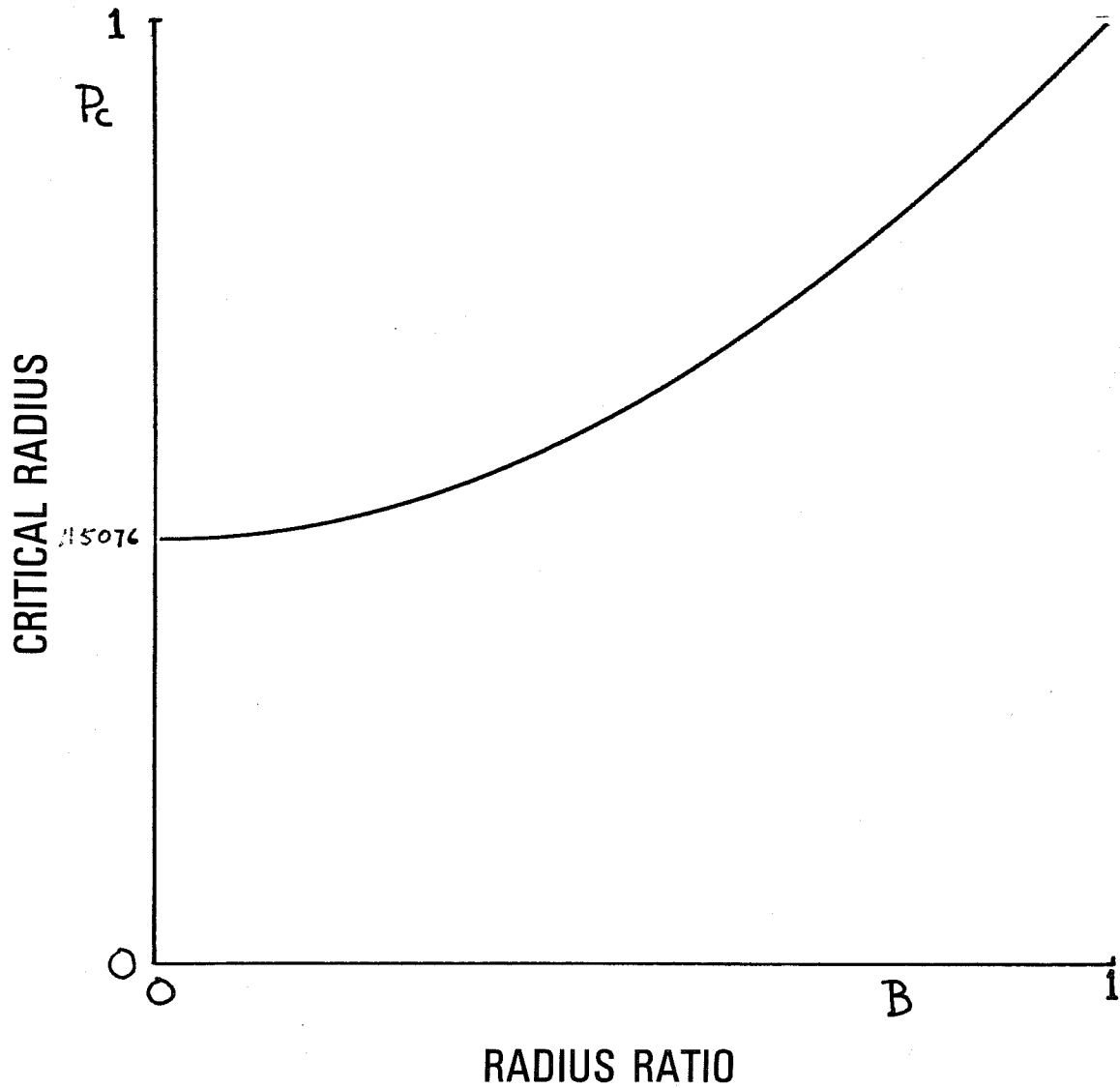


FIGURE A3 - Dimensionless Critical Radius P_c vs. Radius Ratio $B \equiv r_c / r_t$

APPENDIX A-2

DIMENSIONLESS FUNCTIONS OF B

B	Q	X	PC	Y
0.8700	-0.0015696	-0.000893374	0.87588	0.38350
0.8720	-0.0014965	-0.000850095	0.87770	0.38509
0.8740	-0.0014258	-0.000808335	0.87952	0.38673
0.8760	-0.0013575	-0.000768085	0.88134	0.38834
0.8780	-0.0012914	-0.000729237	0.88317	0.38997
0.8800	-0.0012276	-0.000691815	0.88500	0.39160
0.8820	-0.0011659	-0.000655746	0.88683	0.39316
0.8840	-0.0011064	-0.000621054	0.88866	0.39476
0.8860	-0.0010489	-0.000587433	0.89050	0.39638
0.8880	-0.0009935	-0.000555508	0.89234	0.39800
0.8900	-0.0009402	-0.000524438	0.89418	0.39986
0.8920	-0.0008889	-0.000495017	0.89603	0.40135
0.8940	-0.0008395	-0.000466571	0.89788	0.40309
0.8960	-0.0007920	-0.000439294	0.89973	0.40474
0.8980	-0.0007463	-0.000413147	0.90159	0.40649
0.9000	-0.0007025	-0.000388122	0.90345	0.40817
0.9020	-0.0006605	-0.000364180	0.90531	0.40985
0.9040	-0.0006202	-0.000341284	0.90717	0.41159
0.9060	-0.0005816	-0.000319393	0.90904	0.41336
0.9080	-0.0005447	-0.000298535	0.91091	0.41498
0.9100	-0.0005093	-0.000278607	0.91278	0.41660
0.9120	-0.0004756	-0.000259635	0.91466	0.41824
0.9140	-0.0004435	-0.000241615	0.91654	0.41992
0.9160	-0.0004128	-0.000224442	0.91842	0.42184
0.9180	-0.0003836	-0.000208178	0.92030	0.42322
0.9200	-0.0003558	-0.000192721	0.92219	0.42511
0.9220	-0.0003294	-0.000178065	0.92408	0.42682
0.9240	-0.0003045	-0.000164238	0.92597	0.42847
0.9260	-0.0002807	-0.000151107	0.92787	0.43066
0.9280	-0.0002583	-0.000138765	0.92977	0.43207
0.9300	-0.0002370	-0.000127110	0.93167	0.43433
0.9320	-0.0002171	-0.000116203	0.93358	0.43579
0.9340	-0.0001984	-0.000105944	0.93548	0.43762
0.9360	-0.0001806	-0.000096265	0.93739	0.43945
0.9380	-0.0001640	-0.000087258	0.93931	0.44141
0.9400	-0.0001485	-0.000078825	0.94122	0.44263
0.9420	-0.0001340	-0.000070994	0.94314	0.44519
0.9440	-0.0001205	-0.000063729	0.94506	0.44617
0.9460	-0.0001079	-0.000056934	0.94699	0.44971
0.9480	-0.0000963	-0.000050730	0.94892	0.44946
0.9500	-0.0000855	-0.000044927	0.95085	0.45166
0.9520	-0.0000756	-0.000039647	0.95278	0.45459
0.9540	-0.0000665	-0.000034793	0.95472	0.45557
0.9560	-0.0000581	-0.000030364	0.95665	0.45630
0.9580	-0.0000504	-0.000026294	0.95860	0.46143
0.9600	-0.0000435	-0.000022643	0.96054	0.46240
0.9620	-0.0000373	-0.000019379	0.96249	0.46680
0.9640	-0.0000317	-0.000016436	0.96444	0.46533
0.9660	-0.0000266	-0.000013751	0.96639	0.46973
0.9680	-0.0000222	-0.000011478	0.96834	0.46875
0.9700	-0.0000182	-0.000009397	0.97030	0.47852
0.9720	-0.0000148	-0.000007631	0.97226	0.48047

LISTED ON

```
PROGRAM VISCOSIT; ( to calculate and print tables of "Correction Times"
                  to be subtracted from the measured time of fall
                  between observing stations at SS and SF cm from
                  release point; for different values of fluid density.)
```

```
(Program constants and values updated 12/19/81 )
```

```
CONST RHOCYL=7.7608; (gm/cc avg density of cylinder)
      RCYL=0.3840; (cm radius; RTUBE is a variable so B can be.)
      G=979.19; (cm/(sec*sec) in Socorro)
      SS=1.24; SF=10.66; (cm)
```

```
VAR LOTYM, DELTYM, MU, TM, B, XOFB, YOFB, RTUBE,
     DELS, CT, TH : REAL;
     IPG, IRHO, ITM, NP, IA : INTEGER;
     RHO, C, TCM, UTM, TMIN : ARRAY(1..6) OF REAL;
     FOUT : TEXT;
```

```
FUNCTION TFALM(S, UT, TD : REAL): REAL; (TO CALCULATE TIME OF FALL
                                         OF CYLINDER IN TUBE, FROM RELEASE POINT
                                         TO -S
```

```
S in cm.
```

```
UT cm/sec is terminal velocity
```

```
TD sec is decay time of acc. )
```

```
CONST DEL=4.0E-7; NLIMIT=25;
```

```
VAR T1, T2, T3, S1, S2, S3 : REAL;
     I : INTEGER;
     SW : BOOLEAN;
```

```
FUNCTION ESM(T, UTT, TOD : REAL): REAL; (calculates negative distance
                                         from release point that cylinder
                                         will fall in the time T seconds
                                         if terminal velocity is UTT and
                                         decay time of acceleration is
                                         TOD sec. Both UTT and TOD are
                                         entered as positive numbers.)
```

```
CONST XL=0.003;
```

```
VAR X : REAL;
```

```
BEGIN
```

```
  X := T/TOD;
```

```
  IF X < XL THEN
```

```
    ESM:=0.5*UTT*X*T*(1-X/3+SQR(X)/12)
```

```
  ELSE IF X < 18 THEN
```

```
    ESM:=UTT*(T+TOD*(EXP(-X)-1))
```

```
  ELSE
```

```
    ESM:=UTT*(T-TOD);
```

```
END;
```

```
BEGIN; (FUNCTION TFALM(S, UT, TD))
```

```
  T1:=S/UT; T2:=SQR(2*S*TD/UT);
```

```
  IF T2>T1 THEN T1:=T2;
```

```
  S1:=ESM(T1, UT, TD);
```

```
  T2:=1.05*T1;
```

```
  S2:=ESM(T2, UT, TD);
```

```

WHILE SW= TRUE DO
  BEGIN
    T3:= T1+(T2-T1)*(S-S1)/(S2-S1);
    S3:=ESM/(T3,UT,TD);
    T1:=T2; S1:=S2;
    T2:=T3; S2:=S3;
    I:=I+1;
    SW:=(I<NLIMIT) AND (ABS(S2-S1)>DEL);
  END; (WHILE)
TFALM:=T2;
END; (function TFALM(S,UT,TD))

FUNCTION TF(UT,TD :REAL):REAL; (given UT and TD, to calculate what fall
                                time in seconds would be between
                                the observing stations at SS and SF)
  BEGIN
    TF:=TFALM(SF,UT,TD)-TFALM(SS,UT,TD);
  END;

FUNCTION MUFT(FTY : REAL):REAL; (To calculate MU from a falltime
                                measured between SS and SF )
  CONST NLIM=20; DEB=1.0E-6;
  VAR MU1,MU2,MU3,FT1,FT2,FT3 : REAL;
      JB : INTEGER;
      SB : BOOLEAN;

  FUNCTION FTM(MOO:REAL):REAL; (To calculate fall time in fluid of
                                viscosity MOO, as entered in poises.)
    VAR UTMU,TCMU : REAL;
    BEGIN
      UTMU:=UTM*IA3/MOO;
      TCMU:=TCM*IA3/MOO;
      FTM:=TF(UTMU,TCMU);
    END;

  BEGIN (function MUFT)
    MU1:=FTY*CEIA3;
    FT1:=FTM(MU1);
    IF FT1<=TM*IA3 THEN FT1:=TM*IA3*1.01;
    MU2:=1.05*MU1;
    FT2:=FTM(MU2);
    JB:=0; SB:=TRUE;
    WHILE SB=TRUE DO
      BEGIN
        MU3:=MU1+(MU2-MU1)*(TM-FT1)/(FT2-FT1);
        FT3:=FTM(MU3);
        MU1:=MU2; FT1:=FT2;
        MU2:=MU3; FT2:=FT3;
        JB:=JB+1;
        SB:=(JB<NLIM) AND (ABS(FT2-TM)>DEB);
      END; (while)
    MUFT:=MU2;
  END; (function MUFT)

PROCEDURE ENTRDATA;
  BEGIN
    WRITE('ENTER VALUE OF B ( radius ratio ) ');
    READLN(B);
  END;

```

```

WRITELN('RTUBE = ',RTUBE:6:4);
WRITE('ENTER -X(B) ');
READLN(XOFB);
WRITE('ENTER Y(B) ');
READLN(YOFB);
WRITELN('ENTER SIX VALUES OF FLUID DENSITY FOR COLUMNS OF RESULTS ');
DELS:=SF-SS;
FOR IA:=1 TO 6 DO BEGIN
  READLN (RHOCIA);
  CIAJ:=C*RCYL*RCYL*XOFB*(RHOCYL-RHOCIA)/(2*DELS);
  UTMCIAJ:=CIAJ*DELS;
  TCMCIAJ:=RTUBE*RTUBE*XOFB*(0.5*B*D*RHOCYL+YOFB*RHOCIA);
  TMINICIAJ:=SQRT(2*TCMCIAJ/UTMCIAJ)*(SQRT(SF)-SQRT(SS));
  END; (loop on IA)
WRITE('ENTER START TIME AND TIME INCR. IN SEC ');
READLN(LOTYM,DELYM);
WRITE('ENTER NUMBER OF PAGES TO DO ');
READLN(NP);
END; ( PROCEDURE ENTRDATA)

BEGIN (MAIN)
  ENTRDATA;
  REWRITE(FOUT,'REOUT');
  FOUT:=CHR(17); PUT(FOUT); (SELECT PRINTER)
  FOR IPG:=1 TO NP DO
    BEGIN
      FOUT:=CHR(12); PUT(FOUT);(FORMFEED)
      WRITE(FOUT,'page ',IPG);
      WRITELN(FOUT,'CORRECTION TIMES for VISCOSITIES from TIME of FALL(170)');
      WRITELN(FOUT,'of CYLINDER in TUBE(149)');
      WRITELN(FOUT,'Rcyl=',RCYL:6:4,'cm, Rtube=',RTUBE:6:4,'cm, B=',R:7:4,
        ',-X(B)=',XOFB,', RHOCyl=',RHOCYL:6:4,'gm/cc. ');
      WRITELN(FOUT,'Y(B)=',YOFB:8:6,' Obs. stations at ',SS:4:2,' and ',SF:5:2,
        'cm from release point. ');
      WRITE(FOUT,' C= ');
      FOR IA:=1 TO 6 DO BEGIN
        TH:=CIAJ*100;
        WRITE(FOUT,TH:11:4);
      END;
      WRITELN(FOUT);
      WRITELN(FOUT,'for fluid densities(155)');
      WRITE(FOUT,' TIME ');
      FOR IA:=1 TO 6 DO WRITE(FOUT,' rhoC',IA,' ]= ');
      WRITELN(FOUT);
      WRITE(FOUT,' sec ');
      FOR IA:=1 TO 6 DO WRITE(FOUT,RHOCIA:11:4);
      WRITELN(FOUT);
      WRITELN(FOUT);
      FOR ITM:=1 TO 50 DO
        BEGIN
          TM:=LOTYM+(ITM-1+(IPG-1)*50)*DELYM;
          WRITE(FOUT,TM:7:4,' ');
          FOR IA:=1 TO 6 DO
            BEGIN
              IF TM>TMINICIAJ THEN MU:=100*MUFT(TM); (MUFT is in POISE)
              CT:=TM-MU/(CIAJ*100);
              IF TM<=TMINICIAJ THEN WRITE(FOUT,' ');
              ELSE
                WRITE(FOUT,CT:11:5);
            END;
          END;
        END;
    END;

```

```
WRITE(LK, FOUT) *
END * (LOOP ON ITM FOR 50 LINES IN TABLE)
END * (LOOP ON IPG FOR NP PAGES IN TABLE)
CLOSE(FOUT, NORMAL) *
END. (PROGRAM VISCOSIT)
```

CORRECTION TIMES for VISCOSITIES from TIME of FALL
of CYLINDER in TUBE

TIME sec	rho[1]= 0.6000	rho[2]= 0.6500	rho[3]= 0.7000	rho[4]= 0.7500	rho[5]= 0.8000	rho[6]= 0.8500
0.1100	0.09574	0.09765	0.09960	0.10159	0.10360	0.10566
0.1200	0.07971	0.08136	0.08304	0.08475	0.08650	0.08828
0.1300	0.06679	0.06821	0.06967	0.07115	0.07267	0.07421
0.1400	0.05627	0.05751	0.05878	0.06007	0.06130	0.06273
0.1500	0.04766	0.04873	0.04984	0.05096	0.05211	0.05329
0.1600	0.04055	0.04149	0.04246	0.04344	0.04445	0.04547
0.1700	0.03466	0.03548	0.03633	0.03719	0.03807	0.03897
0.1800	0.02974	0.03047	0.03121	0.03197	0.03274	0.03354
0.1900	0.02563	0.02627	0.02692	0.02757	0.02827	0.02897
0.2000	0.02216	0.02273	0.02330	0.02387	0.02450	0.02512
0.2100	0.01923	0.01973	0.02024	0.02076	0.02130	0.02185
0.2200	0.01674	0.01718	0.01764	0.01810	0.01858	0.01906
0.2300	0.01462	0.01501	0.01541	0.01582	0.01625	0.01668
0.2400	0.01279	0.01314	0.01350	0.01387	0.01425	0.01464
0.2500	0.01122	0.01153	0.01186	0.01218	0.01252	0.01287
0.2600	0.00986	0.01014	0.01043	0.01073	0.01103	0.01134
0.2700	0.00869	0.00893	0.00917	0.00946	0.00973	0.01001
0.2800	0.00765	0.00788	0.00811	0.00835	0.00860	0.00885
0.2900	0.00675	0.00694	0.00717	0.00738	0.00761	0.00783
0.3000	0.00596	0.00615	0.00634	0.00653	0.00673	0.00694
0.3100	0.00527	0.00544	0.00561	0.00578	0.00597	0.00615
0.3200	0.00466	0.00481	0.00496	0.00512	0.00529	0.00546
0.3300	0.00412	0.00425	0.00440	0.00454	0.00469	0.00484
0.3400	0.00364	0.00376	0.00389	0.00402	0.00416	0.00430
0.3500	0.00322	0.00333	0.00344	0.00356	0.00369	0.00381
0.3600	0.00284	0.00294	0.00305	0.00316	0.00327	0.00338
0.3700	0.00251	0.00260	0.00270	0.00280	0.00290	0.00300
0.3800	0.00221	0.00230	0.00238	0.00247	0.00257	0.00266
0.3900	0.00195	0.00203	0.00211	0.00219	0.00227	0.00236
0.4000	0.00172	0.00179	0.00186	0.00193	0.00201	0.00209
0.4100	0.00151	0.00158	0.00164	0.00171	0.00178	0.00185
0.4200	0.00133	0.00139	0.00144	0.00151	0.00157	0.00163
0.4300	0.00117	0.00122	0.00127	0.00133	0.00138	0.00144
0.4400	0.00102	0.00107	0.00112	0.00117	0.00122	0.00127
0.4500	0.00090	0.00094	0.00098	0.00103	0.00107	0.00112
0.4600	0.00079	0.00082	0.00086	0.00090	0.00094	0.00097
0.4700	0.00069	0.00072	0.00075	0.00079	0.00083	0.00087
0.4800	0.00060	0.00063	0.00066	0.00069	0.00073	0.00076
0.4900	0.00052	0.00055	0.00058	0.00060	0.00064	0.00067
0.5000	0.00045	0.00048	0.00050	0.00053	0.00056	0.00058
0.5100	0.00039	0.00041	0.00044	0.00046	0.00049	0.00051
0.5200	0.00034	0.00036	0.00038	0.00040	0.00042	0.00045
0.5300	0.00030	0.00031	0.00033	0.00035	0.00037	0.00039
0.5400	0.00025	0.00027	0.00029	0.00030	0.00032	0.00034
0.5500	0.00022	0.00023	0.00025	0.00026	0.00028	0.00029
0.5600	0.00019	0.00020	0.00021	0.00023	0.00024	0.00026
0.5700	0.00016	0.00017	0.00018	0.00020	0.00021	0.00022
0.5800	0.00014	0.00015	0.00016	0.00017	0.00018	0.00019
0.5900	0.00012	0.00013	0.00014	0.00015	0.00016	0.00017
0.6000	0.00010	0.00011	0.00012	0.00012	0.00013	0.00014

DATA: CAL1, TEXT

LISTED ON

PROGRAM CALIP2; (To calibrate four Validyne differential pressure transducers, using manometers on each side.)

CONST C=1.4198E-2 ; (Conversion to psi, if C in Socorro=979.19)

VAR I,J,NR,NRD,K,NRSP ; INTEGER;
 X,Y,VR,RHO,H1,H2,DEN,A,B,SIGMA,P,DH ; REAL;
 U : ARRAY[1..4] OF REAL;
 S : ARRAY[1..4,1..5] OF REAL;
 FOUT; TEXT;
 DATE; STRING;

PROCEDURE MOVEOUT(ADDRESS;DATA;INTEGER); EXTERNAL;

PROCEDURE MOVEIN(ADDRESS;INTEGER) VAR DATA;INTEGER); EXTERNAL;

PROCEDURE GETV(CN;INTEGER) VAR R ; REAL); (to get transducer voltage)

CONST ZZ=4.88281E-3; (volts per least count on ADC)

ADR=-3828; ADC=-3826; (addresses of Analog Devices ADC)

VAR IV ; INTEGER;

BEGIN

MOVEOUT(ADR,CN);

MOVEOUT(ADC,0);

MOVEIN(ADC,IV);

R:=IV*ZZ;

END; (procedure GETV)

PROCEDURE ENTRY; (to get data from operator)

BEGIN

WRITE('ENTER DATE AS MONTH DAY YEAR ');

READLN(DATE);

WRITE('ENTER DENSITY OF TEST LIQUID, RHO= ');

READLN(RHO);

WRITE('HOW MANY TIMES AT EACH PRESSURE? ');

READLN(NRSP);

WRITELN('ENTER 999 for H2 to end program');

END; (procedure ENTRY)

PROCEDURE STRTPRINT; (to initiate printer output.)

BEGIN

REWRITE (FOUT, 'REMOUT:');

FOUT:= CHR(17); PUT (FOUT); (select printer)

WRITELN(FOUT,

'CALIBRATION OF FOUR DIFFERENTIAL PRESSURE TRANSDUCERS ',DATE);

WRITELN(FOUT, 'RHO= ',RHO:6:4);

WRITELN(FOUT, ' (',NRSP,' READINGS MADE AT EACH PRESSURE)');

WRITELN(FOUT,;

WRITELN(FOUT, ' TRANSDUCER VOLTAGES');

WRITELN(FOUT, 'RDING H2-H1 P(psi) DP1 DP2 DP3 DP4');

END; (of procedure STRTPRINT)

PROCEDURE LEASQ; (Given the array S[I,J] and NRD, computes and prints the intercepts and slopes of least square fits of four sets of pressure vs. transducer voltage.)

BEGIN

NRD:=NRD-1;

WRITELN(FOUT);

WRITELN(FOUT,

'Least Square Fitting Parameters, ',NRD,' readings of each transducer');

```

WRITELN(FOUT,'      A,psi/volt      B,psi      SIGMA,psi');
WRITELN(FOUT);
FOR I:=1 TO 4 DO BEGIN
  DEN:=NRD*SCI,4]-SQR(SCI,1])*(in psi*psi)
  A:=(NRD*SCI,3]-SCI,1]*SCI,2])/DEN*(in volts/psi)
  B:=(SCI,4]*SCI,2]-SCI,3]*SCI,1])/DEN*(in volts)
  SIGMA:=SCI,5]+SQR(A)*SCI,4]+NRD*SQR(B)-2*A*SCI,3]-2*B*SCI,2]
                                     +2*A*B*SCI,1]:(volts)
  IF SIGMA>0 THEN SIGMA:=SQRT(SIGMA/(NRD-1)) ELSE SIGMA:=0;
  SIGMA:=ABS(SIGMA/A)*(now in psi)
  B:=B/A*(now in psi)
  A:=1/A*(now in psi/volt)
  WRITELN(FOUT,'  DP',I,'      ',A:9:6,B:10:6,SIGMA:10:6);
END*(loop on I, transducer number)
END*(procedure LEASQ)

```

BEGIN

```

ENTRY;
STRTPRINT;
NRD:=1; NRSP:=1;
FOR I:=1 TO 4 DO BEGIN
  FOR J:=1 TO 5 DO SCI,J]:=0;
END*(loop on I)
REPEAT
  WRITE('ENTER HEIGHT OF FIXED COLUMN IN cm, H1= ');
  READLN(H1);
  WRITE('ENTER HEIGHT OF MOVEABLE COLUMN IN CM, H2= ');
  READLN(H2);
  IF H2<>999 THEN BEGIN
    DH:=H2-H1;
    P:=DH*RHO*C*(in psi)
    FOR K:=1 TO NRSP DO BEGIN
      FOR I:= 1 TO 4 DO BEGIN
        GETX(I,VR);
        VC1]:=VR;
        SCI,1]:=SCI,1]+P;
        SCI,2]:=SCI,2]+VR;
        SCI,3]:=SCI,3]+P*VR;
        SCI,4]:=SCI,4]+SQR(P);
        SCI,5]:=SCI,5]+SQR(VR);
      END*(loop on I)
    END*(loop on K)
    WRITELN(FOUT,NR:3,DH:9:2,P:8:4,VC1]:9:3,VC2]:7:3,VC3]:7:3,VC4]:7:3);
    WRITELN('RDING H2-H1 P(=psi)      DP1      DP2      DP3      DP4');
    WRITELN(NR:3,DH:9:2,P:8:4,VC1]:9:3,VC2]:7:3,VC3]:7:3,VC4]:7:3);
    WRITELN;
    NR:=NR+1; NRD:=NRD+NRSP;
  END (if H2 not 999)
UNTIL H2=999;
LEASQ*(if H2 =999)
CLOSE (FOUT,NORMAL);
END.

```

DAT3:DEL2.TEXT

LISTED ON

PROGRAM DELTA1; (To measure and display input and output pressures during flow in core. Also calculates average time derivatives, and prints an ongoing record .)

(Modified with Marginalarm to beep if sleeve pressure sets lower than an adjustable margin above P in. Variable for this is CMAR.)

(Modified 7/10/81 to give correct dp/dt's)

```
CONST   TPS=60;
VAR     NSNT,NUPI,NUPS,NLINES,NRP,KK,LINELIMIT,
        LOMARGN,NI,XDAZ,XPREV,DA   : INTEGER;
        LBY,LSINB,LSCLK,LTAB,LT,TARGTYH,LTPM   : INTEGER[9];
        PINOFF,POUTOFF              : REAL;
        MS,DS,YS,DATE,TKT          : STRING;
        FOUT                         : TEXT;
        SUMP                         : ARRAY[1..6] OF REAL;
```

```
PROCEDURE MOVEIN(ADDRESS:INTEGER;VAR DATA:INTEGER); EXTERNAL;
PROCEDURE MOVEOUT(ADDRESS,DATA:INTEGER); EXTERNAL;
```

```
PROCEDURE TIKLOK; (Calls time and translates into # of ticks since boot-up. LT is passed as a global variable.)
```

```
VAR     I,J       : INTEGER;
        LI,LJ     : INTEGER[9];
        U,V       : REAL;
```

```
BEGIN
  TIME(I,J);
  U:=I; V:=J;
  IF U<0 THEN LI:=I+LBY ELSE LI:=I;
  IF V<0 THEN LJ:=J+LBY ELSE LJ:=J;
  LT:=LI*LBY+LJ;
END; (Procedure TIKLOK)
```

```
PROCEDURE START; (Asks current date and time, interval for screen update, and # of screen updates per printout. Also initializes sums )
```

```
VAR     SH,SM,SS,MO,YR      : INTEGER;
        LSH,LSM,LSS        : INTEGER[9];
```

```
BEGIN
  LTPM:=TPS*TPS;
  WRITE('ENTER DATE, AS THREE INTEGERS - MONTH,DAY,YEAR ');
  READLN(MO,DA,YR);
  STR(MO,MS);
  STR(DA,DS);
  DATE:=CONCAT(MS,'/',DS,'/',YS);
  WRITELN(' ',DATE);
  WRITE('ENTER CURRENT TIME AS THREE INTEGERS - HRS,MIN,SEC ');
  READLN(SH,SM,SS);
  LSH:=SH; LSM:=SM; LSS:=SS;
  LSCLK:= TPS*(LSS+TPS*(LSM+TPS*LSH)); (Start time in ticks since midnite)
```

```

TIKLOK:=LSINB#LT# (ticks since boot)
LTAB:=LSCLK-LSINB# (Tick time at boot)
WRITE('ENTER INTERVAL DESIRED BETWEEN SCREEN UPDATES (SEC) ');
READLN(NSNT);
WRITE('ENTER # OF SCREEN UPDATES BEFORE PRINT ');
READLN(NUPS);
NUPD:=0;
WRITE('ENTER LINELIMIT ');
READLN(LINELIMIT);
TARGTYM:=NSNT*TPS+LSINB# (tick time for next UPDATE.)
NRP:=NSNT*2-2# (# of pressure readings per screen update)
REWRITE(FOUT,'PEMOUT:');
FOUT#:=CHR(17); PUT(FOUT);
STR(LSCLK,TKT); WRITELN(FOUT,'LSCLK= ',TKT);
STR(LSINB,TKT); WRITELN(FOUT,'LSINB= ',TKT);
STR(LTAB,TKT); WRITELN(FOUT,'LTAB= ',TKT);
WRITELN(FOUT,'NSNT = ',NSNT,' NUPS= ',NUPS,' NRP= ',NRP);
WRITELN(FOUT,' DATE TIME Pi Po DP ',
' dPi/dt dPo/dt dDP/dt ');
END# (procedure start)

```

PROCEDURE OFFSET# (checks with operator if zero offset on input and output transducers is correct)

```

VAR CH : CHAR;
BEGIN
WRITE ('Pi offset= ',PINOFF,' psi. Is that OK? (Y/N) ');
READLN(CH);
IF CH<>'Y' THEN BEGIN
WRITE('ENTER NEW VALUE OF PINOFF ');
READLN(PINOFF);
END# (IF)
WRITE ('Po offset= ',POUTOFF,' psi. Is that OK? (Y/N) ');
READLN(CH);
IF CH<>'Y' THEN BEGIN
WRITE('ENTER NEW VALUE OF POUTOFF ');
READLN(POUTOFF);
END# (IF)
END# (procedure OFFSET)

```

PROCEDURE MARGINALARM(VAR LOMARGN : INTEGER)# (measures sleeve pressure and compares it with Pinut. If margin is less than MARGINLIMIT, then:

- a) displays warning
- b) counts up LOMARGN
- c) sounds beer alarm. }

```

CONST ADR=-3828; ADC=-3826; (ADC addresses)
VCR=-28; TON=2055; TOFF=7; (beeping address and constants)
CMAR=40; (will make MARGINLIMIT about 58.6 psi.)
PZ=1.46484; (psi/count if 10V is 3000 psis.)

```

```

VAR PSL,PIN,PD : REAL;
JSL,JIN,JD,I,J,H : INTEGER;

```

```

BEGIN
MOVEOUT(ADR,5);
MOVEOUT(ADC,0);
MOVEIN(ADC,JIN);
MOVEOUT(ADR,7);
MOVEOUT(ADC,0);
MOVEIN(ADC,JSL);

```

001:=05L 01P:=ROUND(PINOFF/PZ);

IF JD<CHAR THEN

BEGIN

WRITELN(' * * SLEEVE PRESSURE MARGIN WARNING ! * * ');

PSL:=PZ*JSL; PIN:=PZ*JIN+PINOFF; PD:=JD*PZ;

WRITELN(' P SLEEVE = ',PSL:6:1,' psi , P INPUT = ',PIN:6:1,' psi ');

WRITELN(' PRESSURE MARGIN IS ONLY ',PD:6:1,' psi ');

LOMARGN:=LOMARGN+1;

FOR I:=1 TO 10 DO

BEGIN

FOR J:=1 TO 200 DO H:=H+1;

MOVEOUT(VCR,TON);

FOR J:=1 TO 200 DO H:=H-1;

MOVEOUT(VCR,TOFF);

END; (loop on I)

END; (if)

END; (procedure ALARM)

PROCEDURE UPDATE; (calls GETPS NPR times, does least square fits to both Pi and Po to set average P's and dP/dt's)

VAR S; ARRAY[1..5,1..2] OF REAL;

P, DEN, PAV, SLP, SIG; ARRAY[1..2] OF REAL;

T, DT, DP, DSLP, SI; REAL;

K, L, M, N, JJ, MC, NC, SC; INTEGER;

LUP, LUPP, LU; INTEGER[9];

PROCEDURE CLOK; (Translates LT, the # of ticks since boot at the previous call to TIME, into clock-on-th-wall time, to the nearest second.)

VAR RSAH; INTEGER;

LTX, LTSEC; INTEGER[9];

BEGIN

XPREV:=XDAZ;

LTX:= LT+LTAB;

LTSEC:= (LTX+30) DIV TPS;

HC:= TRUNC(LTSEC DIV LTPM);

RSAH:= TRUNC(LTSEC-HC*LTPM); (remaining sec after hours div'n)

MC:=RSAH DIV TPS;

SC:=RSAH MOD TPS;

XDAZ:= HC DIV 24;

IF (XDAZ>XPREV) THEN BEGIN

DA:=DA+1;

STR(DA,DS);

DATE:=CONCAT(MS,'/',DS,'/',YS);

END; (if)

HC:= HC MOD 24;

END; (procedure CLOK)

PROCEDURE PROUT; (to print out a record of P's etc.)

VAR PRP; ARRAY[1..6] OF REAL;

KP; INTEGER;

BEGIN

IF NUPD=1 THEN

FOR KP:=1 TO 6 DO SUMPKP:=0;

SUMPE1:=SUMPE1+PAVE1;

SUMPE2:=SUMPE2+PAVE2;

```

SUMPC3J:=SUMPC3J+IP#
SUMPC4J:=SUMPC4J+SLPC1J#
SUMPC5J:=SUMPC5J+SLPC2J#
SUMPC6J:=SUMPC6J+DSLP#
IF NUPI=NUPS THEN BEGIN
  NUPI:=1#
  FOR KP:=1 TO 6 DO
    PRPCKPJ:=SUMPCKPJ/NUPS#
    WRITELN(FOUT,DATE,HC:3,MC:3,SC:3,PRPC1J:8:1,PRPC2J:7:1,PRPC3J:7:2,
            PRPC4J:10:3,PRPC5J:8:3,PRPC6J:8:3)#
    NLINES:=NLINES + 1#
  END (if)
ELSE NUPI:= NUPI+1#
END# (procedure PROUT)

```

```

PROCEDURE GETPS(VAR PIN,POUT : REAL); (to get input and output
                                       pressures from transducers)
CONST ADR=-3928# ADC=-3926# ( addresses of A-to-D )
      PZ=1.46484 # (psi per count if 10V is 3000 psis)
VAR JIN,JOUT : INTEGER#

```

```

BEGIN
  MOVEOUT(ADR,5)#
  MOVEOUT(ADC,0)#
  MOVEIN(ADC,JIN)#
  MOVEOUT(ADR,6)#
  MOVEOUT(ADC,0)#
  MOVEIN(ADC,JOUT)#
  PIN:=PZ*JIN+PINOFF#
  POUT:=PZ*JOUT+POUTOFF#
END# (procedure GETPS(PIN,POUT))

```

```

PROCEDURE FILLS# ( updates sums SEK,LJ )
BEGIN
  DT:=TRUNC(LT-TARGETM)#
  FOR L:=1 TO 2 DO
    BEGIN
      SE1,LJ:=SE1,LJ+DT#
      SE2,LJ:=SE2,LJ+PCLJ#
      SE3,LJ:=SE3,LJ+PCLJ*DT#
      SE4,LJ:=SE4,LJ+DT*DT#
      SE5,LJ:=SE5,LJ+PCLJ*PCLJ#
    END# (loop on L)
  END# (procedure FILLS)

```

```

BEGIN (procedure UPDATE)
  FOR K:=1 TO 5 DO BEGIN
    FOR L:=1 TO 2 DO SEK,LJ:=0#
  END# (loop on K)
  TIKLOK# LUP:=LT#
  LUPP:=LUP-1#
  FOR N:=1 TO NRP DO
    BEGIN
      REPEAT TIKLOK UNTIL LT>LUPP#
      GETPS(PC1J,PC2J)#
      FILLS#
      LUPP:=LT#
    END# (loop on N thru NRP)
  FOR L:=1 TO 2 DO
    BEGIN

```

```

PAVELJ:=(SC1,LJ*SC3,LJ-SC4,LJ*SC2,LJ)/DENCLJ# (in psi)
SLPCLJ:=- (SC1,LJ*SC2,LJ-NRP*SC3,LJ)/DENCLJ# (psi change betw reads)
SI:=SC5,LJ+NRP*SQR(PAVELJ)+SC4,LJ*SQR(SLPCLJ)-2*PAVELJ*SC2,LJ
-2*SLPCLJ*SC3,LJ+2*PAVELJ*SLPCLJ*SC1,LJ#
IF SI>0 THEN SIGELJ:=SQR(SI/(NRP-1)) ELSE SIGELJ:=0#
SLPCLJ:=SLPCLJ*NRP/NSNT# (to put SLP or dP/dt in psi/sec)
END# (loop on L to calc. avgs P's and dP/dt's)
WRITELN#
WRITELN( ' TIME Pi Po DP dPi/dt',
' dPo/dt dDP/dt' )#
CLOCK#
DP:=PAVELJ-PAVE2J#
DSLPL:=SLPCLJ-SLPE2J#
WRITELN( HC:2,MC:3,SC:3,PAVELJ:7:1,PAVE2J:6:1,DP:8:2,SLPCLJ:11:3,
SLPE2J:9:3,DSLPL:8:3 )#
TARGTYM:=TARGTYM + NSNT*TPS#
PROUT#
END# (procedure UPDATE)

```

```

BEGIN (MAIN)
LOMARGN:=0#
LBY:=65536#
PINDOFF:=-27.2# POUTOFF:=9.3#
OFFSET#
START#
NURD:=1#
NLINES:=0#
FOR KK:=1 TO 6 DO SUMPCKK:=0#
UPDATE#
WHILE NLINES<LINELIMIT DO
BEGIN
REPEAT TIKLOK UNTIL LT>TARGTYM#
MARGINALARM(LOMARGN)#
UPDATE#
END#
WRITELN( 'LOMARGN= ',LOMARGN)#
WRITELN( FOUT, ' LOMARGN= ',LOMARGN)#
CLOSE( FOUT,NORMAL)#
END. (MAIN)

```

DAT2:CONS.TEXT

LISTED ON

PROGRAM CONS: (calls procedure PROFL to take conductivity data, and
prints out record of conductivity profile with MINIGRAF)
(NO FORMFEED AFTER PRINT)
(CORRECTED 9/21/81)

CONST SN=6; L=114; AREA=25.74; RSTAN=732;(ohms)

VAR Y, CRMN, CRMX, MESSULT, CS : REAL;

LOMN, LOMX, I : INTEGER;

CR : ARRAY(0..113) OF REAL;

AV : ARRAY(1..6) OF INTEGER;

CD : ARRAY(0..113) OF INTEGER;

JPR:ARRAY(1..114) OF INTEGER;

DATE : STRING ;

CH : CHAR;

FOUT : TEXT ;

PROCEDURE MOVEOUT(ADDRESS,DATA:INTEGER); EXTERNAL;

PROCEDURE MOVEIN(ADDRESS:INTEGER; VAR DATA:INTEGER);EXTERNAL;

PROCEDURE PROFL:(to take, process and store data for conductivity profile)

CONST DELX=6.604E-1;(cm between adjacent electrodes on core)

DROUT=-158; ADR=-3828; ADC=-3826; ZZ= 4.00291E-3;(volts per bit)

ASW=8192; BSW=16384; ASX=8318; BSX=16510;

VAR J,LOB,SRA,SRB,CA,CB,CN,IS : INTEGER;

PROCEDURE GETC (JS: INTEGER; VAR P : INTEGER);

BEGIN

MOVEOUT(DROUT,JS);(sends the word JS from DRV11 to digital mux)

MOVEOUT(ADR,CN);(sends channel # to ADC)

MOVEOUT(ADC,0); (starts conversion)

MOVEIN(ADC,P);(sets value from ADC and calls it P)

END; (of proc GETC)

BEGIN (procedure PROFL)

CRMN:=1000; CRMX:=0; MESSULT:=0;

CN:=8;

FOR J:=0 TO 119 DO BEGIN

IF J<6 THEN AVEJ+1:=0;

IF J<114 THEN LOB:=J

ELSE IF J<117 THEN LOB:=113+2*(J-113) ELSE LOB:=112+2*(J-113);

GETC((LOB+ASW),CA);(sets volts from el. pair LOB, Current dir. A)

GETC(ASX,SRA);(sets volts from std resistor,Current direction A)

MOVEOUT(DROUT,0); (cuts current to zero)

GETC((LOB+BSW),CB);(volts from electrode pair LOB, current dir. B)

GETC(BSX,SRB);(sets voltage from standard resistor, current B)

MOVEOUT(DROUT,0);(cuts current back to zero)

IF J<114 THEN BEGIN

CRLOBJ:=CA-CB;

IF CA<>CB THEN CRCLOBJ:=(SRA-SRB)/(CA-CB) (conductivity ratio)

ELSE CRCLOBJ:=1+LOB/100 ; (default,if measured CA=CB)

IF CRCLOBJ<CRMN THEN BEGIN

CRMN:=CRCLOBJ;

LOMN:=LOB;

END;

IF CRCLOBJ>CRMX THEN BEGIN

CRMX:=CRCLOBJ;

LOMX:=LOB;

```

        END#
        END (if J<114,calc'ns and finding extrema)
ELSE IF SRA<>SRB THEN
    BEGIN
        AVEJ-113J:=CA-CB;
        MESSULT:=MESSULT + ABS((CA-CB)/(SRA-SRB));(sums asymmetries )
    END# ( calc'ns for asymmetre signals voltages. )
END# (loop on J to read and store ratios and diffs of signal voltages.)
CS:=100*CRMN*DELX/(AREA*RSTAN);
CRMN:=CRMN*CS/CRMX;
END# (PROCEDURE PROFL, which sets values of:
        MESSULT - sum of asymmetre voltase ratios.
        CS - conductivity of most conductive section
                (in mhos/meter).
        LOMX - electrode pair at which CS measured.
        CRMN - minimum conductivity in mhos/meter.
        LOMN - electrode pair at which CRMN was measured.)

```

```

PROCEDURE MINIGRAF(L,SN:INTEGER); (TO PLOT CONDUCTIVITY PROFILE ON P. TIGER)
VAR BU,BL,BS,BT : BOOLEAN;
    I,J,K,IL,P,SNH : INTEGER;
BEGIN (MINIGRAF)
    SNH:=SN DIV 2;
    IF ODD(SN) THEN SNH:=SNH+1;
    WRITELN(FOUT);
    WRITELN(FOUT,' OUTPUT FROM MINIGRAF ');
    WRITELN(FOUT,' STRIP LENGTH IS ',L:6,', STRIP NO. IS ',SN);
    WRITELN(FOUT);
    FOUT:=CHR(3); PUT(FOUT); (GO TO GRAPHICS MODE)
    FOR J:= SN DOWTO 1 DO BEGIN
        FOR I:=1 TO L DO BEGIN
            IL:=0; (IL is dot printing variable - 0 makes no dot)
            BU:= JPREIJ<6*J;
            BL:= JPREIJ>=6*(J-1);
            IF BU AND BL THEN BEGIN
                K:=6- JPREIJ MOD 6 ;
                IL:=1; (puts dot in uppermost row of 6 dot strip)
                WHILE K >1 DO BEGIN
                    IL:=IL*2; (IL=2**N puts dot in (N+1)th row of strip)
                    K:=K-1;
                END# (WHILE)
            END#(IF BU AND BL)
            BS:=(NOT( BU AND BL )); BT:=(I MOD 10 =0);
            IF BS AND BT THEN BEGIN (CHANGE IL FOR SCALE DOTS)
                IF J=1 THEN IL:=32;
                IF J=SNH THEN BEGIN
                    IF SN MOD 2 =0 THEN IL:=1 ELSE IL:=8;
                END# (IF J=SNH)
                IF J=SN THEN IL:=1;
            END# (IF BS & BT)
            FOUT:= CHR(IL); PUT(FOUT); (PRINT A DOT OR NOT)
        END# (LOOP ON I FOR ONE STRIP)
        FOUT:= CHR(3); PUT(FOUT);
        FOUT:= CHR(11); PUT(FOUT); (MOVE TO NEXT STRIP)
    END# (LOOP ON J, FOR SN STRIPS )
    FOUT:=CHR(3); PUT(FOUT);
    FOUT:=CHR(2); PUT(FOUT); (3,2 PUTS BACK IN CHAR.MODE)
    WRITELN(FOUT);
    WRITELN(FOUT,' END OF MINIGRAF');
END#(MINIGRAF PROCEDURE)

```

```

BEGIN (CHAIN)
WRITE('ENTER DATE AND TIME ')*
READLN( DATE)*
WRITE(' WANT A LIST OF CRCIJ and CA-CB ? (Y/N) ')*
READLN( CH)*
REWRITE( FOUT, 'REMOUT: ')*
FOUT := CHR(17)* PUT( FOUT)*
WRITELN( FOUT, 'output from CONDOC, ', DATE)*
WRITELN( FOUT, ' INPUT END OF CORE AT LEFT OF PROFILE, ')*
PROFL*
Y := SN*6*
FOR I := 1 TO L DO JPREIJ := ROUND( Y*CREL - IJ/CRMX)* (turned around, top
input end of core on left in printed profile)

MINIGRAF( L, SN)*
WRITELN( FOUT, 'CMAX= ', CS, ' mhos/meter AT ', LOMX)*
WRITELN( FOUT, 'CMIN= ', CRMN, ' mhos/meter AT ', LOMN)*
WRITELN( FOUT, ' ASYMMETRY VOLTAGE= ', MECSULT)*
WRITELN( FOUT, 'AVC1J:6, ', 'AVC3J:6, ', 'AVC6J:6)*
WRITELN( FOUT, ' INPUT LEFT OK ', 'AVC4J:6)*
WRITELN( FOUT, ' ', 'AVC2J:6, ', 'AVC5J:6)*
IF CH = 'Y' THEN
BEGIN
WRITELN( FOUT)*
WRITELN( FOUT, '(Input end of core at top of list.)*
WRITELN( FOUT, ' I CR (CA-CB)*
FOR I := 113 DOWNT0 0 DO WRITELN( FOUT, I:5, ' ', CRCIJ:11:4, ' ', CDCIJ)*
( list 'em backwards so they're from input end of core )
END*
WRITELN( FOUT)*
WRITELN( FOUT)*
CLOSE( FOUT, NORMAL)*
END.

```

APPENDIX C-1

Calibration of Differential Pressure Gauges

CALIBRATION OF FOUR DIFFERENTIAL PRESSURE TRANSDUCERS 11/19/81 14:59
 RHO= 0.7530
 (10 READINGS MADE AT EACH PRESSURE)

RDING	H2-H1	P(Psi)	TRANSDUCER VOLTAGES			
			DP1	DP2	DP3	DP4
1	0.00	0.0000	0.000	0.000	-0.005	-0.005
2	23.50	0.2512	0.488	0.498	0.479	0.488
3	40.80	0.4362	0.830	0.869	0.840	0.850
4	64.50	0.6896	1.333	1.362	1.338	1.357
5	91.10	0.9740	1.895	1.899	1.885	1.924
6	109.50	1.1707	2.280	2.305	2.285	2.314
7	128.50	1.3738	2.666	2.686	2.681	2.715
8	114.75	1.2268	2.383	2.407	2.373	2.412
9	98.00	1.0477	2.046	2.061	2.036	2.061
10	81.30	0.8692	1.704	1.694	1.685	1.714
11	56.35	0.6024	1.167	1.182	1.172	1.191
12	32.55	0.3480	0.669	0.674	0.679	0.698
13	14.65	0.1566	0.308	0.303	0.288	0.308
14	0.00	0.0000	0.005	0.000	-0.005	0.000

Least Square Fitting Parameters, 140 readings of each transducer

	A,psi/volt	B,psi	SIGMA,psi
DP1	0.514706	0.000295	0.004544
DP2	0.511074	0.001297	0.003927
DP3	0.511998	-0.003983	0.003547
DP4	0.505900	-0.001324	0.003525

(DP - 36, ± 5 psi diaphragms)

APPENDIX C-2
 A Miscible Displacement
 (Selected Data Sheets)

LSClk= 3375600 ,LSINB= 1568421 ,LTAB= 1807179

NSNT = 10, NUPS= 6, NRP= 38

LINELIMIT = 150

HIPIN= 300.0 , LOPIN= 200.0

POFF[1..7]=] -0.016, -0.001, 0.005, 0.006, 1.172, 4.102, 0.0

DATE	TIME	Pi	Po	DP	Pmarsn	PSLV	DP1	DP2	DP3	DP4
11/9/81	15 39 52	198.2	170.6	27.56	191.0	395.5	0.004	0.001	0.004	0.001
11/9/81	15 40 52	222.9	185.8	37.12	171.6	392.6	0.009	0.002	0.006	0.001
11/9/81	15 41 52	224.2	186.1	38.14	167.4	391.1	0.010	0.002	0.006	0.001
11/9/81	15 42 52	224.8	186.3	38.55	164.6	389.6	0.010	0.002	0.007	0.001
11/9/81	15 43 52	225.5	186.1	39.38	161.7	385.3	0.010	0.002	0.007	0.001

— Conductivity = CMAX

CONDUCTIVITY PROFILE

— Conductivity = 0

INPUT END OF CORE AT LEFT OF CONDUCTIVITY PROFILE.

CMAX= 1.30832E-2 mhos/meter AT 99

CMIN= -3.02399E-2 mhos/meter AT 12

ASYMMETRY VOLTAGE= 1.79131E-1

Erroneous negative values for conductivity, obtained at electrodes #12 and #51, results from open circuits there.

10 24 28
 INPUT LEFT OK -27 -10
 -46

DATE	TIME	Pi	Po	DP	Pmarsn	PSLV	DP1	DP2	DP3	DP4
11/9/81	15 44 52	226.3	186.2	40.16	157.9	383.8	0.011	0.002	0.007	0.001
11/9/81	15 45 52	226.6	185.9	40.69	155.2	380.9	0.011	0.002	0.006	0.001
11/9/81	15 46 52	226.9	185.6	41.30	152.0	377.9	0.011	0.002	0.006	0.001
11/9/81	15 47 52	226.0	184.2	41.82	150.5	375.0	0.010	0.002	0.007	0.001
11/9/81	15 48 52	226.6	184.1	42.54	149.1	373.5	0.011	0.002	0.007	0.001

average of NA CMAX s is 0.01491 mhos/meter

DATE	TIME	Pi	Po	DP	Pmarsn	PSLV	DP1	DP2	DP3	DP4
11/9/81	15 49 52	225.3	182.3	43.03	149.0	375.0	0.010	0.002	0.006	0.001
11/9/81	15 50 52	227.0	183.9	43.06	148.7	375.0	0.011	0.002	0.006	0.001
11/9/81	15 51 52	226.7	183.8	42.90	148.6	376.5	0.011	0.002	0.006	0.001
11/9/81	15 52 52	228.2	184.5	43.65	148.5	376.5	0.011	0.002	0.006	0.001
11/9/81	15 53 52	228.1	184.7	43.42	148.3	377.9	0.011	0.002	0.007	0.001

— C = 1.0

Horizontal Scale Marks on Minigraph are at 10 electrode intervals, or 6.604 cm apart on core.

— C = 0.0

0 20 40 60 80 100

INPUT END OF CORE AT LEFT OF CONDUCTIVITY PROFILE.

CMAX= 1.30557E-2 mhos/meter AT 99
 CMIN= -9.34300E-2 mhos/meter AT 12
 ASYMMETRY VOLTAGE= 1.77950E-1

10 23 27
 INPUT LEFT OK -28
 -51 -13

Differential pressure transducers
 remained zeroed during this run.

DATE	TIME	Pi	Po	DP	Pmargin	PSLV	DP1	DP2	DP3	DP4
11/9/81	15 54 52	181.5	178.9	2.62	187.4	366.2	0.010	0.001	0.006	0.001
11/9/81	15 55 52	172.2	170.7	1.46	192.3	361.8	0.008	0.001	0.007	0.001
11/9/81	15 56 52	163.9	162.3	1.59	194.9	356.0	0.007	0.001	0.003	0.001
11/9/81	15 57 52	155.9	154.3	1.64	197.1	350.1	0.005	0.001	0.006	0.001
11/9/81	15 58 52	148.4	146.6	1.81	200.2	345.7	0.004	0.001	0.003	0.000

Concentration
 Profile

INPUT END OF CORE AT LEFT OF CONDUCTIVITY PROFILE.

CMAX= 1.28516E-2 mhos/meter AT 99
 CMIN= -1.30599E-1 mhos/meter AT 12
 ASYMMETRY VOLTAGE= 1.86675E-1

10 25 33
 INPUT LEFT OK -29
 -49 -14

DATE	TIME	Pi	Po	DP	Pmargin	PSLV	DP1	DP2	DP3	DP4
11/9/81	15 59 52	146.4	141.9	4.48	198.1	348.6	0.003	0.001	0.002	0.000
11/9/81	16 0 52	215.1	182.9	32.24	149.6	366.2	0.008	0.002	0.005	0.001
11/9/81	16 1 52	219.7	183.4	36.30	147.3	369.1	0.010	0.002	0.006	0.001
11/9/81	16 2 52	220.2	182.4	37.84	147.7	370.6	0.011	0.002	0.006	0.001
11/9/81	16 3 52	221.1	182.5	38.59	148.3	372.1	0.011	0.002	0.006	0.001

INPUT END OF CORE AT LEFT OF CONDUCTIVITY PROFILE.

CMAX= 1.29285E-2 mhos/meter AT 99
 CMIN= -8.41199E-2 mhos/meter AT 12
 ASYMMETRY VOLTAGE= 1.84356E-1

12 23 31
 INPUT LEFT OK -27
 -47 -15

DATE	TIME	Pi	Po	DP	Pmargin	PSLV	DP1	DP2	DP3	DP4
------	------	----	----	----	---------	------	-----	-----	-----	-----

INPUT END OF CORE AT LEFT OF CONDUCTIVITY PROFILE.

CHAX= 1.25401E-2 mhos/meter AT 7
CMIN= -1.61230E-2 mhos/meter AT 12
ASYMMETRY VOLTAGE= 1.87256E-1

6 14 -9
INPUT LEFT OK -18
-44 -31

DATE	TIME	Pi	Po	DP	Pmarsh	PSLV	DP1	DP2	DP3	DP4
11/9/81	16 19 52	236.6	185.9	50.67	149.9	386.7	0.010	0.002	0.007	-0.007
11/9/81	16 20 52	235.1	183.4	51.65	150.9	383.8	0.009	0.002	0.006	-0.007
11/9/81	16 21 52	234.0	182.1	51.92	149.5	383.8	0.009	0.002	0.006	-0.007
11/9/81	16 22 52	237.4	185.0	52.48	150.0	388.2	0.009	0.002	0.005	-0.007
11/9/81	16 23 52	239.5	186.0	53.52	149.9	389.6	0.009	0.002	0.005	-0.007

INPUT END OF CORE AT LEFT OF CONDUCTIVITY PROFILE.

CHAX= 6.72322E-2 mhos/meter AT 0
CMIN= -1.24644E-2 mhos/meter AT 12
ASYMMETRY VOLTAGE= 2.41522E-1

4 15 -35
INPUT LEFT OK -19
-47 -33

DATE	TIME	Pi	Po	DP	Pmarsh	PSLV	DP1	DP2	DP3	DP4
11/9/81	16 24 52	239.8	185.7	54.15	150.0	388.2	0.009	0.002	0.005	-0.006
11/9/81	16 25 52	238.6	184.0	54.57	151.3	389.6	0.009	0.002	0.005	-0.006
11/9/81	16 26 52	240.0	184.9	55.12	151.1	391.1	0.009	0.002	0.006	-0.006
11/9/81	16 27 52	240.2	184.3	55.91	150.9	391.1	0.009	0.002	0.006	-0.006
11/9/81	16 28 52	239.0	182.7	56.24	152.6	391.1	0.009	0.002	0.005	-0.006

INPUT END OF CORE AT LEFT OF CONDUCTIVITY PROFILE.

CHAX= 1.65763E-2 mhos/meter AT 0
CMIN= -1.15190E-2 mhos/meter AT 12
ASYMMETRY VOLTAGE= 2.74498E-1

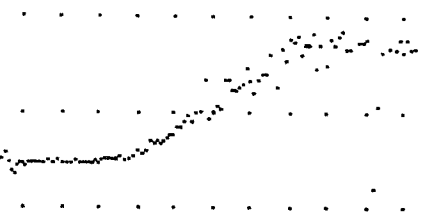
5 15 -48
INPUT LEFT OK -16

CMAX= 2.45777E-2 mhos/meter AT 13
 CMIN= -4.61986E-3 mhos/meter AT 12
 ASYMMETRY VOLTAGE= 7.01457E-1
 -8 79
 INPUT LEFT OK -63
 -58

107

88

DATE	TIME	Pi	Po	DP	Pmarsh	PSLV	DP1	DP2	DP3	DP4
11/9/81	17 54 52	215.3	182.9	32.35	224.9	439.5	0.010	0.002	0.007	-0.003
11/9/81	17 55 52	202.4	185.2	17.21	236.8	443.8	0.010	0.002	0.005	-0.003
11/9/81	17 56 52	202.9	181.5	21.41	236.8	443.8	0.010	0.002	0.006	-0.003
11/9/81	17 57 52	234.6	183.3	51.26	209.5	445.3	0.011	0.002	0.004	-0.003
11/9/81	17 58 52	241.9	183.8	58.07	203.7	448.2	0.011	0.002	0.006	-0.003

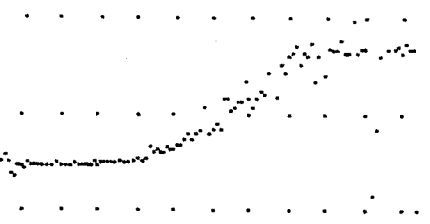


INPUT END OF CORE AT LEFT OF CONDUCTIVITY PROFILE.
 CMAX= 2.52005E-2 mhos/meter AT 13
 CMIN= -4.53729E-3 mhos/meter AT 12
 ASYMMETRY VOLTAGE= 7.08897E-1
 -1 79
 INPUT LEFT OK -78
 -41

111

91

DATE	TIME	Pi	Po	DP	Pmarsh	PSLV	DP1	DP2	DP3	DP4
11/9/81	17 59 52	266.1	184.6	81.52	184.3	448.2	0.011	0.002	0.006	-0.003
11/9/81	18 0 52	280.9	184.5	96.42	171.2	452.6	0.011	0.002	0.005	-0.003
11/9/81	18 1 52	274.0	183.5	90.47	177.2	452.6	0.011	0.002	0.005	-0.003
11/9/81	18 2 52	267.2	183.4	83.80	184.0	454.1	0.011	0.002	0.005	-0.003
11/9/81	18 3 52	261.6	183.9	77.70	189.3	452.6	0.011	0.002	0.005	-0.003



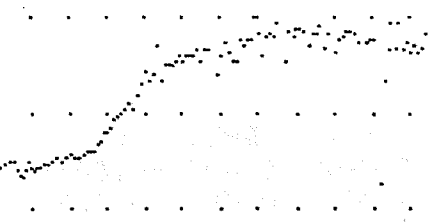
INPUT END OF CORE AT LEFT OF CONDUCTIVITY PROFILE.
 CMAX= 4.31114E-2 mhos/meter AT 13
 CMIN= -1.56450E-1 mhos/meter AT 0
 ASYMMETRY VOLTAGE= 7.56100E-1
 15 74
 INPUT LEFT OK -75
 7

128

71

DATE	TIME	Pi	Po	DP	Pmarsh	PSLV	DP1	DP2	DP3	DP4
------	------	----	----	----	--------	------	-----	-----	-----	-----

11/9/81	17	4	52	233.3	183.3	50.02	184.1	417.5	0.009	0.002	0.004	-0.003
11/9/81	17	5	52	245.3	184.5	60.84	175.1	420.4	0.009	0.002	0.005	-0.003
11/9/81	17	6	52	211.1	181.7	29.46	204.1	414.5	0.009	0.002	0.008	-0.004
11/9/81	17	7	52	199.7	182.6	17.13	214.4	417.5	0.009	0.002	0.006	-0.004
11/9/81	17	8	52	214.3	183.2	31.02	202.2	416.0	0.009	0.002	0.003	-0.004



INPUT END OF CORE AT LEFT OF CONDUCTIVITY PROFILE.

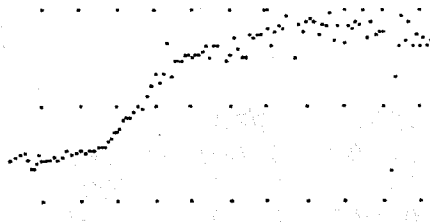
CMAX= 1.80179E-2 mhos/meter AT 13

CMIN= -5.87444E-3 mhos/meter AT 12

ASYMMETRY VOLTAGE= 5.02246E-1

1 -14 154
 INPUT LEFT OK -15
 -66 -81

DATE	TIME	Pi	Po	DP	Pmargin	PSLV	DP1	DP2	DP3	DP4
11/9/81	17 9 52	199.8	181.8	17.98	214.5	420.4	0.009	0.002	0.006	-0.004
11/9/81	17 10 52	219.5	181.8	37.69	198.3	420.4	0.009	0.002	0.007	-0.003
11/9/81	17 11 52	194.1	182.3	11.80	220.9	416.0	0.009	0.002	0.005	-0.004
11/9/81	17 12 52	236.4	184.9	51.49	184.8	421.9	0.010	0.002	0.005	-0.003
11/9/81	17 13 52	233.6	183.4	50.14	187.8	420.4	0.010	0.002	0.005	-0.003



INPUT END OF CORE AT LEFT OF CONDUCTIVITY PROFILE.

CMAX= 1.66745E-2 mhos/meter AT 13

CMIN= -7.48426E-3 mhos/meter AT 12

ASYMMETRY VOLTAGE= 4.99024E-1

-2 -13 146
 INPUT LEFT OK -15
 -74 -74

DATE	TIME	Pi	Po	DP	Pmargin	PSLV	DP1	DP2	DP3	DP4
11/9/81	17 14 52	244.6	183.9	60.72	179.2	418.9	0.010	0.002	0.006	-0.003
11/9/81	17 15 52	224.7	183.0	41.69	195.7	418.9	0.010	0.002	0.004	-0.003
11/9/81	17 16 52	222.5	184.0	38.52	197.9	420.4	0.010	0.002	0.005	-0.003
11/9/81	17 17 52	219.0	183.4	35.60	201.7	420.4	0.009	0.002	0.007	-0.003
11/9/81	17 18 52	214.3	182.7	31.60	206.1	421.9	0.009	0.002	0.004	-0.003



Table 1

"Foam" Generation

<u>Surfactant</u> *	<u>Mfr.</u> **	<u>Concentration Range</u> ***	
Monateric ADFA	1	3.3% - 12.4%	(produced longest lasting foams)
Alipal CD-128	2	4.1% - 26%	
Deriphath 160	3	12.4% - 19.3%	
Deriphath BAW	3	3.3% - 14.1%	
Monateric ADA	1	3.3% - 14.1%	

* concentration of surfactant in water was 10% in all above cases.

** 1 is Mona Industries, Patterson, NJ

2 " GAF Corporation, New York, NY

3 " Henkel Corporation, Hawthorne, CA

*** fractional flow rate of aqueous phase over which water-continuous foam-like emulsion with iso-octane could be produced.

Table 2a. - Solubilities of Polymers in Liquid/Supercritical CO₂

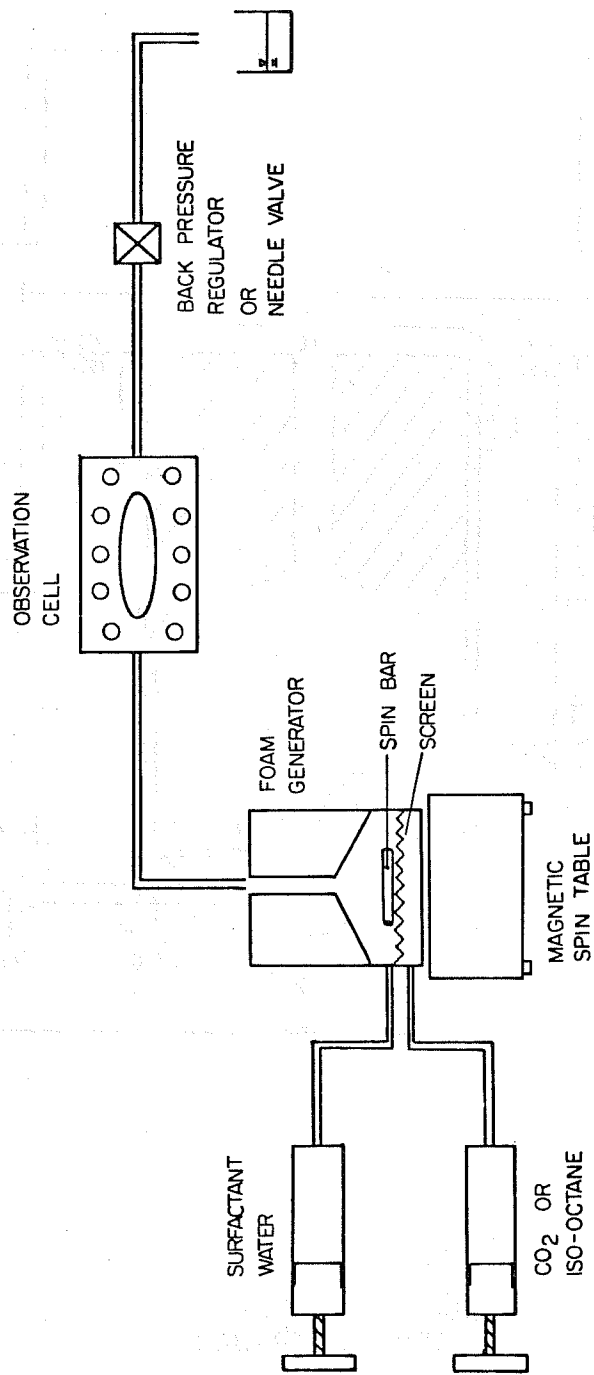
No.	Polymer	Form of the polymers	Temperature, °C	Pressure, PSI	Density of CO ₂ , gm/cc	Solubility, mg./lit.	Observations and Comments
1	Poly (methyl-oxirane)	Waxy solid	25.5	2100	0.865	>8000	Optically active
2	Poly(butene)	Viscous liquid	25.5	2600 - 3400	0.890 to 0.930	>8000	Atactic Mw = 10,000
3	Poly(butene)	Viscous liquid	25.5	3400- 3800	0.930 to 0.945	>5000	Atactic Mw = 25,000
4	Poly(butene)	Solid	25.5	2500	0.89	Nil	Isotactic low mol. weight
5	Poly(n-butyl methacrylate isobutyl methacrylate 50:50)	Beads	20.5	2200	0.90	650	Commercial polymer
6	Poly (benzyl methacrylate)	Beads	25	2000- 2500	0.853 to 0.888	1170	Commercial polymer
7	Poly (ace-naphthalene)	Solid	20	1000	0.80	2533	Commercial polymer
8	Poly(buta-diene)	Viscous liquid	25.5	2800	0.900	2456	Mw = 30,000

Table 2b. - Solubilities of Polymers in Liquid/Supercritical CO₂ (Cont'd.)

No.	Polymer	Form of the Polymers	Temperature, °C	Pressure, PSI	Density of CO ₂ , gm/cc	Solubility, mg./lit.	Observations and Comments
9	Poly(1-vinyl naphthelene)	Solid	25.5	3160	0.918	2210	Commerical polymer
10	Poly(ethyl thiirane)	Solid	25.5	3120	0.915	1400	Atactic, racemic polymer
11	Poly(isobutylene)	Viscous liquid	25.5	2950	0.908	4000	low mol. wt. <i>Atactic</i>
12	Aluminium palmatate	Solid	25.5	3200	0.920	2315	
13	Cetyl trimethyl ammonium bromide	Solid	25.5	2900	0.905	Nil	
14	Poly(Propylene)	Solid	24	2000	0.865 approx.	Nil	Commercial polymer <i>MW=15,000</i>
15	Alkyl phenol formaldehyde condensate	Viscous liquid	25.5	2000	0.855	Nil	Polymer precipitation in the presence of CO ₂
16	Poly (methyl thiirane)	Solid	25.5	2600	0.890	Nil	Mw 500,000 optically active

Table 2c. - Solubilities of Polymers in Liquid/Supercritical CO₂ (Cont'd.)

No.	Polymer	Form of the Polymers	Temperature, °C	Pressure, PSI	Density of CO ₂ , gm/cc	Solubility, mg./lit.	Observations and Comments
17	Poly (ethylene oxide)	Solid	25.5	2500	0.888	Nil	Mw 600,000
18	Poly(vinyl chloride)	Solid	25.5	3100	0.915	Nil	Commerical polymer
19	Poly (isoprene)	Solid	25.5	2800	0.9	Nil	Cis polymer
20	Poly (acrylonitrile)	Solid	25.5	2800	0.9	Nil	Commerical polymer
21	Poly(n-decyl methacrylate)	In toluene solution	25.5	2800	0.9	1298 inclusive solvent	Visual observations indicated no polymer precipitation from its toluene solutions
22	Poly(butene)	Viscous liquid	32.9	2800-2900	0.86	>8000	Atactic mol.wt. 10,000
23	Poly(butene)	Viscous liquid	30	3300	0.925	5614	Atactic mod.wt. 25,000



FOAM GENERATION EXPERIMENTS

FIGURE 1

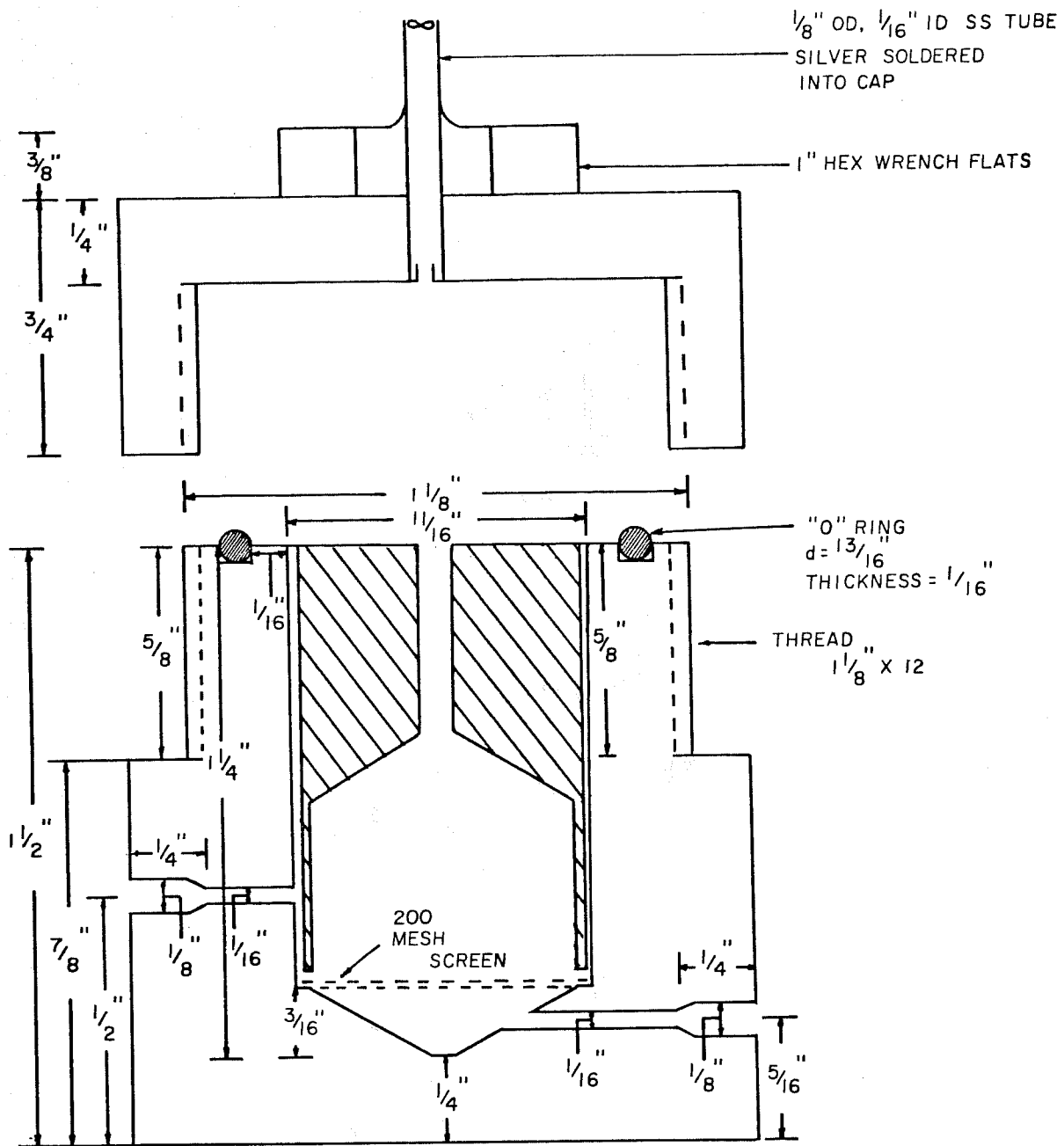
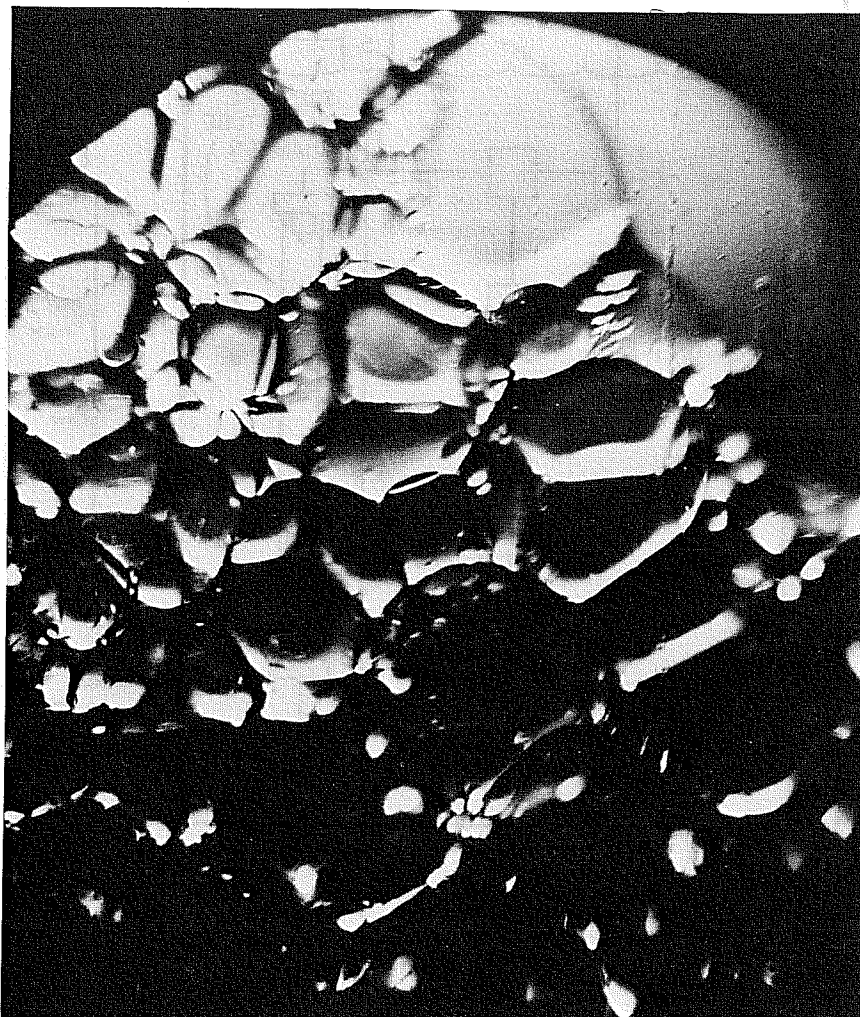


FIGURE 2
 FOAM GENERATOR FOR USE
 WITH MAGNETIC STIR-BAR

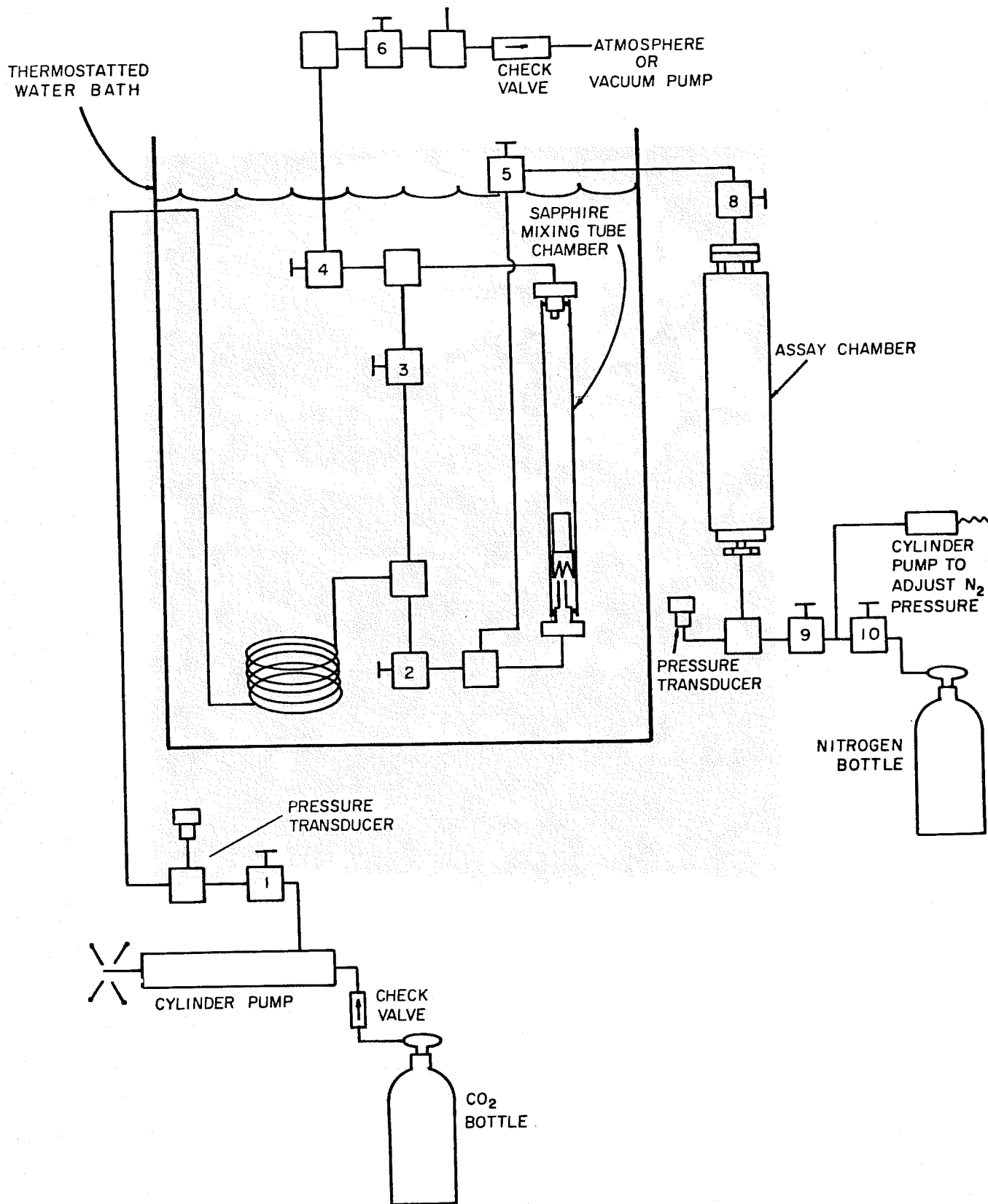


1 mm

FIGURE 3

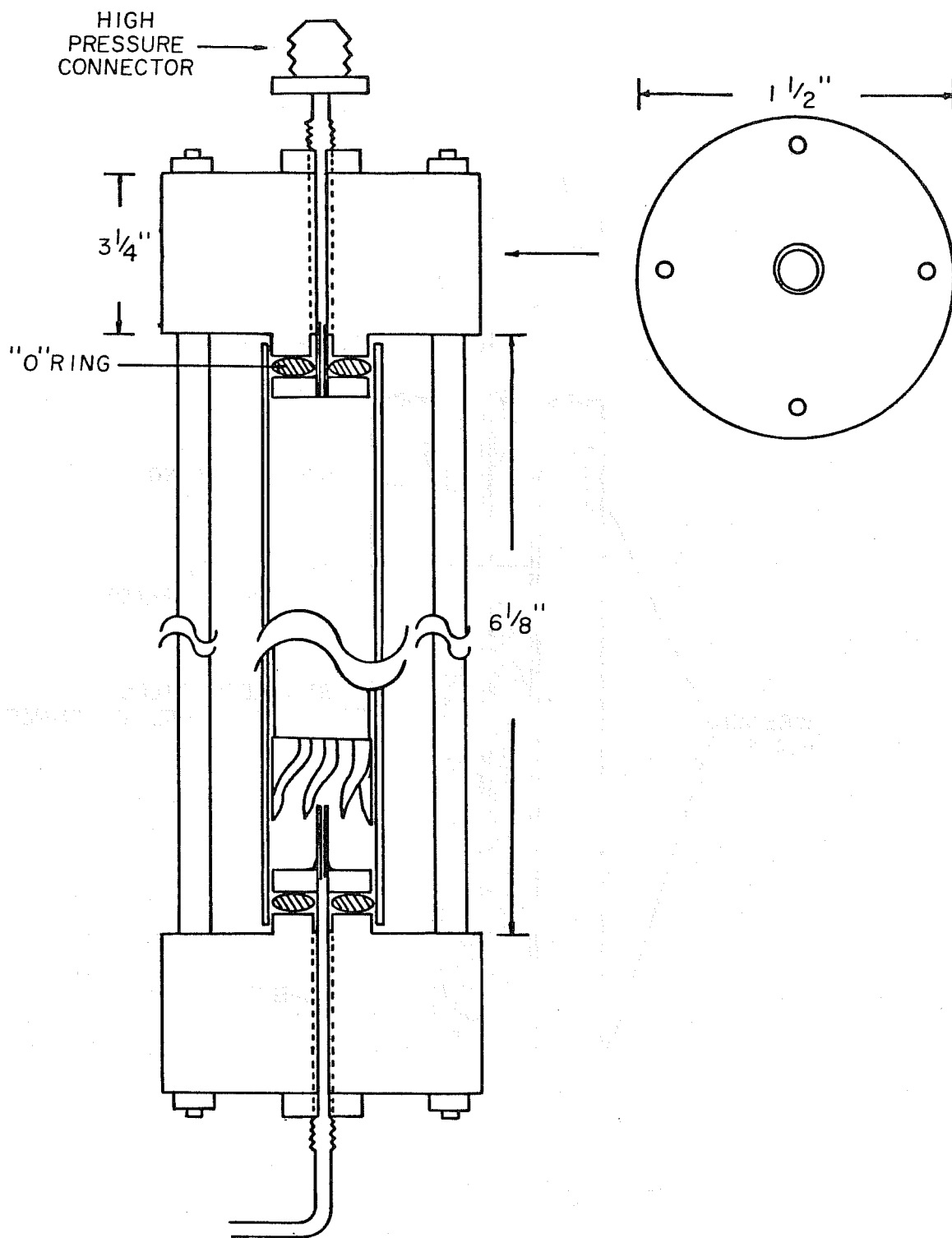
Foam-like Dispersion of Iso-octane
in Aqueous Solution, 10% ADFA*

*Mona Industries, Patterson, New Jersey



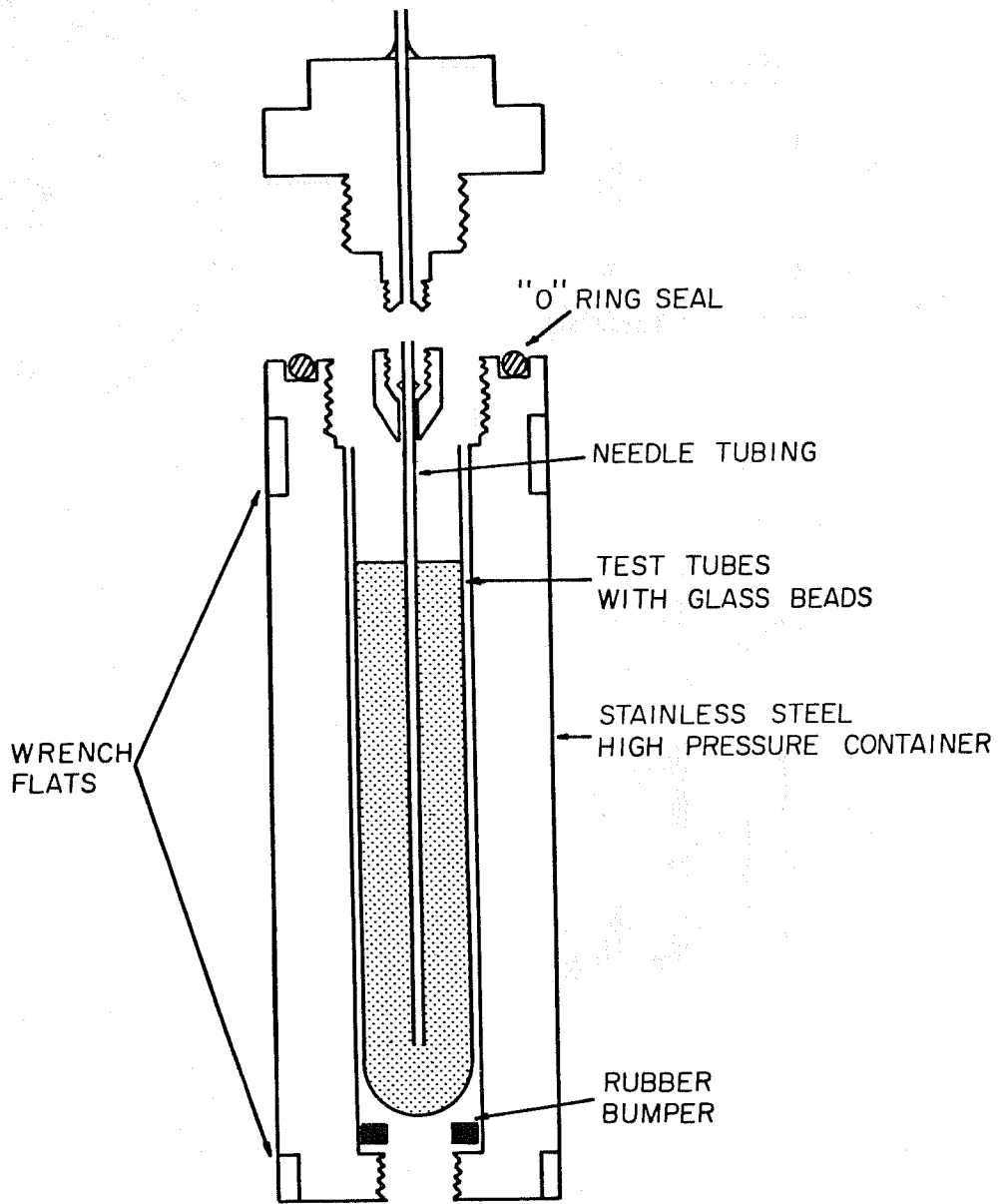
APPARATUS TO MEASURE SOLUBILITY IN DENSE CO₂

FIGURE 4



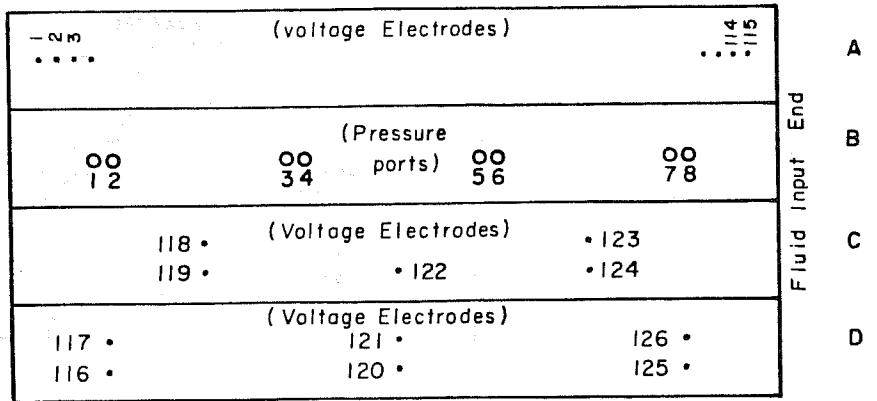
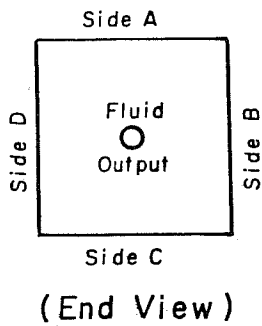
DETAIL OF SAPPHIRE TUBE MIXING CELL

FIGURE 5



DETAIL OF ASSAY CHAMBER

FIGURE 6



(Side View)

Multiplexor
Address

Voltage measured
Between electrodes

- 0
- 1
- 2
- 3
- 4
- 5
- 6
- 7
- ⋮
- 113
- 115
- 117
- 119
- 120
- 122
- 124
- 126
- 127

- 1 and 2
- 2 and 3
- 3 and 4
- 4 and 5
- 5 and 6
- 6 and 7
- 7 and 8
- 8 and 9
- ⋮
- 114 and 115

Side A
Electrodes

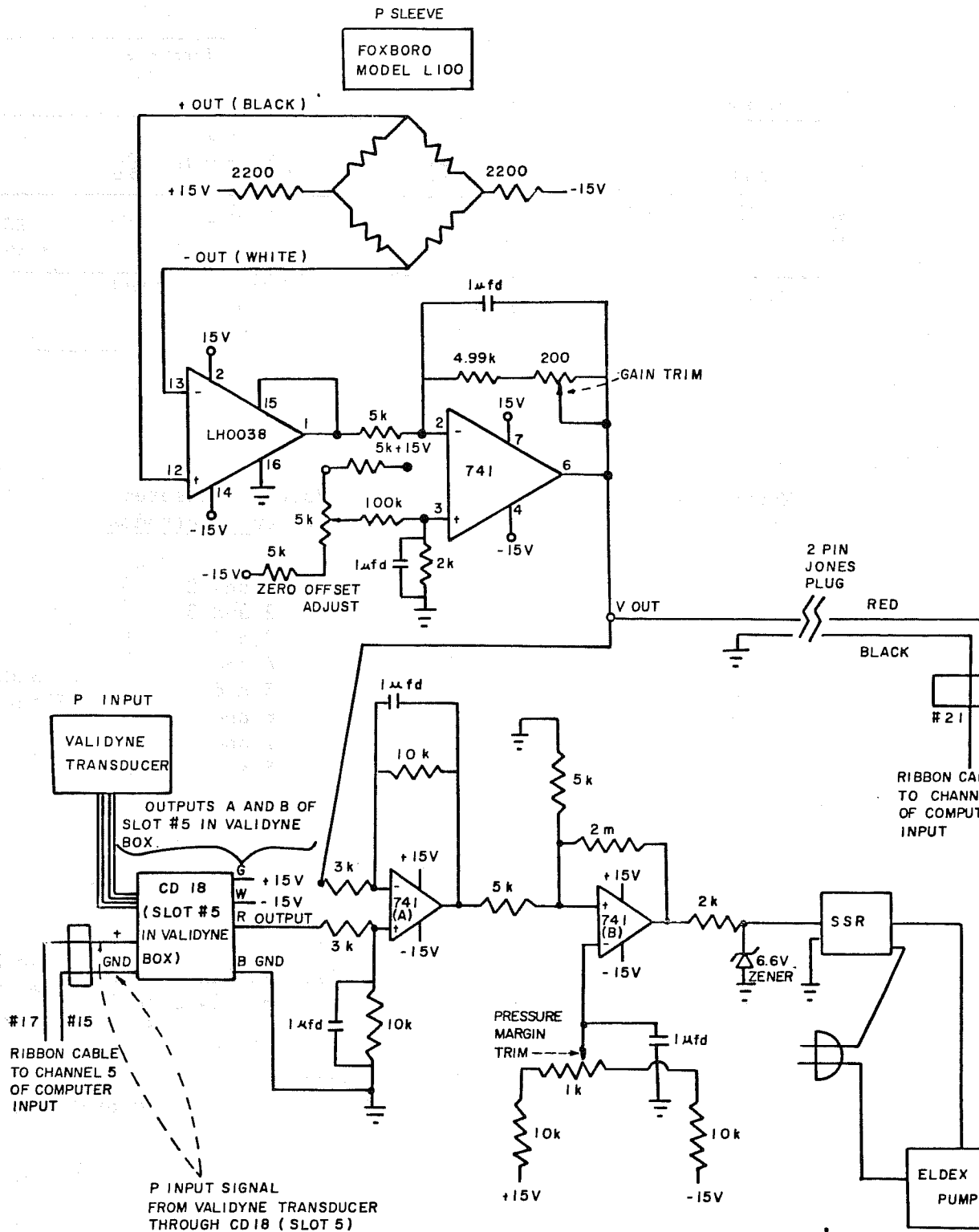
- 116 and 117 side D
- 118 and 119 side C
- 120 and 121 side D
- 121 and 122 edge DC
- 123 and 124 side C
- 125 and 126 side D

Checking
Electrodes

Voltage across Rstandard
Voltage across Rtemperature

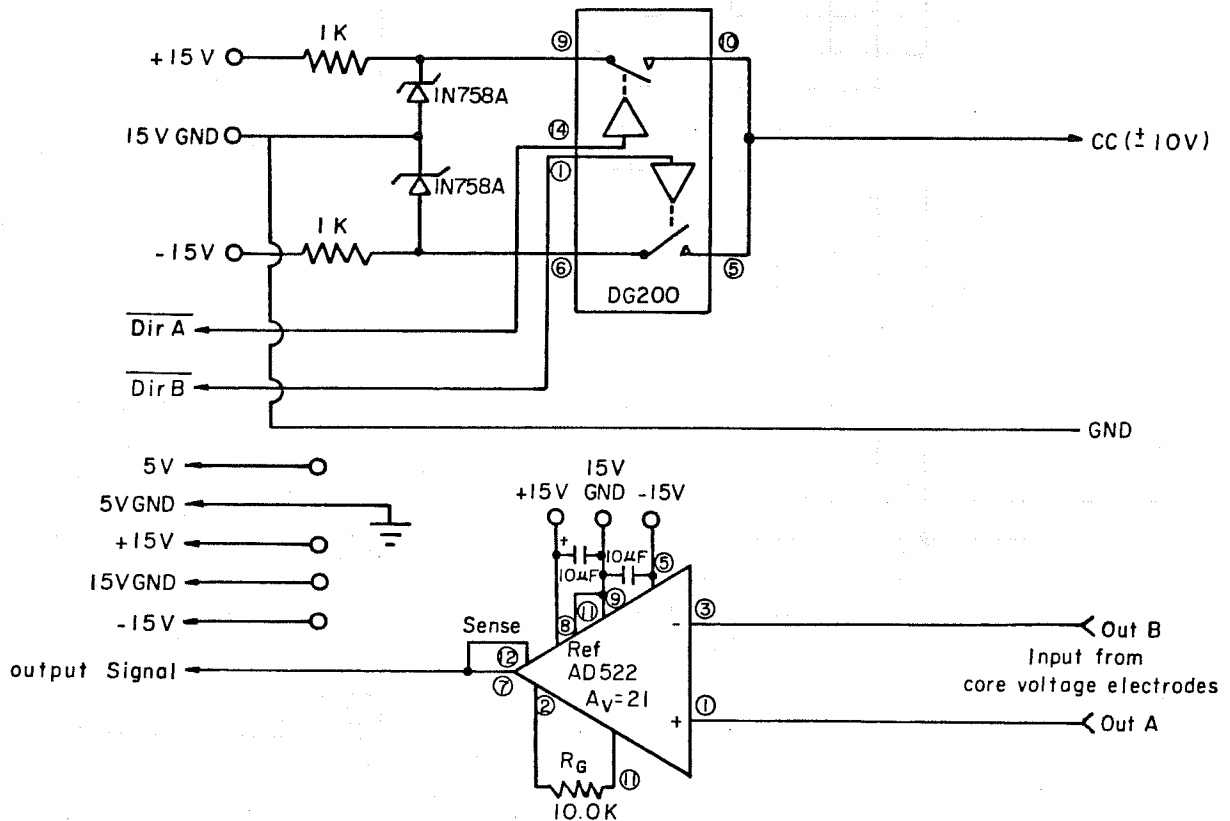
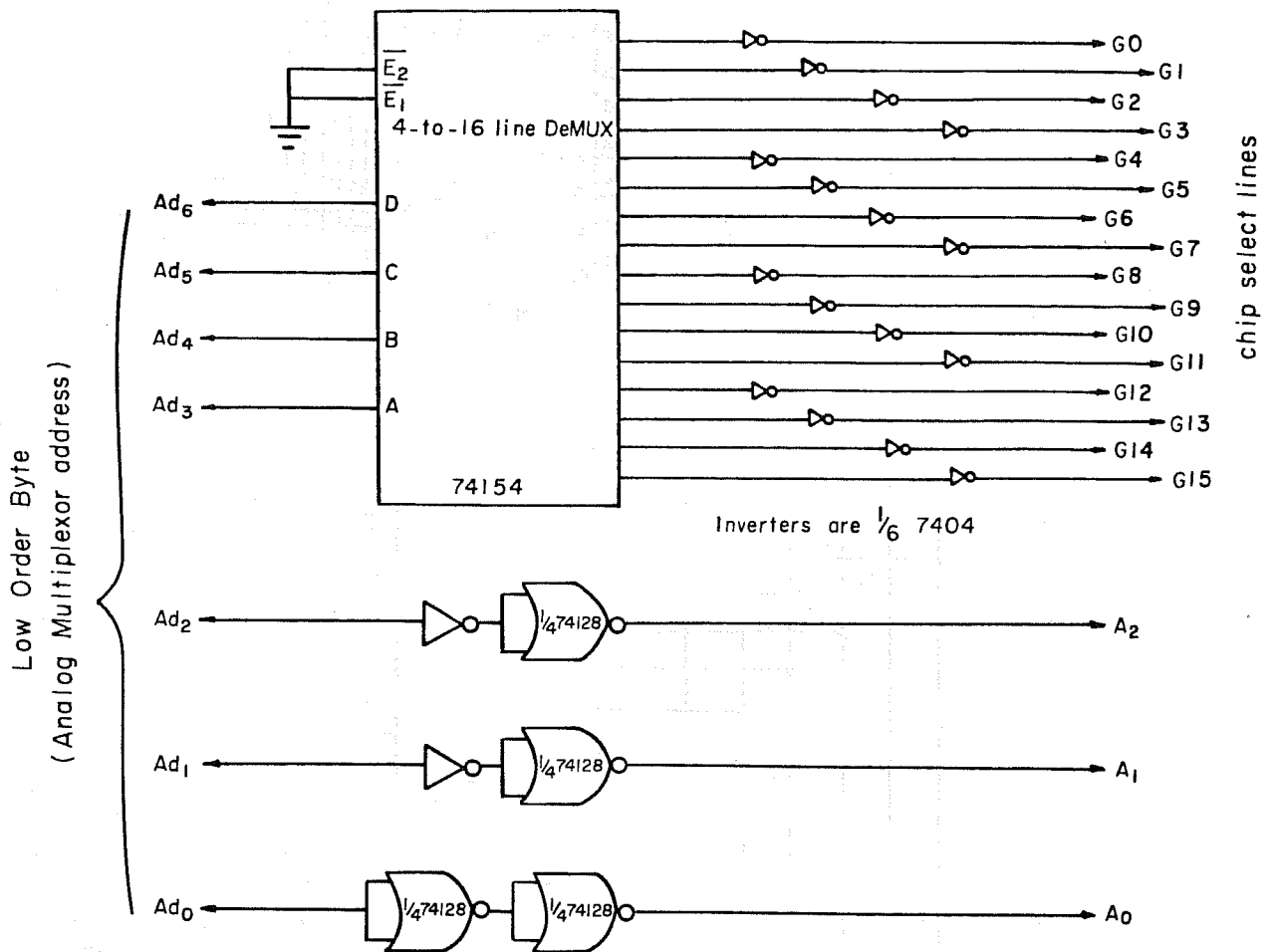
ELECTRODE AND PRESSURE TAP NUMBERING

FIGURE 9



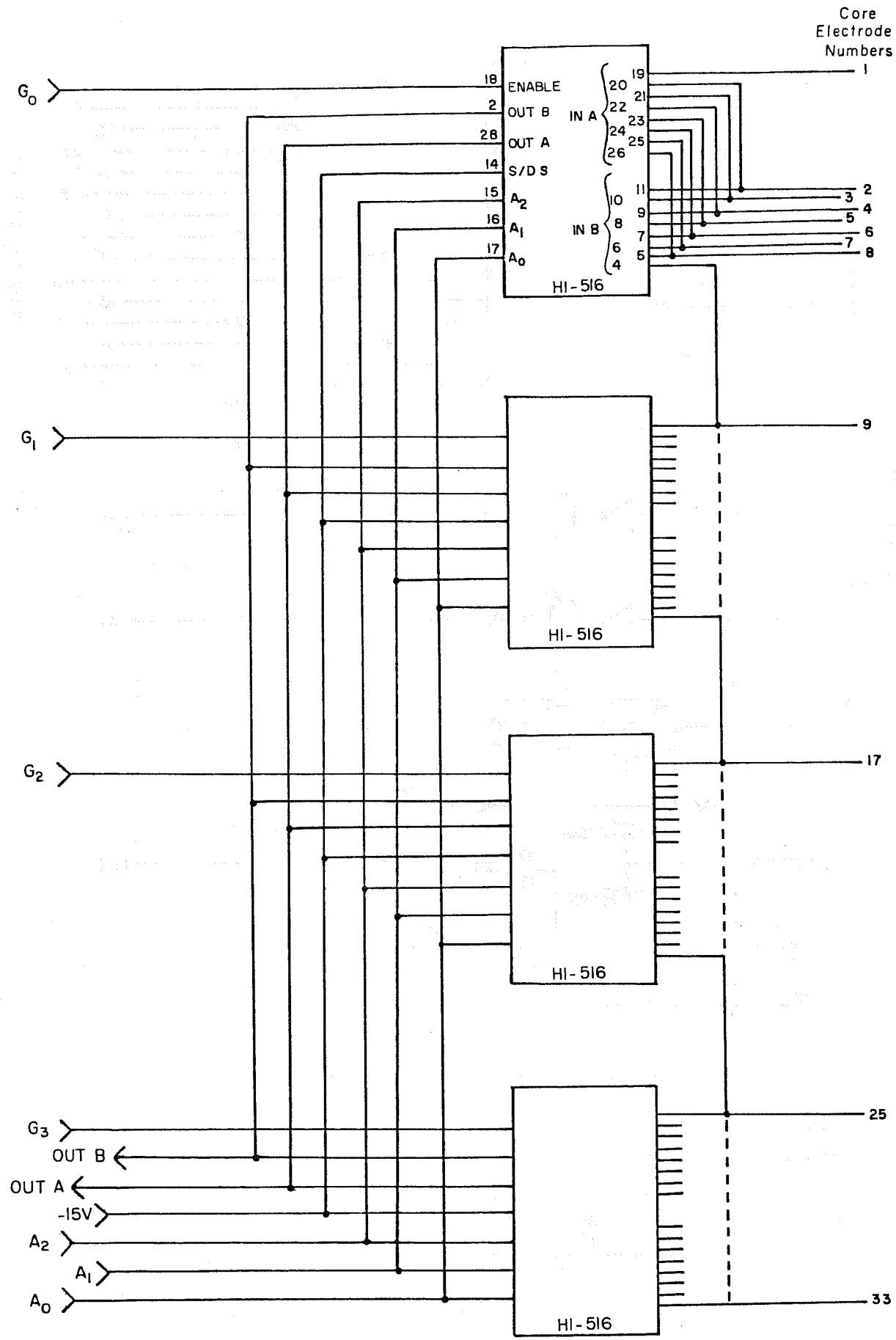
"SLEEVE" PRESSURE REGULATOR

FIGURE 10



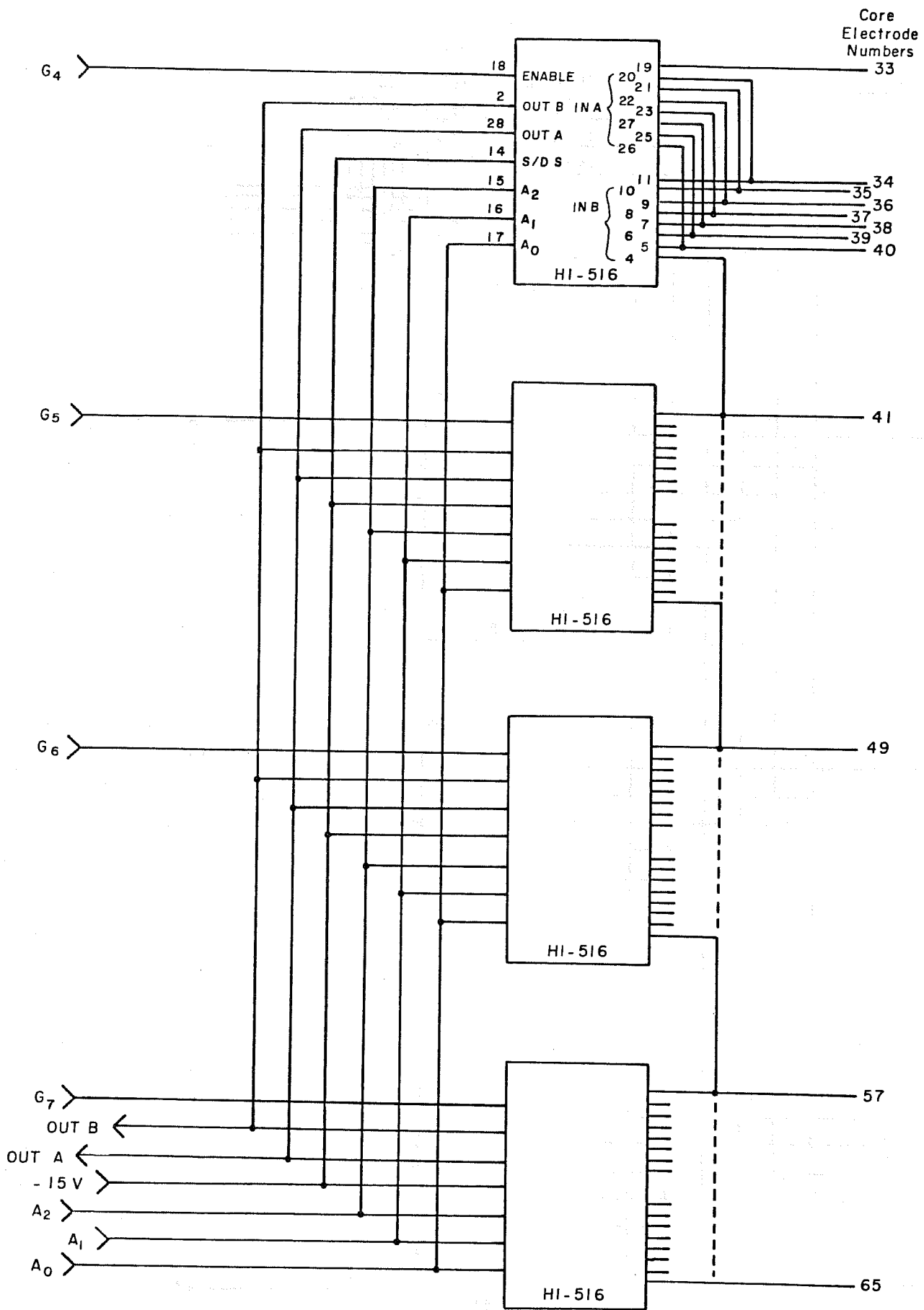
ANALOG MULTIPLEXOR - BOARD 1A

Core
Electrode
Numbers



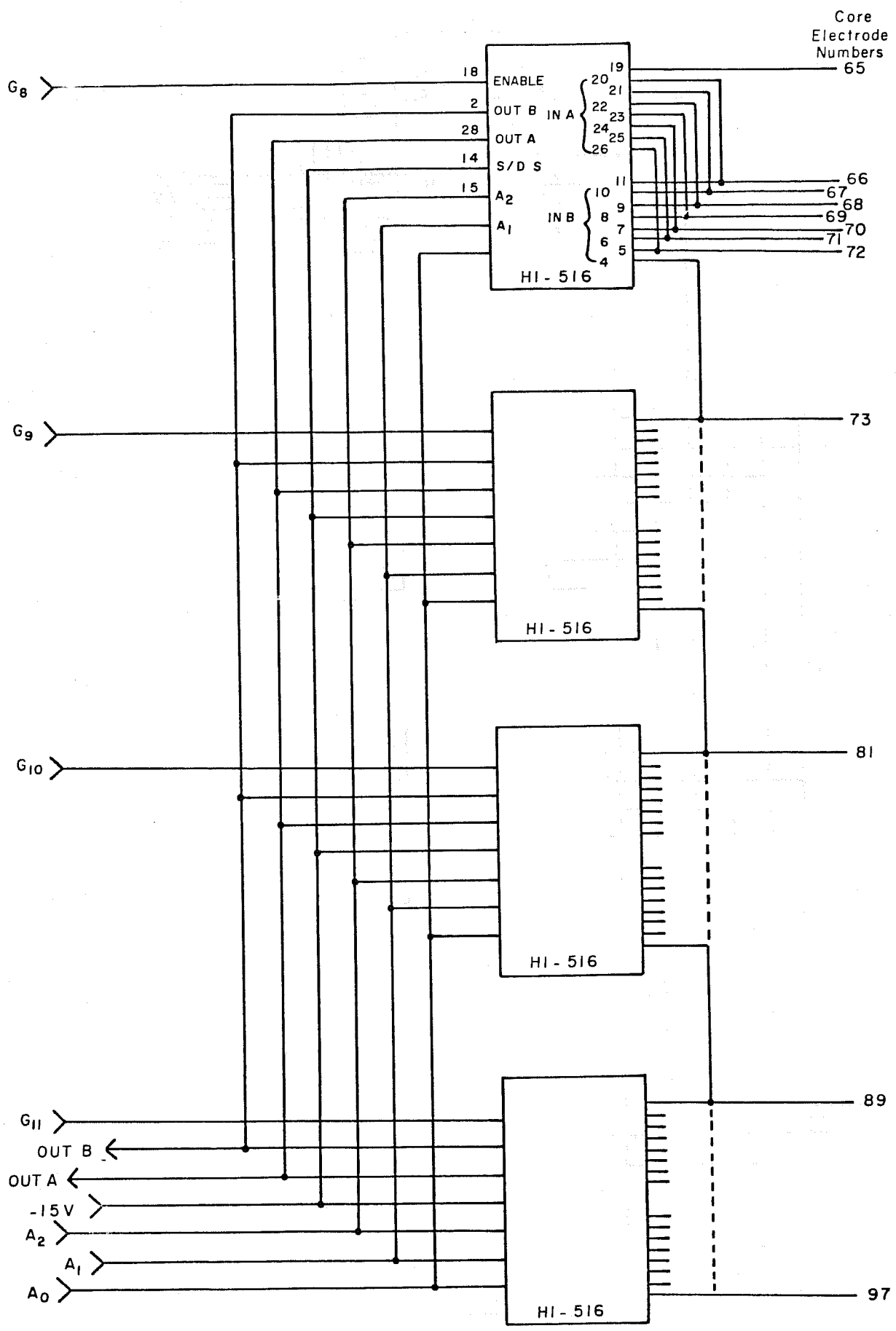
ANALOG MULTIPLEXOR - BOARD 1B

FIGURE 12



ANALOG MULTIPLEXOR - BOARD 2

FIGURE 13



ANALOG MULTIPLEXOR - BOARD 3

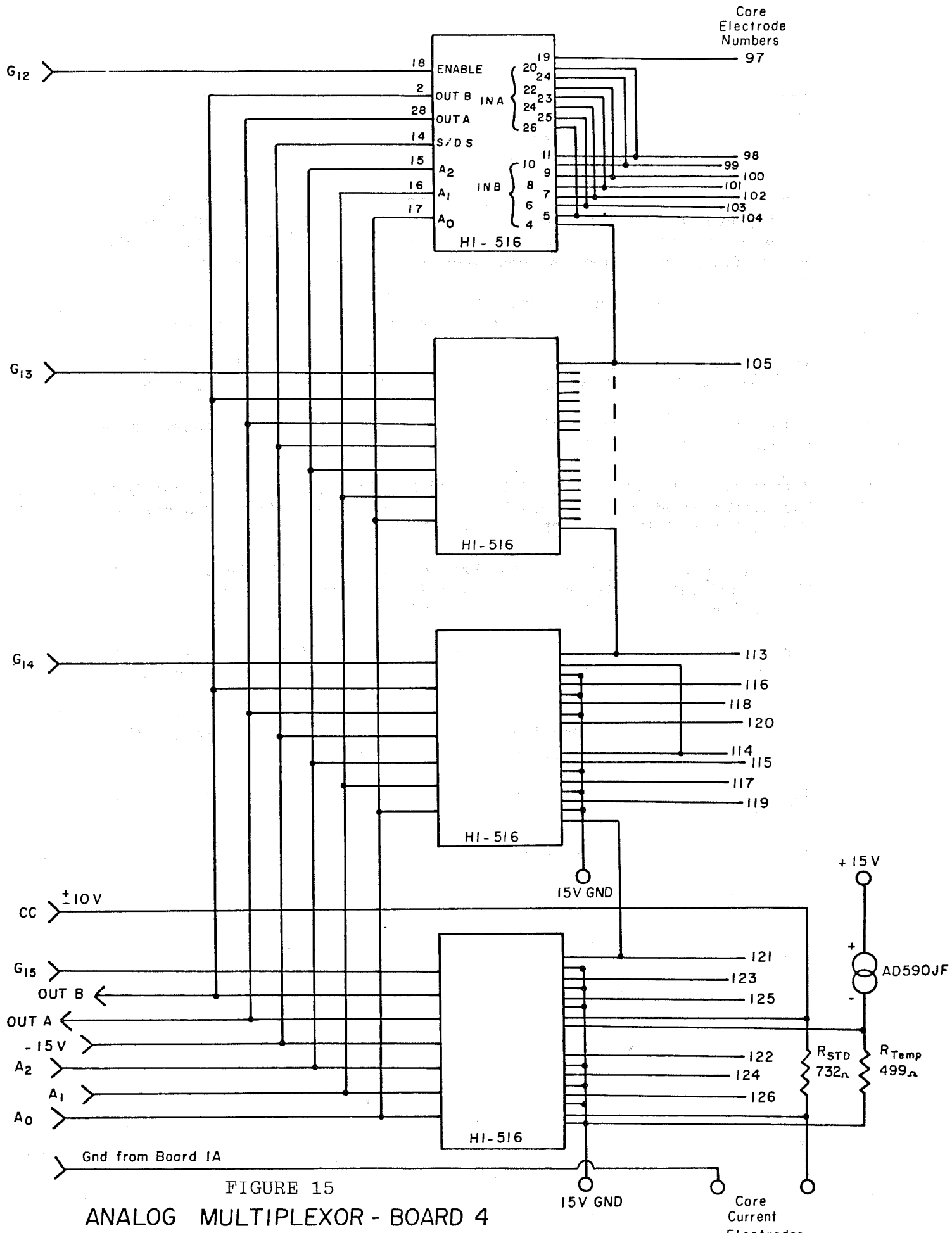


FIGURE 15

ANALOG MULTIPLEXOR - BOARD 4

REFERENCES

- 1 Taber, J.J. and Heller, J.P., "Mobility Control for CO₂ Floods-A Literature Survey," PRRC 80-29, Prepared for the DOE under contract DE-AC21-79MC10689 and for the New Mexico Energy and Minerals Department under contract 68R-3307.
- 2 Taber, J.J. and Heller, J.P., "Development of Mobility Control Methods to Improve Oil Recovery by CO₂," First Annual Report PRRC 80-39, Prepared for the DOE under contract DE-AC21-79MC10689 and for the New Mexico Energy and Minerals Department under contract 68R-3307.
- 3 Hutchinson, C.A. and Braun, P.H., "Phase Relations of Miscible Displacement in Porous Media," AICHE Journal, 7, (1961), pp 64-74.
- 4 Yellig, W.F. and Metcalfe, R.S., "Determination and Prediction of CO₂ Minimum Miscibility Pressures," JPT, 32, (January 1980), pp 160-168.
- 5 Holm, L.W., and Josendal, V.A., "Mechanisms of Oil Displacement by Carbon Dioxide," JPT, 16, (1974), pp 1427-1438.
- 6 Rathmell, J.J., Stalkup, F.I., and Hassinger, R.C., "A Laboratory Investigation of Miscible Displacement by CO₂," SPE 3483, Presented at the 46th Annual Meeting, SPE-AIME (1971).
- 7 Chuoke, R.L., Van Meurs, P., and Van der Poel, C., "The Instability of Slow, Immiscible, Viscous Liquid-Liquid Displacements in Permeable Media," Trans. AIME, 216, (1959), pp 188-194.
- 8 Perkins, T.K., Johnston, O.C., and Hoffman, R.N., "Mechanics of Viscous Fingering in Miscible Systems," SPEJ 5, (Dec. 1965), pp 301-317.
- 9 Perrine, R.L., "The Development of Stability Theory for Miscible Liquid-Liquid Displacement," SPEJ 1, (Mar. 1961), pp 17-25.
- 10 Heller, J.P., "Onset of Instability Patterns Between Miscible Fluids in Porous Media," Journal App. Phys., 37, (1966), pp 1566-1579.
- 11 Heller, J.P., "The Interpretation of Model Experiments for the Displacement of Fluids Through Porous Media," AICHE Journal, 9, (1963), pp 452-459.
- 12 Blackwell, R.J., Rayne, J.R., and Terry, W.M., "Factors Influencing the Efficiency of Miscible Displacement," Trans AIME-SPE, 216 (1959), pp 1-8.
- 13 Van Meurs, P. and Van der Poel, C., "A Theoretical Description of Water-Drive Processes Involving Viscous Fingering," Trans. AIME, 213, (1958), pp 103-112.
- 14 San Filippo, G.P. and Guckert, L.G., "Development of a Pilot CO₂ Flood in the Rock Creek-Big Injun Field, Roane County, WV" ERDA Enhanced Methods, C/3-1 to C/3-15, (August 1977).

- 15 Kane, A.V., "Performance Review of a Large Scale CO₂-WAG PROJECT SACROC UNIT-Kelly Snyder Field," SPE 7091, 5th Symp. on Improved Oil Recovery, Tulsa, (1978).
- 16 Caudle, B.H., and Dyes, A.B., "Improving Miscible Displacement by Gas-Water Injection," Trans. AIME, 213, (1958), pp 281-284.
- 17 Blackwell, R.J., Terry, W.M., Rayne, J.R., Lindley, D.C. and Henderson, J.R., "Recovery of Oil by Displacement with Water-Solvent Mixtures," Trans. AIME 219, (1960), pp 293-300.
- 18 Bernard, G.G., Holm, L.W., and Harvey, C.P., "Use of Surfactant to Reduce CO₂ Mobility in Oil Displacement," SPE #8370, Presented at the 54th Annual Fall Meeting SPE-AIME, Las Vegas, (1979).
- 19 Sagert, N.H., and Quinn, M.J., "Surface Viscosities at High Pressure Gas-Liquid Interfaces," J. Coll. Int. Sci., 65 (July 1978), pp 415-422.
- 20 Heller, J.P., Donaruma, L.G., and Dandge, D.K., "Measuring Solubilities of Polymers in Dense CO₂" (Presented at ACS Polymer Division Meeting, NYC Aug 1981). Polymer Preprints 22 #2, p 59-60 (Aug 1981).
- 21 Patton, J.T., Belkin, H., Holbrook, S. and Kuntamukkula, M., "Enhanced Oil Recovery CO₂ Foam Flow Flooding," First Annual Report, New Mexico State University/DOE Contract ET78C013259 (October 1979).
- 22 McCutcheon's Emulsifiers and Detergents, North American Edition. MC Publishing Co., 175 Rock Road, Glen Rock, NJ (1981).
- 23 Francis, A.W., "Solvent Extraction with Liquid Carbon Dioxide," Ind. and Eng. Chem, 47, (1955), pp 230-233.
- 24 Francis, A.W., "Ternary Systems of Liquid CO₂," Journ. Phys. Chem., 58, 6 (December 1954), pp 1099-1114.
- 25 Stahl, E., Schulz, W., Schuetz, E. and Willing, E., "A Quick Method for the Microanalytical Evaluation of the Dissolving Power of Supercritical Gases," Angew. Chem. Int'l Ed. Engl., 17, (1978), pp 731-738.
- 26 Lohrenz, John, Swift, G.W., and Kurata, F., "An Experimentally Verified Theoretical Study of the Falling Cylinder Viscometer," AICHE J., 6 (Dec. 1960) p 547-550.
- 27 Meister, J.J., "A Porous, Permeable Carbonate for Use in Oil Recovery Experiments," JPT 30 (Nov. 1978), pp.1632-1634.

